Hereditary Early-onset Parkinsonism
The Role of the FBXO7 Protein

Tianna Zhao

The studies presented in this thesis were financially supported by:
Erasmus MC Rotterdam
“Internationaal Parkinson Fonds” – The Netherlands
Netherlands Organization for Scientific Research (NWO, VIDI grant n.4600268033).

The printing of this thesis was financially supported by:
Erasmus University Rotterdam
Department of Clinical Genetics, Erasmus MC
“Internationaal Parkinson Fonds” – The Netherlands
J.E. Jurriaanse Stichting

ISBN: 978-94-6182-172-0
Cover: Guanqun Wu
Layout: Peng Lu
Printed by: Off Page, Amsterdam

Hereditary Early-onset Parkinsonism
The Role of the FBXO7 Protein

Erfelijke Parkinsonisme op jonge leeftijd
De rol van het FBXO7 eiwit

Proefschrift

ter verkrijging van de graad van doctor aan de
Erasmus Universiteit Rotterdam
op gezag van de rector magnificus
Prof.dr. H.G. Schmidt
en volgens besluit van het College voor Promoties

De openbare verdediging zal plaatsvinden op
woensdag 17 oktober 2012 om 13.30 uur

door

Tianna Zhao

geboren te Zao Zhuang

Promotiecommissie

Promotoren:	Prof.dr. V. Bonifati
	Prof.dr. B.A. Oostra
Overige leden:	Prof.dr. O. Bandmann
	Dr. E. Aronica
	Dr. N. Galjart

Table of Contents

Chapter 1	General introduction and Scope of the thesis	7
Chapter 2	*FBXO7* Mutations Cause Autosomal Recessive, Early-onset Parkinsonian-Pyramidal Syndrome	41
Chapter 3	Loss of Nuclear Activity of the FBXO7 Protein in Patients with Parkinsonian-Pyramidal Syndrome (PARK15)	59
Chapter 4	Dopaminergic neuronal loss and dopamine-dependent locomotor defects in Fbxo7-deficient zebrafish	87
Chapter 5	The expression of the FBXO7 proteins in the normal human brain and in Parkinson's disease	111
Chapter 6	General discussion	127
Summary/Samenvatting/总结		141
Curriculum Vitae		150
PhD Portfolio		151
List of Publications		152
Acknowledgements		153

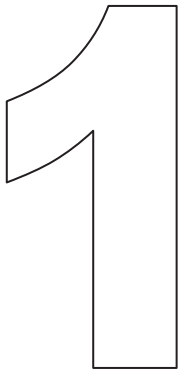

General introduction

Parkinson's disease – clinical and pathologic aspects

Idiopathic Parkinson's disease (idiopathic parkinsonism, PD) is the second most common neurodegenerative disorder after Alzheimer's disease, and it affects 1-2% of the population above the age of 60 years-old [1]. The cardinal motor clinical features of the disease consist of resting tremor, bradykinesia, muscular rigidity, and postural instability. This motor syndrome is sustained by the degeneration of the nigral dopaminergic neurons, resulting in dopamine deficiency at the level of the striatal synaptic terminals [2,3].

The pathogenesis of PD remains poorly understood, and, as a consequence, no treatment is available to stop or even slow the disease progression [4,5]. The restoration of the dopamine levels (using the natural precursor levodopa, or different dopamine agonist compounds), is currently the foundation of the symptomatic pharmacological therapy for PD [6,7]. Of note, some non-motor symptoms such as autonomic, sleep, and cognitive disturbances are increasingly recognized as integral components of PD [8]. These non-motor symptoms are sustained by deficit at the level of different, non-dopaminergic brain pathways, and are therefore largely refractory to dopamine-replacement therapies [9].

The pathologic hallmarks of PD are the severe loss of dopaminergic neurons in the substantia nigra, and the presence of eosinophilic inclusions, termed Lewy bodies (LBs) or Lewy neurites (LNs) in the surviving neurons (Figure 1) [10]. LBs are round-shaped cytoplasmic inclusion bodies, while LNs are spindle-like or thread-like inclusions within the neuronal processes [5,10,11]. Pathologically aggregated forms of the α-synuclein protein represent the main component of LBs and LNs, and indeed, the presence of α-synuclein immunoreactive inclusions (together with dopaminergic neuronal loss) has become the gold standard criterion for the neuropathological diagnosis of PD and diffuse Lewy body disease (DLB) [12,13]. Furthermore, α-synuclein is also the major component of the glial cytoplasmic inclusions, the pathological hallmark of a different neurodegenerative disorder, termed Multiple System Atrophy (MSA). The term "α-synucleinopathy" is currently adopted to indicate the whole spectrum of neurodegenerative diseases, characterized by misfolding and aggregation of α-synuclein [10].

Most PD patients experience the onset of their motor symptoms after the age of 60 years-old [1,2]. However, in some patients, the symptoms of the disease

develop much earlier. “Early-Onset Parkinsonism” is the terminology used to indicate the patients presenting with a parkinsonian syndrome before the age of 40 years-old. These cases can be further divided into “Young-onset parkinsonism” (YOP, symptomatic onset between the ages of 21 and 40) and “Juvenile-onset parkinsonism” (JP, below the age of 21) [14]. YOP accounts for ~3-10% of all cases of parkinsonism [15,16]. As a group, the YOP patients usually display slower disease progression, more frequent dystonia at onset, less cognitive decline, and more frequent dyskinesias in response to levodopa treatment [17]. JP is relatively rare, at least in Western countries, is often familial, and more frequently associated with atypical clinical and pathological features. In contrast, YOP is less commonly familial, and usually displays clinical symptoms and pathology similar to classical, late-onset PD [18].

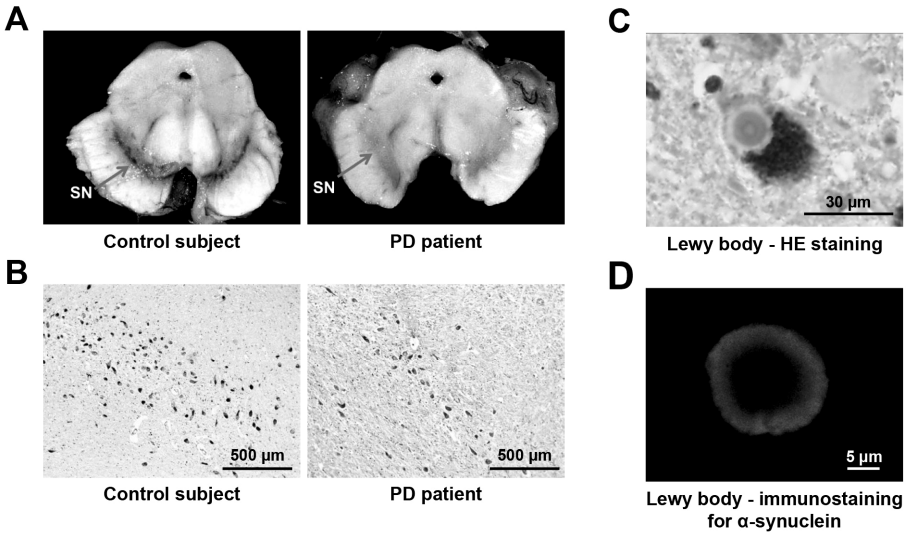

Figure 1 Macroscopic and microscopic neuropathological features of PD.
Midbrain sections show normal substantia nigra (SN) and SN degeneration in PD patient (A). Representative H&E staining shows loss of dopaminergic neurons in SN (B) and the presence of lewy body (C) in PD patient. Lewy body was stained using α-synuclein antibody (D).
Figure 1A is reproduced from Mandel, et al. EPMA Journal (2010), 1(2):273-92, with permission.

The molecular pathogenesis of PD

Abnormalities in several important cellular pathways and systems are suspected to play some roles in the pathogenesis of PD, including mitochondrial dysfunctions, oxidative stress, proteasomal and autophagic dysfunctions, neuroinflammation, excitotoxicity, and apoptosis [4,5,19]. However, the exact

molecular mechanisms causing neurodegeneration in PD remain mostly unknown [20,21]. It is commonly assumed that in most patients, PD is caused by an interaction of multiple genetic susceptibilities and environmental factors. According to the epidemiological studies, some environmental risk factors such as rural living, consumption of well water and pesticide exposure increase the risk of PD [1]. Humans intoxicated with MPTP (1-methyl-4-phenyl-1,2,3,6-tetrahydropyridine) can develop a permanent parkinsonian syndrome, that is clinically nearly identical to PD [22,23,24]. Conversely, cigarette smoking and coffee drinking reduce the risk for developing PD [1,25].

Table 1 Current catalogue of confirmed parkinsonism-causing genes

Locus	Gene	Symptoms onset	Inheritance	Clinical phenotype	Pathology
PARK1	*SNCA*	early onset	Autosomal dominant	typical parkinsonism	LB positive
PARK8	*LRRK2*	typical late onset	Autosomal dominant	typical parkinsonism	LB positive in most cases
PARK17	*VPS35*	typical late onset	Autosomal dominant	typical parkinsonism	Not available
PARK2	*parkin*	early onset	Autosomal recessive	typical parkinsonism	LB negative in most cases
PARK6	*PINK1*	early onset	Autosomal recessive	typical parkinsonism	LB positive (only 1 brain studied)
PARK7	*DJ-1*	early onset	Autosomal recessive	typical parkinsonism	Not available
PARK9	*ATP13A2*	early onset	Autosomal recessive	atypical parkinsonism	LB negative
PARK14	*PLA2G6*	early onset	Autosomal recessive	atypical parkinsonism	LB positive
PARK15	*FBXO7*	early onset	Autosomal recessive	atypical parkinsonism	Not available

Over the past few years, the rapid development in genetic studies has provided novel clues for understanding of the molecular pathogenesis of PD [5,19,26]. Genome-wide linkage analysis and positional cloning have been successful in identification of several loci and genes in ‘Mendelian’ forms of parkinsonism (Table 1). It is expected that other monogenic forms of parkinsonism will be

identified in the future, as mutations in the above-mentioned genes are not found in other patients.

The autosomal dominant forms of parkinsonism

Mutations in the *α-synuclein* (*SNCA*), *leucine-rich repeat kinase 2* (*LRRK2*), and *vacuolar protein sorting 35* (*VPS35*) genes have been definitely established as the cause of autosomal dominant forms of parkinsonism. Mutations in the *α-synuclein* gene were the first recognized genetic cause of parkinsonism [27]. Three missense mutations (A53T, A30P, and E46K) in this gene are currently known as a cause of disease, but they are detected very rarely in PD families with an autosomal dominant pattern of inheritance. However, duplications or triplications of the entire *α-synuclein* locus are a more frequent type of mutation, detectable in ~1% of the familial PD cases with an autosomal dominant pattern of inheritance [28]. The phenotype associated with *α-synuclein* mutations is often characterized by earlier onset and more aggressive disease progression compared with the typical, idiopathic PD.

The α-synuclein protein was later recognized as the major fibrillar component of LBs [29], the pathological hallmarks in PD, diffuse Lewy body disease, and MSA. Therefore, the α-synuclein protein is considered to be crucial in the pathogenesis of different neurodegenerative diseases, and the term "α-synucleinopathy" was defined to encompass the spectrum of disorders associated with misfolding, and aggregation of this protein [26,30]. In vitro studies revealed that α-synuclein has a high propensity to aggregate, leading to a toxic gain of function as the consequence of aggregation [31].

Another important causative gene in autosomal dominant parkinsonism is *LRRK2.* Mutations in this gene lead to parkinsonism with typical clinical features, including late-onset. Furthermore, they are much more common than the mutations in the other known PD-causing genes. Perhaps, the most impressive aspect of the *LRRK2* gene is the identification of the G2019S mutation, which is present in up to 30-40% of the patients with typical, late-onset PD from North African and Middle Eastern populations [32,33,34]. Besides the G2019S mutation, six other *LRRK2* variants (N1437H, R1441G/C/H, Y1699C, and I2020T) have been definitely identified and confirmed as pathogenic mutations in PD. In addition, polymorphic variants in the *LRRK2* gene such as R1628P and G2385R are common and strong risk factors (odd ratio ~2.5) for sporadic PD in the Chinese Han population [34,35]. *LRRK2* has 51 exons and encodes a large

protein of 286 kDa. The LRRK2 protein contains both a kinase and a GTPase enzymatic activity. The G2019S mutation is located in the kinase domain and has been consistently shown to increase the kinase activity. However, the R1441C, R1441G and Y1699C mutations are present in other domains (ROC-GTPase and COR, C-terminal of ROC), resulting in a reduced GTPase activity [36,37,38]. The normal function of the LRRK2 protein, and the mechanisms leading to disease in the patients with LRRK2 mutations remain poorly understood. Whether the pathways of LRRK2 intersect with those of α-synuclein remains a matter of debate. According to a recent study, the over-expression of LRRK2 accelerated the neuropathology induced by A53T-mutant α-synuclein, which leads to aggregation and toxicity. Moreover, the LRRK2 depletion reduced the accumulation of A53T α-synuclein and delayed its associated pathology. These finding support the contention that α-synuclein and LRRK2 interact in a common pathway leading to dominant parkinsonism [39].

The autosomal recessive forms of parkinsonism

Mutations in each of the three following genes, *parkin (PRKN*), *PTEN induced putative kinase 1* (*PINK1*), and *Parkinson protein 7* (*PARK7*, *DJ-1*) can cause autosomal recessive form of parkinsonism, which is usually characterized by an early-onset and typical clinical signs [40,41,42]. *Parkin* mutations are the most common cause of early onset parkinsonism. More than 100 mutations in *parkin* have been reported, accounting for up to 50% of the cases of familial, early-onset PD compatible with recessive inheritance and around 15% of early onset sporadic cases [43]. The average onset age is in the early 30s in most patients, and only very few late-onset cases have been described up to 70 years of age. Clinically, the patients with *parkin* mutations have good and prolonged response to levodopa. Motor fluctuations- and levodopa-induced dyskinesias are frequently and early observed, whereas marked cognitive or vegetative disturbances are rare [44]. Notably, about 50% of the mutations present in the *parkin* are point mutations detectable by sequencing, while the remaining 50% consists of large genomic deletions or multiplications, which are only detectable by gene-dosage assays [43,45]. The *parkin* gene encodes a protein with ubiquitin-ligase E3-activity [46], which is abolished by the disease-causing mutations, in keeping with a loss-of-function mechanism (as usually evident in autosomal recessive diseases). Covalent attachment of multiple copies of the ubiquitin protein (poly-ubiquitylation) tags proteins for proteasomal degradation. Furthermore, mono-ubiquitylation is involved in other cell processes, such as regulation of gene expression and protein sorting. Therefore, loss of parkin

function might lead to the accumulation of non-ubiquitylated substrates in the brain of patients with parkin mutations [5]. Parkin was shown to localize within the mitochondria of proliferating cells and has been shown to play a role in mitochondrial biogenesis by regulating both transcription and replication of mitochondrial DNA [47]. *Parkin* knockout mice exhibit nigrostriatal deficits in the absence of nigral degeneration, and decreased expression of a number of proteins involved in the protection against oxidative stress [23,48].

Mutations in *PINK1* are a less common cause of autosomal recessive, early-onset parkinsonism, and account for up to ~1-7% of early onset cases in different studies [41,49,50]. The PINK1 protein contains a kinase domain and a mitochondrial targeting peptide, and it localizes (at least in part) to the mitochondria [41]. Elegant studies using transgenic Drosophila models showed that the parkin and PINK1 proteins are functionally linked, with PINK1 acting upstream of parkin in the same neuroprotective pathway [51,52,53]. More recently, PINK1 has been shown to be able to recruit parkin to damaged mitochondria, in order to induce the degradation of these organelles by autophagy (mitophagy) [54]. These findings support the view that the same molecular pathways underlie different forms of recessive, early-onset parkinsonisms, and the dynamic interplay between mitochondrial biogenesis and destruction by autophagy is taking a central place in this scenario [55,56].

Mutations in the *DJ-1* gene cause a third, rare form of autosomal recessive parkinsonism, and are found in ~1-2% of early onset cases [42,57,58]. The DJ-1 protein has antioxidant properties, and depletion of DJ-1 in neuronal cell lines accelerated cell death induced by oxidative stress [59]. The Drosophila *DJ-1* knock-out models display sensitivity to toxins such as paraquat and rotenone. Moreover, inactivation of Drosophila *DJ-1* results in accumulation of reactive oxygen species and dopaminergic neurons degeneration [60,61]. Whether autophagic abnormalities are also involved in the patients with *DJ-1* mutations remains unclear [62,63].

Mutations in the *ATPase type 13 A2* (*ATP13A2*), *phospholipase A2, group VI (PLA2G6*), and *F-box only protein 7* (*FBXO7*) can cause early onset recessive parkinsonism, which is usually complicated by additional symptoms, in varying combinations, including: dystonias, pyramidal signs, oculomotor disturbances, and cognitive decline. The phenotype associated with mutations in *ATP13A2* is characterized by early-onset parkinsonian syndrome associated with pyramidal

signs, dementia and supranuclear gaze palsy (this combination is also termed 'Kufor-Rakeb syndrome') [64,65]. The *ATP13A2* gene encodes a large transmembrane lysosomal protein with ATPase activity. Thus, lysosomal dysfunctions, due to the loss of the ATP13A2 function, are involved in the pathogenesis of this form [65].

Recessive mutations in *PLA2G6* were initially described as the cause of infantile neuroaxonal dystrophy and neurodegeneration with brain iron accumulation [66]. However, mutations in *PLA2G6* were later reported in patients with adult-onset dystonia-parkinsonism with pyramidal signs and cognitive disturbances (also termed PARK14). Intriguingly, brain MRI showed generalized brain atrophy without iron accumulation [67]. The disease onset might occur from childhood to early adulthood, and brain pathology studies showed widespread α-synuclein positive Lewy bodies, particularly severe in the neocortex [68], suggesting further mechanistic links between this rare monogenic disease and the typical, late-onset PD forms.

The *FBXO7* gene and its phenotype

Mutations in the *F-box only protein 7* gene (*FBXO7*) cause PARK15, an autosomal recessive neurodegenerative disease presenting with juvenile-onset, severe levodopa-responsive parkinsonism and pyramidal disturbances [69,70]. This phenotype resembles closely the pallido-pyramidal syndrome (PPS). The combination of JP and pyramidal tract dysfunctions was first described by Charles Davison in 1954 in five patients [71]. Post-mortem examination in those patients revealed abnormalities at the level of the pallidum, substantia nigra, and the corticospinal tract. The term pallido-pyramidal syndrome (PPS) was therefore introduced [71]. Since then, other patients with a similar presentation were reported over the years, usually with juvenile onset, familial aggregation, and frequent parental consanguinity, suggesting an autosomal recessive mechanism of inheritance [70,72,73,74]. The progression of the parkinsonian symptoms in these patients might be relatively slow, and the signs of parkinsonism might develop as a late feature in some familial cases presenting with pyramidal disturbances (spasticity, hyperactive tendon reflexes, and Babinski sign) [69]. Of note, the response to levodopa therapy is usually remarkable and sustained, but it is often limited by severe dyskinesias and psychiatric side effects [69,70,75]. The dramatic abnormality of the nigrostriatal dopaminergic terminals detected in some patients using DaTSCAN-SPECT, the beneficial effects of levodopa and the presence of levodopa-induced dyskinesias

indicate that a dopaminergic lesion at the level of the substantia nigra (rather than the globus pallidum) underlies the parkinsonism in these patients [70]. “Parkinsonian-pyramidal” syndrome appears therefore more appropriate than the older “pallido-pyramidal” syndrome, when referring to this entity [70].

The molecular characterization of these forms gained momentum with the recent identification of one Iranian kindred with PPS [69]. Of note, in the affected members of this family the first clinical signs included pyramidal signs such as spastic weakness and Babinski signs, rather than parkinsonism. However, five to twenty years after the appearance of pyramidal symptoms, three out of ten patients developed parkinsonism; levodopa therapy was administered in one of these patients, with good and sustained response [69]. Genome-wide analysis in the Iranian family yielded linkage to chromosome 22, and a homozygous missense mutation in the *FBXO7* gene was proposed as the disease cause [69]. Different mutations in the same gene were later identified in our laboratory in two Caucasian families with an overlapping phenotype of autosomal recessive, juvenile parkinsonism with pyramidal signs [70]. Compound heterozygous mutations (IVS7+1G/T and T22M) were detected in the patients of one Dutch family, while a homozygous truncating mutation (R498X) was found in the patients of one Italian family [70]. Together with the findings in the Iranian pedigree, our data provided conclusive evidence that *FBXO7* mutations are the cause of a novel genetic disease, which was termed PARK15 (monogenic parkinsonism, type 15). More recently, the same R498X truncating mutation was detected as the cause of disease in patients from two additional families, originating from Pakistan and Turkey [75].

The FBXO7 protein

FBXO7 is a member of the F-box-containing protein family, characterized by a 50 amino acids domain, the “F-box” which usually mediates protein-protein interactions [76,77,78,79]. Proteins carrying the F-box motif are evolutionarily conserved, and present in various species such as yeast, plants, nematodes, flies, and humans. In mammals, 47 F-box proteins are known, and they are divided into three major classes according to their specific interaction domain present in addition to the F-box [76,77]. The “FBXW” proteins contain WD40 repeats [80], while the “FBXL” proteins contain leucine-rich repeats [81]. The remaining class of F-box proteins includes members with no other, or unclassified domains, thus they are termed FBXO, while “O” in FBXO refers to “other” domains [82]. The F-box proteins serve as molecular scaffolds in the

formation of larger protein complexes, and they have been implicated in a range of processes, such as cell cycle, genome stability, development, synapse formation, and circadian rhythms [83]. By binding to the Skp1 protein, the F-box proteins are recruited to SCF (Skp-Cullin1-F-box)-type of E3 ubiquitin ligases. Skp1 also interacts with the scaffold protein Cullin1 at its N terminus, while the C terminus of Cul1 binds to an E2 enzyme. Through this interaction, the SCF-type E3 ubiquitin ligases transfer ubiquitin from E2 to a specific substrate. The F-box proteins provide therefore the substrate specificity. Accordingly, the FBXO7 protein is thought to act as a conventional SCF adaptor [84,85], promoting ubiquitination of substrate proteins. The exact cellular function of the FBXO7 protein remains unknown, but two proteins, the hepatoma up-regulated protein (HURP) and the cellular inhibitor of apoptosis 1 (cIAP1) have been proposed to be substrates of FBXO7 [86,87].

A further complexity is due to the fact that in humans, two *FBXO7* transcripts are expressed as a result of the usage of alternatively spliced 5'-exons (Figure 2). These transcripts encode two FBXO7 protein isoforms of 522 and 443 amino acids (also referred to as isoform 1 and isoform 2). The FBXO7 isoform 1 is longer than isoform 2 because of the presence of an N-terminal ubiquitin-like (Ubl) domain. The remaining domains are present in both isoforms, including an FP (FBXO7/PI31) domain, the F-box domain, and a C-terminal proline-rich region (PRR). The FP domain mediates the interaction of FBXO7 with the proteasome inhibitor protein PI31 [88], while the C-terminal PRR region serves as protein-protein interaction domain and appears to be crucial for the binding of FBXO7 to specific substrates.

There is evidence that the FBXO7 proteins are localized in both the cytoplasm and the nucleus of the cell [89]. More recently, a functional leucine-rich nuclear export sequence (NES) was identified in the F-box domain, and the subcellular localization of FBXO7 was shown to be regulated by the competitive interaction of FBXO7 between Skp1 and the nuclear export protein exportin 1 (CRM1) [90]. According to this model, the binding to Skp1 prevents FBXO7 from contacting CRM1, leading to the accumulation of FBXO7 in the nucleus [90]. Moreover, FBXO7 has been shown to be able to directly interact with the cell cycle regulators p27 and cyclin-dependent kinase 6 (CDK6), in order to enhance the assembly of cyclin D/CDK6 complexes and increase CDK6 activity [91,92].

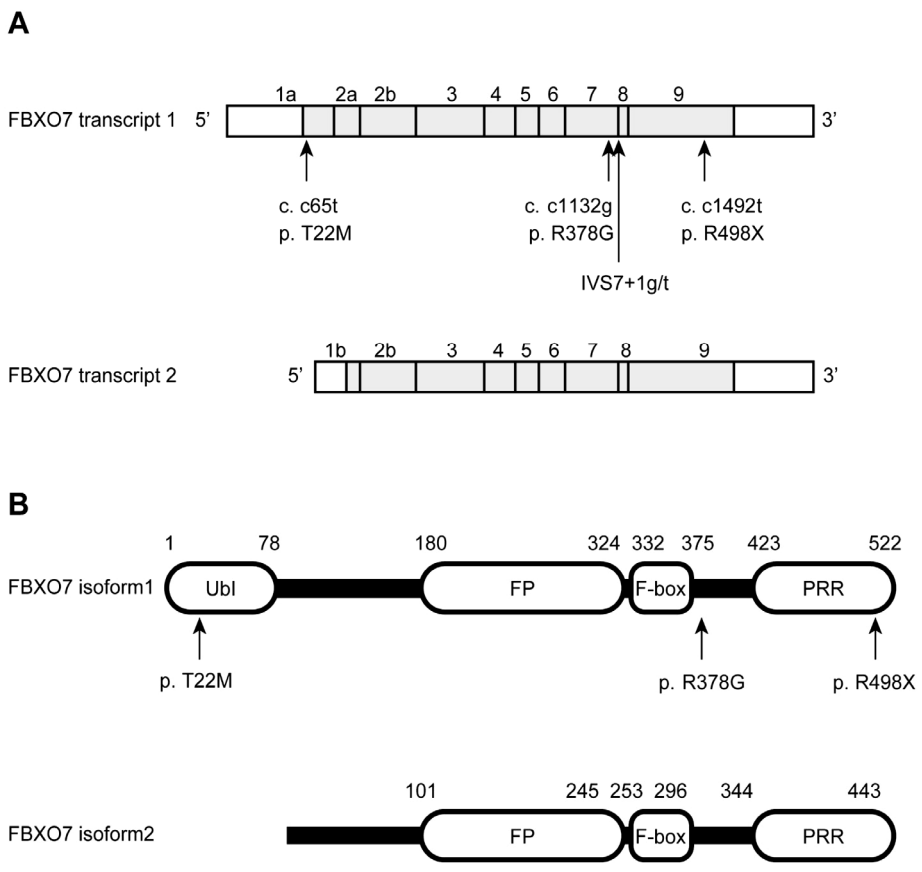

Figure 2 Schematic representation of the *FBXO7* transcripts and protein isoforms.
(A) The *FBXO7* transcripts with location of the mutations found in patients with PARK15.
(B) Domain organization of the two FBXO7 protein isoforms.
Ubl: ubiquitin-like domain; FP: FBXO7/ PI31 domain; F-box: F-box motif; PRR: proline rich domain.

The over-expression of FBXO7 causes CDK6-dependent transformation of immortalized fibroblasts. Furthermore, increased expression of FBXO7 has been detected in human lung cancer and colon carcinomas, and FBXO7 has been proposed to act as a proto-oncogene [91]. However, a different study found no transforming properties of FBXO7 despite high levels of CDK6 in haematopoietic pro-B cells. In mouse, the depletion of the Fbxo7 protein yielded increased levels of precursor pro-B cells and pro-erythroblasts, indicating that FBXO7 has anti-proliferative functions and a cell-cycle-independent role in promoting maturation of precursor cells [93]. Furthermore, FBXO7 has been reported as a negative regulator of the nuclear factor κB (NF-κB) signaling. The NF-κB signal

pathway is activated by tumor necrosis factors-α (TNFα) stimulation and is highly dependent on ubiquitination events. As the components of TNF receptor 1 signaling complex, FBXO7 can bind to either cIAP1 or TNF receptor-associated factor 2, and promote ubiquitination of both proteins, which in turn attenuates the ubiquitination of receptor interacting protein 1 and negatively regulates NF-κB signaling [94].

Modelling PD in Zebrafish

An ideal animal model of PD should reproduce the progressive loss of dopaminergic (DA) neurons pathologically as well as the motor clinical phenotype. Several rodent and non-human primate models of PD have been generated either by administering neurotoxins or by genetic manipulation (transgenic and knockout). These models have provided significant contributions towards a better understanding of the pathogenic mechanisms of PD [95]. However, murine or non-human primate models often are expensive and time-consuming. Disease modelling using Zebrafish has recently become an attractive alternative.

The zebrafish (*Danio rerio*) are vertebrates and thus they are much closer to humans than invertebrate model organisms, such as Drosophila or Caenorhabditis elegans. Due to the availability of a sequenced genome, annotated gene expression atlas, and tools for genetic manipulation (cloning, mutagenesis, and transgenesis) the zebrafish has recently become a powerful model to study human diseases [96,97,98]. Zebrafish are widely used for studying developmental biology because of high fecundity (a few hundred eggs per spawning), external fertilization, transparent embryos and quick development. Transparent embryos enable zebrafish to be visualized and manipulated easily. Moreover, after just 24 hours, the zebrafish can develop from a single cell to a multicellular embryo with differentiated tissues and recognizable organs. Within 5 days of development, larvae are mobile and foraging. The overall generation time of zebrafish is only 2-3 months. Another advantage is that the zebrafish embryos are permeable to small molecules, rendering them convenient for drug screen and chemical toxicity test [99].

Zebrafish genomics

Over the last decade, it has become apparent that all vertebrates have a similar sets of genes, and that biochemical and developmental pathways are highly conserved [100]. The current assembly of the zebrafish genome (Zv9) spans

~1.5 Gb and contains approximately 18,000 genes distributed in 25 chromosomes (http://www.ensembl.org/Danio_rerio). Interestingly, the zebrafish genome contains orthologues for almost all human genes. With the completed sequence of the zebrafish genome, approximately 12,000 expression units have been characterized and annotated, allowing the rapid identification of the orthologues related to human diseases [101]. The Zebrafish Information Network database (www.zfin.org) provides the opportunity to systematically search for gene and miRNA expression patterns [102]. Novel published expression patterns are continually added into the database [103,104]. Additionally, large scale mutagenesis screens have been successfully performed in zebrafish, leading to the identification of hundreds of essential genes for vertebrate development [105,106,107,108,109]. Recently, some of these screens were targeted to the nervous system and yielded phenotypes of relevance for human disease [110,111]. A large number of gene mutants were identified, which are relevant for the development of the forebrain, the spinal cord, and the cerebellum [112,113].

The rapid development in molecular technologies allows us to create genetically modified zebrafish models that mimic pathogenic processes, with the ultimate goal of discovering therapeutic targets and strategies. Different strategies are available to obtain gene-silencing in zebrafish, either temporarily by morpholino injection during the early stages of the embryonic development (transient knockdown), or permanently by establishing stable knockout lines through the so-called TILLING (Targeting Induced Local Lesions In Genomes) method [114,115].

The injection of morpholinos (MOs) is the most widely used technique for transient gene knockdown in zebrafish [116]. MOs are synthetic oligonucleotides of the length of about 25 bases. They are similar to DNA and RNA oligonucleotides, except that the morpholino ring replaces the deoxyribose/ribose ring, and a non-ionic phosphorodiamidate linkage replaces the anionic phosphodiester bond [117]. Compared with conventional oligonucleotides, MOs offer therefore the advantages of being more stable, due to resistance to nucleases. Moreover, MOs do not carry a negatively charged backbone, which enables less interaction with other components of the cell and makes them less toxic. Furthermore, the neutral charge and relatively small size allows MO to quickly diffuse throughout the embryo after microinjection [118].

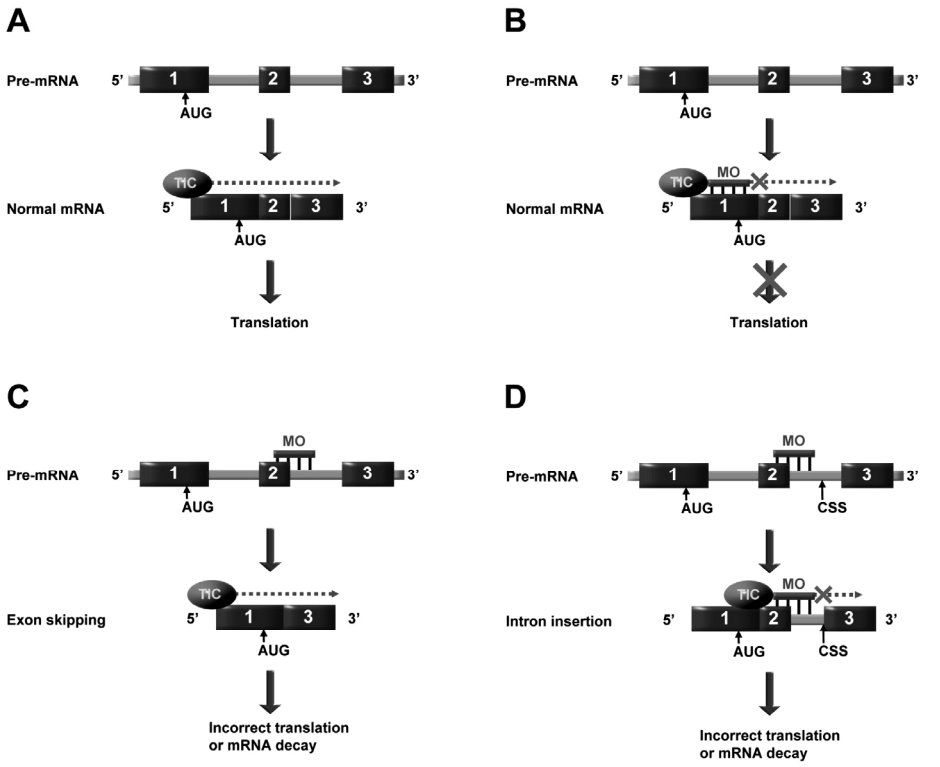

Figure 3 Strategies for MO-mediated gene knockdown.
(A) Normal transcription and translation.
(B) MO is designed to target the 5'-UTR near the translational start site in order to block protein translation.
(C and D) MOs are designed to target the exon-intron boundary to alter pre-mRNA splicing, leading to exon skipping (C) or intron insertion (D).

There are two strategies for MO-mediated gene knockdown in zebrafish (Figure 3). In the first strategy MOs are designed to target the 5'-untranslated region (UTR) of the mRNA near the translational start site in order to block protein translation [119]. In the second strategy, MOs are designed to target the exon-intron boundary, to inhibit the pre-mRNA splicing [120,121]. The MOs are usually injected into single-cell embryos immediately after fertilization, which leads to efficient gene knockdown during the early stages of development.

The specificity of MO-mediated gene knock down is an important issue in zebrafish models, because non-specific MO toxicity, or off-target effects might be often encountered, which are usually caused by the activation of p53-

mediated apoptosis [122,123]. Non-specific MO effects might also cause neuronal death, complicating the interpretation of the neurodegenerative phenotypes observed in zebrafish models. A possible way to control for the above-mentioned nonspecific effects, involves the co-injection of p53-targeting MOs. Furthermore, control MOs (targeting random sequences or containing 5-bases mismatch compared to the target sequence), are often also used. The phenotypes observed with the control MOs are then compared with those induced by gene-targeting MO injection. In addition, a good evidence of MOs specificity is provided when the same phenotype is produced by using two different MOs (one targeting to ATG translation site, and one targeting splicing sites of the same gene), because MOs with different sequences will less likely induce the same non-specific phenotype. In principle, the best evidence in support for the specificity of the MO effects comes from rescuing the phenotypes by injecting the mRNA of the specific gene of interest. However, specific time and/or localization is crucial for many proteins to perform their proper function. It is sometimes very difficult or impossible to accurately reproduce the time course and cell-specific expression pattern of endogenous transcripts by over-expressing exogenous mRNAs. This explains why some real, specific MO effects are not rescued, and this is a well-known phenomenon in zebrafish MO-mediated modelling [121]. Because of the inherent problems and limitations of the MO approach, a new technique known as TILLING has been developed in order to knock out genes permanently in zebrafish. TILLING is a reverse genetic strategy that identifies specific mutations in a gene of interest from chemically mutagenized fish libraries [114,115]. This approach is now well established for the generation of stable mutant lines, but it is limited by the size of the available libraries and the high throughput of the screening methodologies required.

The dopaminergic system in zebrafish

The zebrafish central nervous system is well developed after only 4-5 days post-fertilization, enabling the larvae to perform complex behaviors such as swimming and hunting. The zebrafish central nervous system is conventionally divided into the spinal cord, hindbrain, midbrain and forebrain. Although the structure and scale of the brain are different between zebrafish and humans, the overall organization is similar since some specific regions of the zebrafish brain are often strikingly conserved and relevant to their human counterparts. The dopaminergic (DA) system is well characterized in both embryos and adult zebrafish. Similar to any other vertebrates, zebrafish DA neurons have been described mainly in the olfactory bulb, preoptic region, pretectum, retina, and

ventral diencephalon [97,124,125,126,127]. DA neurons are first detected between 18 and 19 h post fertilization (hpf) in the posterior tuberculum of the ventral diencephalon (vDC), and this cluster of neurons represent the DA system ascending to the striatum, comparable to the nigrostriatal system in human [128,129]. Recent studies revealed important function of DA neurons in the regulation of the motor behaviour in larval and adult zebrafish [130,131].

In the central nervous system the catecholaminergic systems include essentially the DA and noradrenergic (NA) neurons [132,133]. In addition to the tyrosine hydroxylase (TH), NA neurons express the dopamine beta-hydroxylase (DBH) enzyme, which converts dopamine to norepinephrine. TH is the rate-limiting enzyme in the catecholamine synthesis since it catalyzes the transformation of L-tyrosine into L-DOPA (the precursor of dopamine) at the first step of the biosynthesis, and TH is routinely used as the marker to visualize both DA and NA neurons [132,134,135]. Early during the evolution of the vertebrates, two paralogous tyrosine hydroxylase genes, *th1* and *th2*, emerged as a result of a duplication of the ancestral *th* gene [136,137]. *Th1* gene is an orthologue of the mammalian *TH* gene, while *th2* sequence form a separate clade from *th1.* More abundant th2 expression was detected in liver, kidney, heart, and gills [134]. Furthermore, *th1* and *th2* display different expression profiles in the zebrafish brain. Th1 is expressed in DA neurons of telencephalon and the NA neurons of hindbrain, whereas the localization of th2 is restricted to diencephalon with more abundant expression in the hypothalamus [137]. Th2 expression in brain development is later than th1, since th2 is poorly detected during embryonic stages but highly expressed in the juvenile brain, suggesting that th1 expressing neurons may provide dopaminergic activity during the embryonic development of brain, while th2 contributes more to DA synthesis at juvenile or adult stage [138].

Due to its specific expression in DA neurons, the dopamine transporter gene (*dat*, *slc6a3*) is often used as a more appropriate marker of DA neurons [128,139,140]. The genomic structure of this gene is highly conserved between human and zebrafish [127]. The dopamine transporter protein (DAT) mediates the reuptake of dopamine from the synaptic cleft into the presynaptic terminal in order to regulate the intensity and duration of DA signalling at synapses [141]. Recently, a transgenic *dat:eGFP* (enhanced green fluorescent protein) zebrafish line was generated, with eGFP expressed under the control of cis-regulatory elements of the *dat* gene. Therefore, in this line DA neurons labelled with eGFP

can be directly visualized under the microscope in the ventral diencephalon [142].

Current zebrafish models of PD

As mentioned above, the zebrafish ventral diencephalic DA neurons are functionally homologous to the substantia nigra in the human brain. Furthermore, the orthologues of some human PD-related genes, including *LRRK2*, *parkin*, *DJ-1*, and *PINK1*, have been identified in zebrafish. Knockdown of each of these genes has recently been developed, establishing the zebrafish as a novel and useful model organism for studying the pathogenesis of PD [129,143,144,145,146,147].

Parkin is thought to play critical roles in mitochondrial function together with the products of other PD related genes such as *PINK1* and *DJ-1*. The zebrafish *parkin* gene encodes a protein of 458 amino acids, which is highly conserved between zebrafish and humans, with 62% identity in its functional domains. MO-mediated *parkin* knockdown caused the loss of th^+ neurons in the vDC, and it also decreased the activity of the mitochondrial respiratory chain complex I. These features are consistent with those seen in patients with *parkin* mutations [144]. A similar neuronal loss was not observed in another study, but *parkin* overexpression in zebrafish prevented the cell death induced by proteotoxic stress, supporting a neuroprotective activity of the parkin protein [148].

The zebrafish Pink1 protein displays 54% amino acid identity to its human orthologue. An initial study reported severe developmental phenotypes accompanied with ~40% reduction in the number of th^+ neurons, in MO-mediated *Pink1* knockdown zebrafish [149]. Other groups have been unable to detect gross alterations in the number of DA neurons in the vDC. However, they did report aberrant patterning of the DA neurons, and these neurons were more susceptible to the toxicity of MPTP. Furthermore, *Pink1* knock down morphants showed impaired response to tactile stimuli and reduced swimming locomotor [150,151]. Similar to *parkin*, the *Pink1* knockdown also induced mitochondrial defects such as loss of cristae and a reduced number of mitochondria, supporting the contention that pink1 and parkin work together in the same mitochondrial pathway, as previously described in the Drosophila models [51,52,97].

The zebrafish dj-1 protein is expressed throughout the embryogenesis and ubiquitously in all adult tissues with particular abundance in the brain. The zebrafish dj-1 displays 83% of amino acid identity with its human homologue [152,153]. *Dj-1* knockdown using MO did not affect the number of DA neurons, but increased the susceptibility of DA neurons to the pro-oxidant hydrogen peroxide and the proteasome inhibitor MG132. In combination with MG132 exposure, the dj-1 depletion caused a marked loss of DA neurons, which was rescued by pharmacological inhibitors of apoptosis [123,153].

The zebrafish orthologue of human LRRK2 also displays a highly conserved amino acid sequence. In a first study, the deletion of the C-terminal WD40 domain of lrrk2 caused a significant loss of vDC DA neurons and PD-like locomotor defects [147]. However, these phenotypes were not reproduced by another group using the same MOs and the same zebrafish line [154]. Last, an ortholog of *α-synuclein* has not been identified in zebrafish. However, the other synuclein family members such as β- and γ-synuclein are expressed widely in DA neurons, and the effects of their knockdown suggest that these proteins are necessary for the maintenance of the DA function and normal locomotion in zebrafish [155].

Using zebrafish as a model for studying neurodegenerative disease is a relatively new concept, but rapid improvements in the genetic manipulation have already produced a large number of transgenic and mutant lines of biomedical relevance. The zebrafish has been established as a powerful model for studying neurodegenerative disease, including Parkinson's, Huntington's, and Alzheimer's disease [96,97,98]. Furthermore, the same zebrafish models can now be used to rapidly screen for modifier genes, and for disease-modifying therapeutic compounds [99].

Scope of the thesis

The work described in this thesis is aimed to study the role of FBXO7 proteins in early-onset Parkinsonism. In **Chapter 2**, we characterize pathogenic mutations in the *FBXO7* gene in two families with early-onset, progressive parkinsonism and pyramidal tract dysfunctions. This work provided the conclusive evidence that *FBXO7* is the disease-causing gene in this newly-identified autosomal recessive form, which we termed PARK15.

Very little was known about the two protein isoforms, which are predicted to be encoded by *FBXO7*, and nothing was known about their expression in the human brain. In **Chapter 3**, we describe the characterization of these proteins in normal human cells and the consequences of mutations in cells derived from PARK15 patients. In parallel with the above-mentioned *in vitro* experiments, in **Chapter 4** we report the development of the first *in vivo* model of PARK15 by transient, morpholino-mediated knockdown of the homologous gene *Fbxo7* in zebrafish. This model displays both the pathologic and behavioral hallmarks of human parkinsonism (dopaminergic neuronal loss and dopamine-dependent bradykinesia), representing therefore a valid tool for investigating the mechanisms of selective dopaminergic neuronal death. Last, in **Chapter 5**, we describe the expression of the FBXO7 proteins in the brain of normal human subjects and of PD patients, and we report the presence of FBXO7 immunoreactivity in the Lewy bodies. The last part, **Chapter 6**, contains a general discussion of the above-mentioned studies, and some perspectives for future investigations.

REFERENCES

1. de Lau LM, Breteler MM (2006) Epidemiology of Parkinson's disease. Lancet Neurol 5: 525-535.
2. Fahn S (2003) Description of Parkinson's disease as a clinical syndrome. Ann N Y Acad Sci 991: 1-14.
3. Jankovic J (2008) Parkinson's disease: clinical features and diagnosis. J Neurol Neurosurg Psychiatry 79: 368-376.
4. Cookson MR, Bandmann O (2010) Parkinson's disease: insights from pathways. Hum Mol Genet 19: R21-27.
5. Corti O, Lesage S, Brice A (2011) What genetics tells us about the causes and mechanisms of Parkinson's disease. Physiol Rev 91: 1161-1218.
6. Poewe W (2009) Treatments for Parkinson disease--past achievements and current clinical needs. Neurology 72: S65-73.
7. Fox SH, Katzenschlager R, Lim SY, Ravina B, Seppi K, et al. (2011) The Movement Disorder Society Evidence-Based Medicine Review Update: Treatments for the motor symptoms of Parkinson's disease. Mov Disord 26 Suppl 3: S2-41.
8. Chaudhuri KR, Odin P, Antonini A, Martinez-Martin P (2011) Parkinson's disease: the non-motor issues. Parkinsonism Relat Disord 17: 717-723.
9. Seppi K, Weintraub D, Coelho M, Perez-Lloret S, Fox SH, et al. (2011) The Movement Disorder Society Evidence-Based Medicine Review Update: Treatments for the non-motor symptoms of Parkinson's disease. Mov Disord 26 Suppl 3: S42-80.
10. Jellinger KA (2012) Neuropathology of sporadic Parkinson's disease: evaluation and changes of concepts. Mov Disord 27: 8-30.
11. Tolosa E, Wenning G, Poewe W (2006) The diagnosis of Parkinson's disease. Lancet Neurol 5: 75-86.
12. Braak H, Ghebremedhin E, Rub U, Bratzke H, Del Tredici K (2004) Stages in the development of Parkinson's disease-related pathology. Cell and tissue research 318: 121-134.
13. Tofaris GK, Spillantini MG (2005) Alpha-synuclein dysfunction in Lewy body diseases. Movement disorders : official journal of the Movement Disorder Society 20 Suppl 12: S37-44.
14. Schrag A, Schott JM (2006) Epidemiological, clinical, and genetic characteristics of early-onset parkinsonism. Lancet neurology 5: 355-363.

15. Schrag A, Ben-Shlomo Y, Quinn NP (2000) Cross sectional prevalence survey of idiopathic Parkinson's disease and Parkinsonism in London. BMJ 321: 21-22.
16. Golbe LI (1991) Young-onset Parkinson's disease: a clinical review. Neurology 41: 168-173.
17. Wickremaratchi MM, Ben-Shlomo Y, Morris HR (2009) The effect of onset age on the clinical features of Parkinson's disease. European journal of neurology : the official journal of the European Federation of Neurological Societies 16: 450-456.
18. Schrag A, Ben-Shlomo Y, Brown R, Marsden CD, Quinn N (1998) Young-onset Parkinson's disease revisited--clinical features, natural history, and mortality. Movement disorders : official journal of the Movement Disorder Society 13: 885-894.
19. Gasser T (2009) Molecular pathogenesis of Parkinson disease: insights from genetic studies. Expert Rev Mol Med 11: e22.
20. Olanow CW (2007) The pathogenesis of cell death in Parkinson's disease--2007. Mov Disord 22 Suppl 17: S335-342.
21. Gupta A, Dawson VL, Dawson TM (2008) What causes cell death in Parkinson's disease? Ann Neurol 64 Suppl 2: S3-15.
22. Langston JW, Ballard P, Tetrud JW, Irwin I (1983) Chronic Parkinsonism in humans due to a product of meperidine-analog synthesis. Science 219: 979-980.
23. Bogaerts V, Theuns J, van Broeckhoven C (2008) Genetic findings in Parkinson's disease and translation into treatment: a leading role for mitochondria? Genes, brain, and behavior 7: 129-151.
24. Priyadarshi A, Khuder SA, Schaub EA, Priyadarshi SS (2001) Environmental risk factors and Parkinson's disease: a metaanalysis. Environmental research 86: 122-127.
25. Hancock DB, Martin ER, Stajich JM, Jewett R, Stacy MA, et al. (2007) Smoking, caffeine, and nonsteroidal anti-inflammatory drugs in families with Parkinson disease. Archives of neurology 64: 576-580.
26. Bonifati V (2007) Genetics of parkinsonism. Parkinsonism Relat Disord 13 (Suppl 3): S233-S241.
27. Polymeropoulos MH, Lavedan C, Leroy E, Ide SE, Dehejia A, et al. (1997) Mutation in the alpha-synuclein gene identified in families with Parkinson's disease. Science 276: 2045-2047.
28. Nuytemans K, Theuns J, Cruts M, Van Broeckhoven C (2010) Genetic etiology of Parkinson disease associated with mutations in the SNCA,

PARK2, PINK1, PARK7, and LRRK2 genes: a mutation update. Human mutation 31: 763-780.
29. Spillantini MG, Schmidt ML, Lee VM, Trojanowski JQ, Jakes R, et al. (1997) Alpha-synuclein in Lewy bodies. Nature 388: 839-840.
30. Spillantini MG, Goedert M (2000) The alpha-synucleinopathies: Parkinson's disease, dementia with Lewy bodies, and multiple system atrophy. Ann N Y Acad Sci 920: 16-27.
31. Conway KA, Harper JD, Lansbury PT (1998) Accelerated in vitro fibril formation by a mutant alpha-synuclein linked to early-onset Parkinson disease. Nature medicine 4: 1318-1320.
32. Lesage S, Durr A, Tazir M, Lohmann E, Leutenegger AL, et al. (2006) LRRK2 G2019S as a cause of Parkinson's disease in North African Arabs. N Engl J Med 354: 422-423.
33. Ozelius LJ, Senthil G, Saunders-Pullman R, Ohmann E, Deligtisch A, et al. (2006) LRRK2 G2019S as a cause of Parkinson's disease in Ashkenazi Jews. N Engl J Med 354: 424-425.
34. Bonifati V (2007) LRRK2 low-penetrance mutations (Gly2019Ser) and risk alleles (Gly2385Arg)-linking familial and sporadic Parkinson's disease. Neurochem Res 32: 1700-1708.
35. Di Fonzo A, Wu-Chou YH, Lu CS, van Doeselaar M, Simons EJ, et al. (2006) A common missense variant in the LRRK2 gene, Gly2385Arg, associated with Parkinson's disease risk in Taiwan. Neurogenetics 7: 133-138.
36. Guo L, Gandhi PN, Wang W, Petersen RB, Wilson-Delfosse AL, et al. (2007) The Parkinson's disease-associated protein, leucine-rich repeat kinase 2 (LRRK2), is an authentic GTPase that stimulates kinase activity. Exp Cell Res 313: 3658-3670.
37. Lewis PA, Greggio E, Beilina A, Jain S, Baker A, et al. (2007) The R1441C mutation of LRRK2 disrupts GTP hydrolysis. Biochem Biophys Res Commun 357: 668-671.
38. Liu M, Dobson B, Glicksman MA, Yue Z, Stein RL (2010) Kinetic mechanistic studies of wild-type leucine-rich repeat kinase 2: characterization of the kinase and GTPase activities. Biochemistry 49: 2008-2017.
39. Lin X, Parisiadou L, Gu XL, Wang L, Shim H, et al. (2009) Leucine-rich repeat kinase 2 regulates the progression of neuropathology induced by Parkinson's-disease-related mutant alpha-synuclein. Neuron 64: 807-827.

40. Kitada T, Asakawa S, Hattori N, Matsumine H, Yamamura Y, et al. (1998) Mutations in the parkin gene cause autosomal recessive juvenile parkinsonism. Nature 392: 605-608.
41. Valente EM, Abou-Sleiman PM, Caputo V, Muqit MM, Harvey K, et al. (2004) Hereditary early-onset Parkinson's disease caused by mutations in PINK1. Science 304: 1158-1160.
42. Bonifati V, Rizzu P, van Baren MJ, Schaap O, Breedveld GJ, et al. (2003) Mutations in the DJ-1 gene associated with autosomal recessive early-onset parkinsonism. Science 299: 256-259.
43. Lucking CB, Durr A, Bonifati V, Vaughan J, De Michele G, et al. (2000) Association between early-onset Parkinson's disease and mutations in the parkin gene. The New England journal of medicine 342: 1560-1567.
44. Bonifati V (2012) Autosomal recessive parkinsonism. Parkinsonism & related disorders 18 Suppl 1: S4-6.
45. Hedrich K, Eskelson C, Wilmot B, Marder K, Harris J, et al. (2004) Distribution, type, and origin of Parkin mutations: review and case studies. Mov Disord 19: 1146-1157.
46. Shimura H, Hattori N, Kubo S, Mizuno Y, Asakawa S, et al. (2000) Familial Parkinson disease gene product, parkin, is a ubiquitin-protein ligase. Nat Genet 25: 302-305.
47. Kuroda Y, Mitsui T, Kunishige M, Shono M, Akaike M, et al. (2006) Parkin enhances mitochondrial biogenesis in proliferating cells. Human molecular genetics 15: 883-895.
48. Palacino JJ, Sagi D, Goldberg MS, Krauss S, Motz C, et al. (2004) Mitochondrial dysfunction and oxidative damage in parkin-deficient mice. The Journal of biological chemistry 279: 18614-18622.
49. Tan EK, Yew K, Chua E, Puvan K, Shen H, et al. (2006) PINK1 mutations in sporadic early-onset Parkinson's disease. Movement disorders : official journal of the Movement Disorder Society 21: 789-793.
50. Bonifati V, Rohe CF, Breedveld GJ, Fabrizio E, De Mari M, et al. (2005) Early-onset parkinsonism associated with PINK1 mutations: frequency, genotypes, and phenotypes. Neurology 65: 87-95.
51. Clark IE, Dodson MW, Jiang C, Cao JH, Huh JR, et al. (2006) Drosophila pink1 is required for mitochondrial function and interacts genetically with parkin. Nature 441: 1162-1166.
52. Park J, Lee SB, Lee S, Kim Y, Song S, et al. (2006) Mitochondrial dysfunction in Drosophila PINK1 mutants is complemented by parkin. Nature 441: 1157-1161.

53. Yang Y, Gehrke S, Imai Y, Huang Z, Ouyang Y, et al. (2006) Mitochondrial pathology and muscle and dopaminergic neuron degeneration caused by inactivation of Drosophila Pink1 is rescued by Parkin. Proc Natl Acad Sci U S A 103: 10793-10798.
54. Narendra DP, Jin SM, Tanaka A, Suen DF, Gautier CA, et al. (2010) PINK1 is selectively stabilized on impaired mitochondria to activate Parkin. PLoS biology 8: e1000298.
55. McCoy MK, Cookson MR Mitochondrial quality control and dynamics in Parkinson's disease. Antioxid Redox Signal 16: 869-882.
56. Deas E, Wood NW, Plun-Favreau H Mitophagy and Parkinson's disease: the PINK1-parkin link. Biochim Biophys Acta 1813: 623-633.
57. Bonifati V, Oostra BA, Heutink P (2004) Linking DJ-1 to neurodegeneration offers novel insights for understanding the pathogenesis of Parkinson's disease. J Mol Med (Berl) 82: 163-174.
58. Hedrich K, Djarmati A, Schafer N, Hering R, Wellenbrock C, et al. (2004) DJ-1 (PARK7) mutations are less frequent than Parkin (PARK2) mutations in early-onset Parkinson disease. Neurology 62: 389-394.
59. Yokota T, Sugawara K, Ito K, Takahashi R, Ariga H, et al. (2003) Down regulation of DJ-1 enhances cell death by oxidative stress, ER stress, and proteasome inhibition. Biochemical and biophysical research communications 312: 1342-1348.
60. Yang Y, Gehrke S, Haque ME, Imai Y, Kosek J, et al. (2005) Inactivation of Drosophila DJ-1 leads to impairments of oxidative stress response and phosphatidylinositol 3-kinase/Akt signaling. Proc Natl Acad Sci U S A 102: 13670-13675.
61. Meulener M, Whitworth AJ, Armstrong-Gold CE, Rizzu P, Heutink P, et al. (2005) Drosophila DJ-1 mutants are selectively sensitive to environmental toxins associated with Parkinson's disease. Current biology : CB 15: 1572-1577.
62. Burbulla LF, Krebiehl G, Kruger R Balance is the challenge--the impact of mitochondrial dynamics in Parkinson's disease. Eur J Clin Invest 40: 1048-1060.
63. Krebiehl G, Ruckerbauer S, Burbulla LF, Kieper N, Maurer B, et al. Reduced basal autophagy and impaired mitochondrial dynamics due to loss of Parkinson's disease-associated protein DJ-1. PLoS One 5: e9367.
64. Najim al-Din AS, Wriekat A, Mubaidin A, Dasouki M, Hiari M (1994) Pallido-pyramidal degeneration, supranuclear upgaze paresis and dementia: Kufor-Rakeb syndrome. Acta neurologica Scandinavica 89: 347-352.

65. Ramirez A, Heimbach A, Grundemann J, Stiller B, Hampshire D, et al. (2006) Hereditary parkinsonism with dementia is caused by mutations in ATP13A2, encoding a lysosomal type 5 P-type ATPase. Nature genetics 38: 1184-1191.
66. Morgan NV, Westaway SK, Morton JE, Gregory A, Gissen P, et al. (2006) PLA2G6, encoding a phospholipase A2, is mutated in neurodegenerative disorders with high brain iron. Nature genetics 38: 752-754.
67. Paisan-Ruiz C, Bhatia KP, Li A, Hernandez D, Davis M, et al. (2009) Characterization of PLA2G6 as a locus for dystonia-parkinsonism. Ann Neurol 65: 19-23.
68. Paisan-Ruiz C, Li A, Schneider SA, Holton JL, Johnson R, et al. (2012) Widespread Lewy body and tau accumulation in childhood and adult onset dystonia-parkinsonism cases with PLA2G6 mutations. Neurobiology of aging 33: 814-823.
69. Shojaee S, Sina F, Banihosseini SS, Kazemi MH, Kalhor R, et al. (2008) Genome-wide linkage analysis of a Parkinsonian-pyramidal syndrome pedigree by 500 K SNP arrays. Am J Hum Genet 82: 1375-1384.
70. Di Fonzo A, Dekker MC, Montagna P, Baruzzi A, Yonova EH, et al. (2009) FBXO7 mutations cause autosomal recessive, early-onset parkinsonian-pyramidal syndrome. Neurology 72: 240-245.
71. Davison C (1954) Pallido-pyramidal disease. J Neuropathol Exp Neurol 13: 50-59.
72. Horowitz G, Greenberg J (1975) Pallido-pyramidal syndrome treated with levodopa. J Neurol Neurosurg Psychiatry 38: 238-240.
73. Nisipeanu P, Kuritzky A, Korczyn AD (1994) Familial levodopa-responsive parkinsonian-pyramidal syndrome. Mov Disord 9: 673-675.
74. Remy P, Hosseini H, Degos JD, Samson Y, Agid Y, et al. (1995) Striatal dopaminergic denervation in pallidopyramidal disease demonstrated by positron emission tomography. Ann Neurol 38: 954-956.
75. Paisan-Ruiz C, Guevara R, Federoff M, Hanagasi H, Sina F, et al. (2010) Early-onset L-dopa-responsive parkinsonism with pyramidal signs due to ATP13A2, PLA2G6, FBXO7 and spatacsin mutations. Mov Disord 25: 1791-1800.
76. Cenciarelli C, Chiaur DS, Guardavaccaro D, Parks W, Vidal M, et al. (1999) Identification of a family of human F-box proteins. Curr Biol 9: 1177-1179.

77. Winston JT, Koepp DM, Zhu C, Elledge SJ, Harper JW (1999) A family of mammalian F-box proteins. Curr Biol 9: 1180-1182.
78. Ilyin GP, Rialland M, Pigeon C, Guguen-Guillouzo C (2000) cDNA cloning and expression analysis of new members of the mammalian F-box protein family. Genomics 67: 40-47.
79. Kipreos ET, Pagano M (2000) The F-box protein family. Genome Biol 1: REVIEWS3002.
80. Smith TF, Gaitatzes C, Saxena K, Neer EJ (1999) The WD repeat: a common architecture for diverse functions. Trends Biochem Sci 24: 181-185.
81. Kobe B, Kajava AV (2001) The leucine-rich repeat as a protein recognition motif. Curr Opin Struct Biol 11: 725-732.
82. Jin J, Cardozo T, Lovering RC, Elledge SJ, Pagano M, et al. (2004) Systematic analysis and nomenclature of mammalian F-box proteins. Genes Dev 18: 2573-2580.
83. Ho MS, Ou C, Chan YR, Chien CT, Pi H (2008) The utility F-box for protein destruction. Cell Mol Life Sci 65: 1977-2000.
84. Patton EE, Willems AR, Tyers M (1998) Combinatorial control in ubiquitin-dependent proteolysis: don't Skp the F-box hypothesis. Trends Genet 14: 236-243.
85. Skowyra D, Craig KL, Tyers M, Elledge SJ, Harper JW (1997) F-box proteins are receptors that recruit phosphorylated substrates to the SCF ubiquitin-ligase complex. Cell 91: 209-219.
86. Chang YF, Cheng CM, Chang LK, Jong YJ, Yuo CY (2006) The F-box protein Fbxo7 interacts with human inhibitor of apoptosis protein cIAP1 and promotes cIAP1 ubiquitination. Biochem Biophys Res Commun 342: 1022-1026.
87. Hsu JM, Lee YC, Yu CT, Huang CY (2004) Fbx7 functions in the SCF complex regulating Cdk1-cyclin B-phosphorylated hepatoma up-regulated protein (HURP) proteolysis by a proline-rich region. J Biol Chem 279: 32592-32602.
88. Kirk R, Laman H, Knowles PP, Murray-Rust J, Lomonosov M, et al. (2008) Structure of a Conserved Dimerization Domain within the F-box Protein Fbxo7 and the PI31 Proteasome Inhibitor. J Biol Chem 283: 22325-22335.
89. Zhao T, De Graaff E, Breedveld GJ, Loda A, Severijnen LA, et al. (2011) Loss of nuclear activity of the FBXO7 protein in patients with parkinsonian-pyramidal syndrome (PARK15). PLoS One 6: e16983.

90. Nelson DE, Laman H (2011) A Competitive binding mechanism between Skp1 and exportin 1 (CRM1) controls the localization of a subset of F-box proteins. The Journal of biological chemistry 286: 19804-19815.
91. Laman H, Funes JM, Ye H, Henderson S, Galinanes-Garcia L, et al. (2005) Transforming activity of Fbxo7 is mediated specifically through regulation of cyclin D/cdk6. Embo J 24: 3104-3116.
92. Laman H (2006) Fbxo7 gets proactive with cyclin D/cdk6. Cell Cycle 5: 279-282.
93. Meziane el K, Randle SJ, Nelson DE, Lomonosov M, Laman H (2011) Knockdown of Fbxo7 reveals its regulatory role in proliferation and differentiation of haematopoietic precursor cells. Journal of cell science 124: 2175-2186.
94. Kuiken HJ, Egan DA, Laman H, Bernards R, Beijersbergen RL, et al. (2012) Identification of F-box only protein 7 as a negative regulator of NF-kappaB signaling. Journal of cellular and molecular medicine.
95. Pienaar IS, Gotz J, Feany MB (2010) Parkinson's disease: insights from non-traditional model organisms. Prog Neurobiol 92: 558-571.
96. Bandmann O, Burton EA (2010) Genetic zebrafish models of neurodegenerative diseases. Neurobiol Dis 40: 58-65.
97. Xi Y, Noble S, Ekker M (2011) Modeling neurodegeneration in zebrafish. Curr Neurol Neurosci Rep 11: 274-282.
98. Kabashi E, Brustein E, Champagne N, Drapeau P (2011) Zebrafish models for the functional genomics of neurogenetic disorders. Biochim Biophys Acta 1812: 335-345.
99. Huang X, Nguyen AT, Li Z, Emelyanov A, Parinov S, et al. (2011) One step forward: the use of transgenic zebrafish tumor model in drug screens. Birth Defects Res C Embryo Today 93: 173-181.
100. King A (2009) Researchers find their Nemo. Cell 139: 843-846.
101. Postlethwait JH (2006) The zebrafish genome: a review and msx gene case study. Genome dynamics 2: 183-197.
102. Sprague J, Bayraktaroglu L, Bradford Y, Conlin T, Dunn N, et al. (2008) The Zebrafish Information Network: the zebrafish model organism database provides expanded support for genotypes and phenotypes. Nucleic acids research 36: D768-772.
103. Thisse C, Thisse B (2008) High-resolution in situ hybridization to whole-mount zebrafish embryos. Nature protocols 3: 59-69.

104. Thisse B, Heyer V, Lux A, Alunni V, Degrave A, et al. (2004) Spatial and temporal expression of the zebrafish genome by large-scale in situ hybridization screening. Methods in cell biology 77: 505-519.
105. Driever W, Solnica-Krezel L, Schier AF, Neuhauss SC, Malicki J, et al. (1996) A genetic screen for mutations affecting embryogenesis in zebrafish. Development 123: 37-46.
106. Haffter P, Granato M, Brand M, Mullins MC, Hammerschmidt M, et al. (1996) The identification of genes with unique and essential functions in the development of the zebrafish, Danio rerio. Development 123: 1-36.
107. Allende ML, Amsterdam A, Becker T, Kawakami K, Gaiano N, et al. (1996) Insertional mutagenesis in zebrafish identifies two novel genes, pescadillo and dead eye, essential for embryonic development. Genes & development 10: 3141-3155.
108. Amsterdam A, Nissen RM, Sun Z, Swindell EC, Farrington S, et al. (2004) Identification of 315 genes essential for early zebrafish development. Proceedings of the National Academy of Sciences of the United States of America 101: 12792-12797.
109. Golling G, Amsterdam A, Sun Z, Antonelli M, Maldonado E, et al. (2002) Insertional mutagenesis in zebrafish rapidly identifies genes essential for early vertebrate development. Nature genetics 31: 135-140.
110. Baier H (2000) Zebrafish on the move: towards a behavior-genetic analysis of vertebrate vision. Current opinion in neurobiology 10: 451-455.
111. Owens KN, Santos F, Roberts B, Linbo T, Coffin AB, et al. (2008) Identification of genetic and chemical modulators of zebrafish mechanosensory hair cell death. PLoS genetics 4: e1000020.
112. Brand M, Heisenberg CP, Jiang YJ, Beuchle D, Lun K, et al. (1996) Mutations in zebrafish genes affecting the formation of the boundary between midbrain and hindbrain. Development 123: 179-190.
113. Heisenberg CP, Brand M, Jiang YJ, Warga RM, Beuchle D, et al. (1996) Genes involved in forebrain development in the zebrafish, Danio rerio. Development 123: 191-203.
114. Wienholds E, van Eeden F, Kosters M, Mudde J, Plasterk RH, et al. (2003) Efficient target-selected mutagenesis in zebrafish. Genome research 13: 2700-2707.
115. Moens CB, Donn TM, Wolf-Saxon ER, Ma TP (2008) Reverse genetics in zebrafish by TILLING. Briefings in functional genomics & proteomics 7: 454-459.

116. Bill BR, Petzold AM, Clark KJ, Schimmenti LA, Ekker SC (2009) A primer for morpholino use in zebrafish. Zebrafish 6: 69-77.
117. Summerton J, Weller D (1997) Morpholino antisense oligomers: design, preparation, and properties. Antisense & nucleic acid drug development 7: 187-195.
118. Nasevicius A, Ekker SC (2000) Effective targeted gene 'knockdown' in zebrafish. Nature genetics 26: 216-220.
119. Summerton J (1999) Morpholino antisense oligomers: the case for an RNase H-independent structural type. Biochimica et biophysica acta 1489: 141-158.
120. Morcos PA (2007) Achieving targeted and quantifiable alteration of mRNA splicing with Morpholino oligos. Biochemical and biophysical research communications 358: 521-527.
121. Eisen JS, Smith JC (2008) Controlling morpholino experiments: don't stop making antisense. Development 135: 1735-1743.
122. Robu ME, Larson JD, Nasevicius A, Beiraghi S, Brenner C, et al. (2007) p53 activation by knockdown technologies. PLoS Genet 3: e78.
123. Bandmann O, Burton EA (2010) Genetic zebrafish models of neurodegenerative diseases. Neurobiology of disease 40: 58-65.
124. Rink E, Wullimann MF (2002) Development of the catecholaminergic system in the early zebrafish brain: an immunohistochemical study. Brain Res Dev Brain Res 137: 89-100.
125. Ma PM (2003) Catecholaminergic systems in the zebrafish. IV. Organization and projection pattern of dopaminergic neurons in the diencephalon. J Comp Neurol 460: 13-37.
126. Ryu S, Holzschuh J, Mahler J, Driever W (2006) Genetic analysis of dopaminergic system development in zebrafish. J Neural Transm Suppl: 61-66.
127. Bai Q, Burton EA (2009) Cis-acting elements responsible for dopaminergic neuron-specific expression of zebrafish slc6a3 (dopamine transporter) in vivo are located remote from the transcriptional start site. Neuroscience 164: 1138-1151.
128. Holzschuh J, Ryu S, Aberger F, Driever W (2001) Dopamine transporter expression distinguishes dopaminergic neurons from other catecholaminergic neurons in the developing zebrafish embryo. Mech Dev 101: 237-243.

129. Flinn L, Bretaud S, Lo C, Ingham PW, Bandmann O (2008) Zebrafish as a new animal model for movement disorders. J Neurochem 106: 1991-1997.
130. Giacomini NJ, Rose B, Kobayashi K, Guo S (2006) Antipsychotics produce locomotor impairment in larval zebrafish. Neurotoxicol Teratol 28: 245-250.
131. Sallinen V, Torkko V, Sundvik M, Reenila I, Khrustalyov D, et al. (2009) MPTP and MPP+ target specific aminergic cell populations in larval zebrafish. J Neurochem 108: 719-731.
132. Schweitzer J, Lohr H, Filippi A, Driever W (2011) Dopaminergic and noradrenergic circuit development in zebrafish. Dev Neurobiol.
133. Tay TL, Ronneberger O, Ryu S, Nitschke R, Driever W (2011) Comprehensive catecholaminergic projectome analysis reveals single-neuron integration of zebrafish ascending and descending dopaminergic systems. Nat Commun 2: 171.
134. Chen YC, Priyadarshini M, Panula P (2009) Complementary developmental expression of the two tyrosine hydroxylase transcripts in zebrafish. Histochem Cell Biol 132: 375-381.
135. Hokfelt T, Johansson O, Fuxe K, Goldstein M, Park D (1976) Immunohistochemical studies on the localization and distribution of monoamine neuron systems in the rat brain. I. Tyrosine hydroxylase in the mes- and diencephalon. Med Biol 54: 427-453.
136. Candy J, Collet C (2005) Two tyrosine hydroxylase genes in teleosts. Biochim Biophys Acta 1727: 35-44.
137. Yamamoto K, Ruuskanen JO, Wullimann MF, Vernier P (2010) Two tyrosine hydroxylase genes in vertebrates New dopaminergic territories revealed in the zebrafish brain. Mol Cell Neurosci 43: 394-402.
138. Filippi A, Mahler J, Schweitzer J, Driever W (2010) Expression of the paralogous tyrosine hydroxylase encoding genes th1 and th2 reveals the full complement of dopaminergic and noradrenergic neurons in zebrafish larval and juvenile brain. J Comp Neurol 518: 423-438.
139. Hersch SM, Yi H, Heilman CJ, Edwards RH, Levey AI (1997) Subcellular localization and molecular topology of the dopamine transporter in the striatum and substantia nigra. J Comp Neurol 388: 211-227.
140. Ciliax BJ, Heilman C, Demchyshyn LL, Pristupa ZB, Ince E, et al. (1995) The dopamine transporter: immunochemical characterization and localization in brain. J Neurosci 15: 1714-1723.

141. Torres GE (2006) The dopamine transporter proteome. J Neurochem 97 Suppl 1: 3-10.
142. Xi Y, Yu M, Godoy R, Hatch G, Poitras L, et al. (2011) Transgenic zebrafish expressing green fluorescent protein in dopaminergic neurons of the ventral diencephalon. Developmental dynamics : an official publication of the American Association of Anatomists 240: 2539-2547.
143. Sun Z, Gitler AD (2008) Discovery and characterization of three novel synuclein genes in zebrafish. Dev Dyn 237: 2490-2495.
144. Flinn L, Mortiboys H, Volkmann K, Koster RW, Ingham PW, et al. (2009) Complex I deficiency and dopaminergic neuronal cell loss in parkin-deficient zebrafish (Danio rerio). Brain 132: 1613-1623.
145. Bretaud S, Allen C, Ingham PW, Bandmann O (2007) p53-dependent neuronal cell death in a DJ-1-deficient zebrafish model of Parkinson's disease. J Neurochem 100: 1626-1635.
146. Anichtchik O, Diekmann H, Fleming A, Roach A, Goldsmith P, et al. (2008) Loss of PINK1 function affects development and results in neurodegeneration in zebrafish. J Neurosci 28: 8199-8207.
147. Sheng D, Qu D, Kwok KH, Ng SS, Lim AY, et al. (2010) Deletion of the WD40 domain of LRRK2 in Zebrafish causes Parkinsonism-like loss of neurons and locomotive defect. PLoS Genet 6: e1000914.
148. Fett ME, Pilsl A, Paquet D, van Bebber F, Haass C, et al. (2010) Parkin is protective against proteotoxic stress in a transgenic zebrafish model. PLoS One 5: e11783.
149. Anichtchik O, Diekmann H, Fleming A, Roach A, Goldsmith P, et al. (2008) Loss of PINK1 function affects development and results in neurodegeneration in zebrafish. The Journal of neuroscience : the official journal of the Society for Neuroscience 28: 8199-8207.
150. Xi Y, Ryan J, Noble S, Yu M, Yilbas AE, et al. (2010) Impaired dopaminergic neuron development and locomotor function in zebrafish with loss of pink1 function. The European journal of neuroscience 31: 623-633.
151. Sallinen V, Kolehmainen J, Priyadarshini M, Toleikyte G, Chen YC, et al. (2010) Dopaminergic cell damage and vulnerability to MPTP in Pink1 knockdown zebrafish. Neurobiology of disease 40: 93-101.
152. Bai Q, Mullett SJ, Garver JA, Hinkle DA, Burton EA (2006) Zebrafish DJ-1 is evolutionarily conserved and expressed in dopaminergic neurons. Brain research 1113: 33-44.

153. Bretaud S, Allen C, Ingham PW, Bandmann O (2007) p53-dependent neuronal cell death in a DJ-1-deficient zebrafish model of Parkinson's disease. Journal of neurochemistry 100: 1626-1635.
154. Ren G, Xin S, Li S, Zhong H, Lin S (2011) Disruption of LRRK2 does not cause specific loss of dopaminergic neurons in zebrafish. PLoS One 6: e20630.
155. Milanese C, Sager JJ, Bai Q, Farrell TC, Cannon JR, et al. (2012) Hypokinesia and reduced dopamine levels in zebrafish lacking beta- and gamma1-synucleins. The Journal of biological chemistry 287: 2971-2983.

COLOUR FIGURES

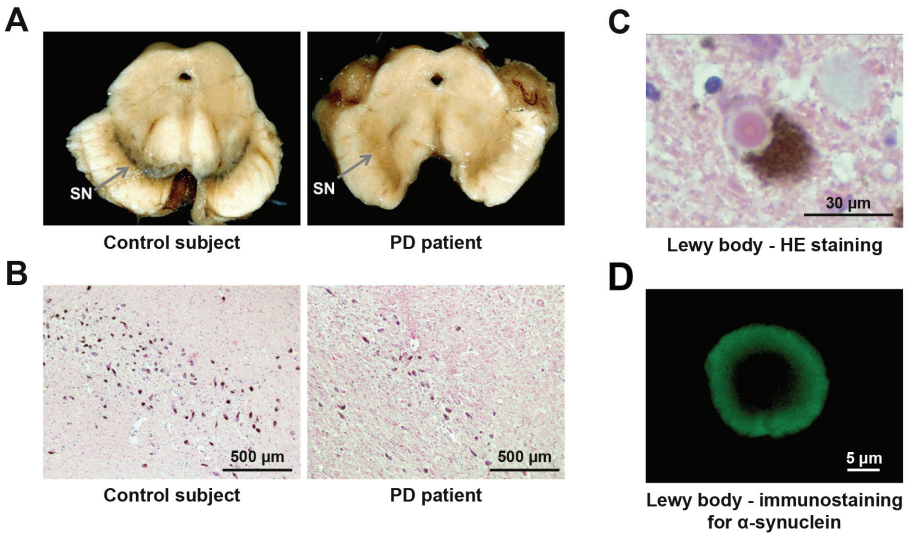

Figure 1 Macroscopic and microscopic neuropathological features of PD.
Midbrain sections show normal substantia nigra (SN) and SN degeneration in PD patient (A). Representative H&E staining shows loss of dopaminergic neurons in SN (B) and the presence of lewy body (C) in PD patient. Lewy body was stained using α-synuclein antibody (D).
Figure 1A is reproduced from Mandel, et al. EPMA Journal (2010), 1(2):273-92, with permission.

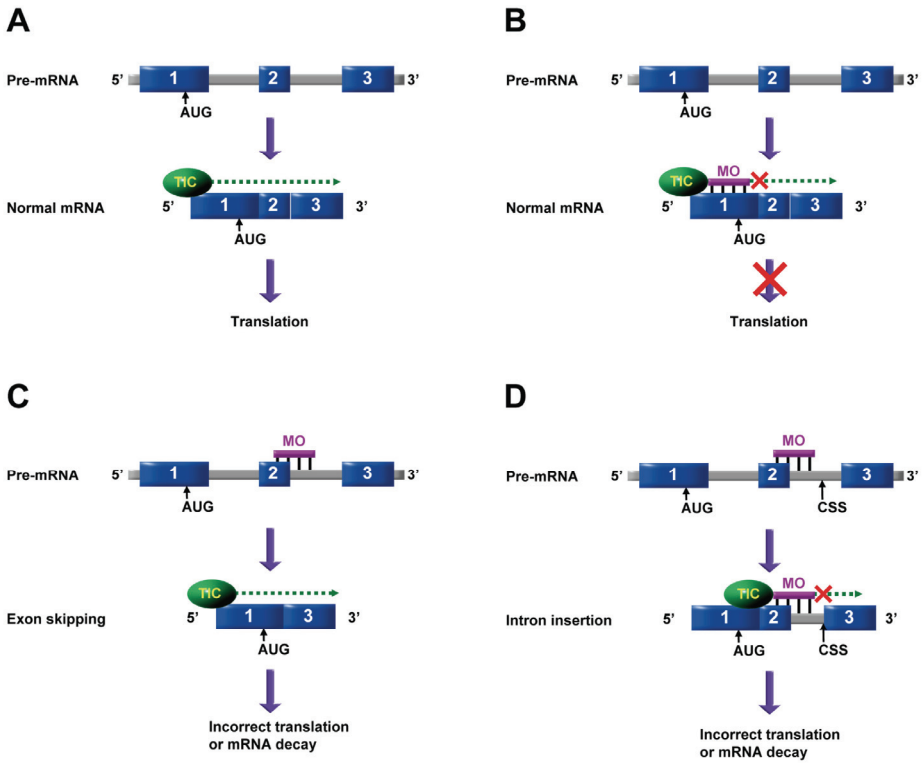

Figure 3 Strategies for MO-mediated gene knockdown.

(A) Normal transcription and translation.

(B) MO is designed to target the 5'-UTR near the translational start site in order to block protein translation.

(C and D) MOs are designed to target the exon-intron boundary to alter pre-mRNA splicing, leading to exon skipping (C) or intron insertion (D).

2

FBXO7 Mutations Cause Autosomal Recessive, Early-onset Parkinsonian-Pyramidal Syndrome

Alessio Di Fonzo, Marieke C. J. Dekker, Pasquale Montagna, Agostino Baruzzi, Ekaterina H. Yonova, Leonor Correia Guedes, Anna Szczerbinska, **Tianna Zhao**, Lorette O. M. Dubbel-Hulsman, Cokkie H. Wouters, Esther de Graaff, Wim J. G. Oyen, Erik J. Simons, Guido J. Breedveld, Ben A. Oostra, Martin W. Horstink, Vincenzo Bonifati

Published in Neurology. 2009 Jan 20;72(3):240-5, and reproduced with permission

ABSTRACT

The combination of early-onset, progressive parkinsonism with pyramidal tract signs has been known as pallido-pyramidal or parkinsonian-pyramidal syndrome, since the first description by Davison in 1954. Very recently, a locus was mapped in a single family with an overlapping phenotype, and an *FBXO7* gene mutation was nominated as the likely disease cause. We performed clinical and genetic studies in two families with early-onset, progressive parkinsonism and pyramidal tract signs. An *FBXO7* homozygous truncating mutation (Arg498Stop) was found in an Italian family, while compound heterozygous mutations (a splice-site IVS7+1G/T mutation and a missense Thr22Met mutation) were present in a Dutch family. We also found evidence of expression of novel normal splice-variants of *FBXO7*. The phenotype associated with *FBXO7* mutations consisted of early-onset, progressive parkinsonism and pyramidal tract signs, thereby matching clinically the pallido-pyramidal syndrome of Davison. The parkinsonism exhibits varying degrees of levodopa-responsiveness in different patients. We conclusively show that recessive *FBXO7* mutations cause progressive neurodegeneration with extrapyramidal and pyramidal system involvement, delineating a novel genetically-defined entity, that we propose to designate as *PARK15*. Understanding how *FBXO7* mutations cause disease will shed further light on the molecular mechanisms of neurodegeneration, with potential implications also for more common forms of parkinsonism, such as Parkinson's disease and multiple system atrophy.

INTRODUCTION

In 1954, Charles Davison described five patients with juvenile parkinsonism and pyramidal tract signs. In one case, necropsy disclosed lesions of the pallidum, ansa lenticularis, substantia nigra, and pyramidal tract [1]. The term "pallido-pyramidal disease", proposed by Davison for this entity, was adopted in the subsequent literature and textbooks [2,3] [OMIM accession number: 260300]. Similar cases have been repeatedly reported [4,5,6,7,8], including several from India [9,10,11,12]. The early onset, the type of familial aggregation, and frequent parental consanguinity suggest autosomal recessive inheritance. It became later evident that the parkinsonian component of this syndrome might exhibit good and sustained response to levodopa [4,6,8]. Brain imaging was unremarkable [6,7,8,9,10,11,12], but positron emission tomography showed marked decrease of striatal fluorodopa uptake [8].

Recently, an Iranian kindred was reported with autosomal recessive, early-onset spastic paraplegia. Interestingly, five to twenty years after the appearance of pyramidal symptoms, three out of the ten patients developed akinetic-rigid parkinsonism without tremor (levodopa-response was favorable in one patient, and not tested in the others) [13]. Linkage mapping in the Iranian family yielded a locus on chromosome 22, and a homozygous missense mutation in the gene encoding the F-box protein 7 *(FBXO7)* was proposed as the likely disease-causing variant [13].

However, association of a single variant with disease does not prove causation, and the role of *FBXO7* mutations remains to be demonstrated. Here, we report three novel pathogenic *FBXO7* mutations in two families, showing unambiguously that recessive *FBXO7* mutations cause a neurodegenerative disease with early-onset, parkinsonian-pyramidal phenotype.

RESULTS

We detected *FBXO7* mutations in both families (Figure 1). In the Italian family (BO) the two affected siblings carry a novel homozygous truncating mutation in exon 9 (c.C1492T, according to the longer *FBXO7* transcript, predicted protein effect p.Arg498Stop). This mutation was present in heterozygous state in both the unaffected parents and in one of the unaffected siblings. The other unaffected sib did not inherit the mutation. In the Dutch family (NIJ), the two affected siblings are compound heterozygous for two novel *FBXO7* mutations: a splice-site mutation (IVS7+1G/T) and a single base substitution in exon 1A

(c.C65T, predicted to lead to the missense protein change p.Thr22Met). This mutation affects only the *FBXO7* isoforms containing exon 1A (Figure 2). The unaffected mother only carried the heterozygous missense c.C65T mutation. Therefore, the remaining mutation (IVS7+1G/T) was most likely transmitted from the father, who was not available for genetic testing. In both families, direct sequencing revealed no additional disease-associated variants. The above-mentioned mutations were not found in ethnically-matched controls: 364 chromosomes tested from the Italian general population (mutation c.C1492T); 300 chromosomes from the Dutch general population (mutation IVS7+1G/T); 348 chromosomes from the Dutch general population (mutation c.C65T).

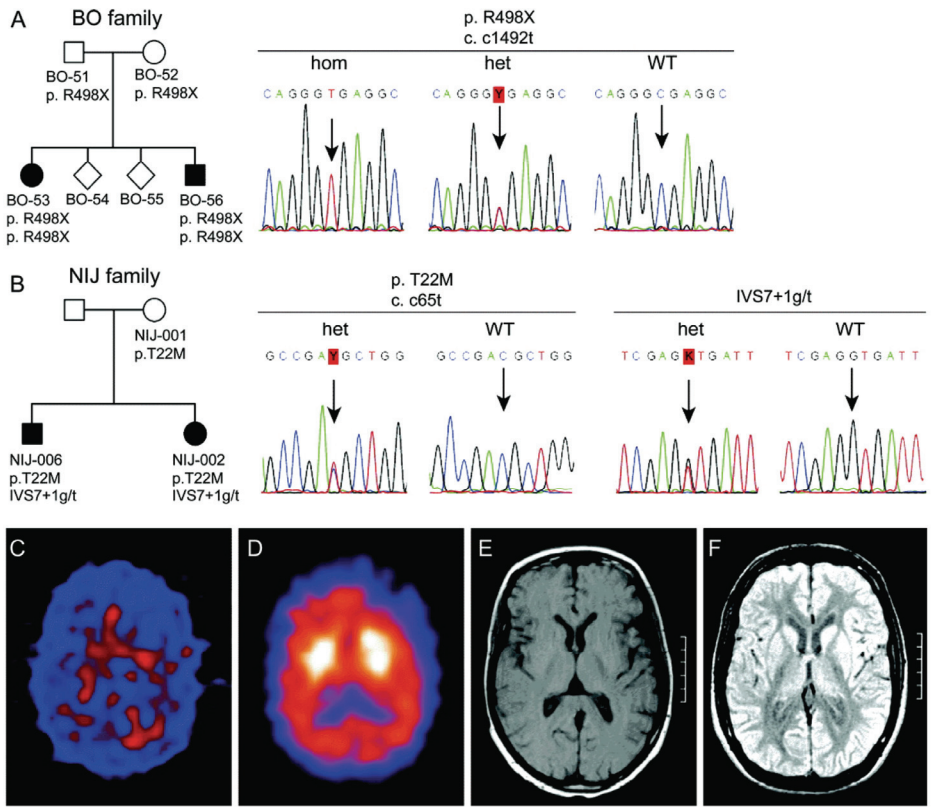

Figure 1 Genetic findings and neuroimaging in families with *FBXO7* mutations.
Black symbols in pedigrees denote affected individuals. To protect privacy, gender of unaffected siblings has been disguised and genotypes are not shown.
(A) Pedigree of the Italian family and electropherograms of mutations.
(B) Pedigree of the Dutch family and electropherograms of mutations.
(C) Brain CIT-SPECT (DaTSCAN-SPECT) in the NIJ-002 patient, showing a severe presynaptic defect of the nigrostriatal dopaminergic systems.
(D) Brain IBZM-SPECT in the NIJ-002 patient, showing the integrity of post-synaptic striatal dopamine receptor-bearing compartment.
(E and F) Normal brain MRI images in the NIJ-002 (E), and BO-56 (F) patient.

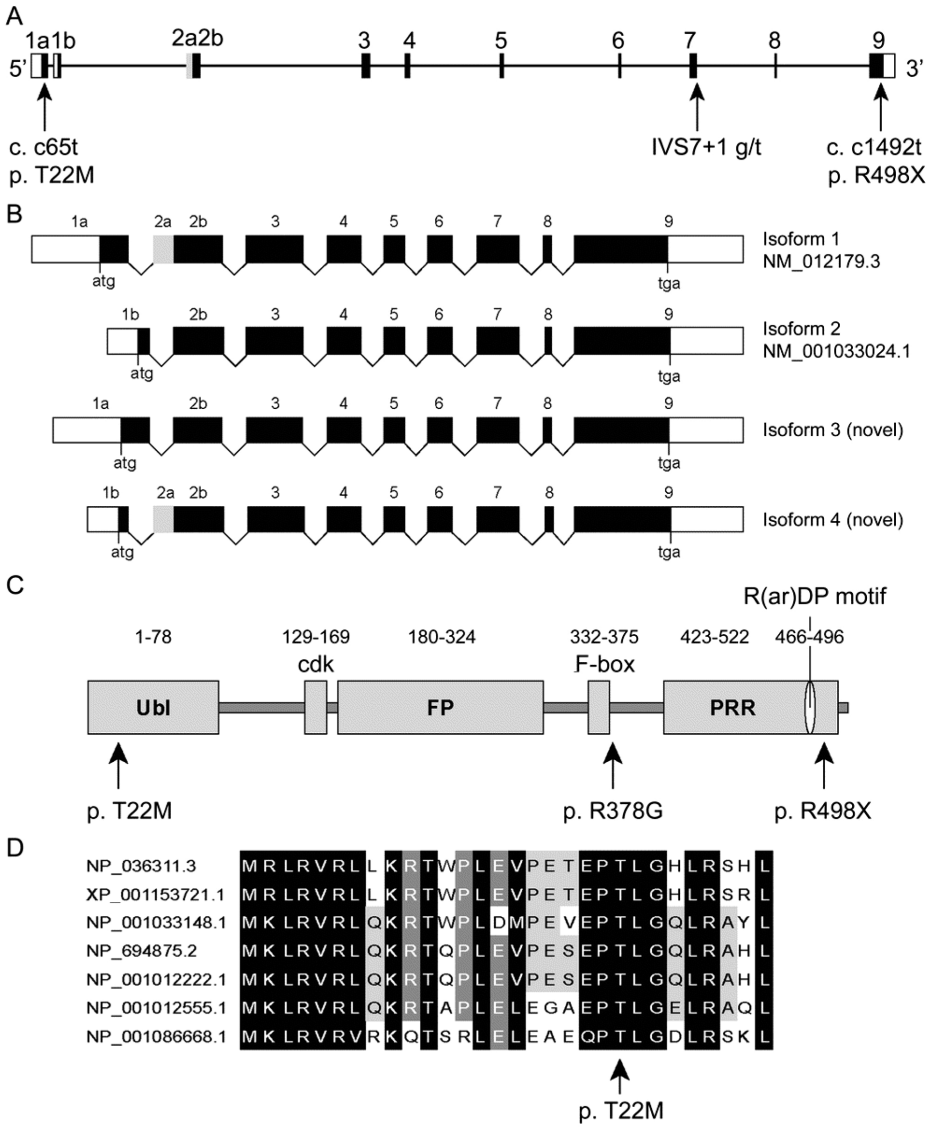

Figure 2 The *FBXO7* gene, transcripts, and protein isoforms.
(A) Genomic structure of the *FBXO7* gene (the genomic size is ~24 kb).
(B) Schematic representation of the *FBXO7* transcripts.
(C) Fbxo7 protein isoform 1 with functional regions and position of mutations identified in this study. The Arg378Gly mutation identified previously by others in an Iranian family is also shown. Ubl: ubiquitin-like region. cdk: cdk6 interaction region. FP: region mediating homo-and heterodimerization of F-Box proteins, and interaction with the PI13 protein. PRR: proline rich region. R(ar)DP: highly conserved motif of still undetermined function ("ar" indicates any aromatic amino acids).
(D) Alignment of Fbxo7 protein homologues in the regions targeted by the mutation identified in the Dutch patients. The closest homologues of the Fbxo7 protein were aligned using the program T-Coffee. GenBank accession numbers are as follows: NP_036311.3 [*Homo sapiens*]; XP_001153721.1 [*Pan troglodytes*]; NP_001033148.1 [*Bos taurus*]; NP_694875.2 [*Mus musculus*]; NP_001012222.1 [*Rattus norvegicus*]; NP_001012555.1 [*Gallus gallus*]; NP_001086668.1 [*Xenopus laevis*].

cDNA analysis from control blood cells and brain tissue confirmed the existence of the two known *FBXO7* transcripts (termed isoform 1 and 2) and also revealed evidence for at least two novel in-frame isoforms (termed isoforms 3 and 4), expressed by alternative combinations of exons 1A or 1B with exons 2A or 2B (for details see Figure 2 and Supplemental Figure E-1). Direct sequencing of the full-length *FBXO7* cDNA in one patient and the mother from the Dutch family confirmed the presence of the heterozygous c.C65T substitution, documenting therefore the expression of both alleles. The splice-site mutation (IVS7+1G/T) removes the invariable splice donor of intron 7, and is therefore expected to disrupt *FBXO7* mRNA splicing. And indeed, multiple aberrant frame-shift splice variants were detected in the patient but not in the unaffected mother, resulting from the activation of premature cryptic splice sites in exon 7 (Supplemental Figure E-2).

The missense mutation p.Thr22Met replaces a highly conserved amino acid in the N-terminal ubiquitin-like domain, one of the known functional domains of the Fbxo7 protein, which is only expressed in the two longer Fbxo7 isoforms (Figure 2). This situation predicts that the two shorter Fbxo7 isoforms are unaltered, which is compatible with some small residual Fbxo7 functional activity in the Dutch patients.

DISCUSSION

The homozygosity and compound heterozygosity for pathogenic mutations detected in the patients from families BO and NIJ represent clearly disease-causing genotypes. Our data convey therefore different important messages. First, they show unambiguously that recessive *FBXO7* mutations are a cause of neurodegeneration in humans, after the initial suggestive evidence provided by Shojaee and colleagues. Second, they show that the phenotypic spectrum associated with *FBXO7* mutations is much broader and less stereotypic than suggested by Shojaee and colleagues, and it encompasses the combination of early-onset, progressive parkinsonism with associated pyramidal tract signs, matching therefore clinically the “pallido-pyramidal syndrome” of Davison. The disease progression seems slow, as patients were alive decades after symptoms onset. Response to levodopa of the parkinsonism is variable, sometimes marked and sustained, but often limited by severe motor and psychiatric side effects. Screening of the *FBXO7* gene should be included in the diagnostic work-up of patients with otherwise unexplained early-onset parkinsonian-pyramidal syndromes.

We agree with others [6] that the term "*parkinsonian-pyramidal syndrome*" should be preferred to "*pallido-pyramidal syndrome"*, in the lack of pathology studies, and because the patients exhibit clinically a combination of parkinsonism and pyramidal disturbance. Moreover, on the basis of the clinical and imaging features, the disease caused by *FBXO7* mutations should be listed among the monogenic parkinsonisms, and termed PARK15 (for monogenic parkinsonism type 15).

The presynaptic nature of the parkinsonism is shown by the dramatic abnormality of DaTSCAN-SPECT, the beneficial effect of levodopa and the presence of levodopa-induced dyskinesias, and, in the patient NIJ-002, the low HVA and compensatory high biopterine levels in spinal fluid, normalized with levodopa therapy. A massive postsynaptic involvement is unlikely because of the normal MRI, normal IBZM-SPECT, and long-lasting beneficial levodopa effect, at least in some patients. The pyramidal signs together with abnormal TMS in patient NIJ-002, confirm the presence of pyramidal tract lesions. The normal MRI and the absence of dementia might help distinguishing this disease from other forms of complicated early-onset parkinsonism (such as PARK9 or neurodegeneration with brain iron accumulation) [14]. The patients from the Italian family carrying a Fbxo7 homozygous truncating mutation exhibit a more severe phenotype than those in the Dutch family, who carry missense and splice mutations, and those in the Iranian family [13], with homozygous missense. This phenotypic variance might correlate with genotypes and with the possible residual Fbxo7 protein activity, but analysis of large number of patients with *FBXO7* mutations is warranted.

Little is known about the function of the Fbxo7 protein. When over-expressed, Fbxo7 shows mainly cytosolic, but also nuclear localization [15,16]. Fbxo7 is a member of the F-box-containing protein (FBP) family, characterized by a ~40-amino acids domain (the F-box). FBPs serve as molecular scaffolds in the formation of protein complexes, and have been implicated in a range of processes, such as cell cycle, genome stability, development, synapse formation, and circadian rhythms [reviewed in [17]]. Through the interaction between F-box and the Skp1 protein, FBPs become part of SCF (Skp1, Cullin1, F-box protein) ubiquitin ligase complexes, and play roles in ubiquitin-mediated proteasomal degradation. However, FBPs might also be involved in ubiquitin-mediated, non-proteasomal pathways, and SCF-independent functions [17]. Fbxo7 also contains an N-terminal ubiquitin-like domain, and a C-terminal

proline-rich region (PRR), crucial for FBPs target specificity [15,17,18]. Fbxo7 is known to interact with different proteins, including the hepatoma up-regulated protein (HURP, a mitotic protein) [18], the inhibitor of apoptosis protein 1 (cIAP1) [16], and the proteasome inhibitor protein PI31 [15]. Last, Fbxo7 has SCF-independent transforming activity by enhancing the interaction of cyclin-dependent-kinase CDK6 with its targets [19]. Whether these or other, still unknown Fbxo7 interacting-proteins, are important for the neuronal function of Fbxo7 and for the mechanisms of neurodegeneration, is unknown. Unraveling the Fbxo7 pathways in neurons and the mechanisms of Fbxo7-linked disease will shed further light on the molecular mechanisms of multiple-system brain degeneration.

SUBJECTS AND METHODS

Two Caucasian families (one Dutch and one Italian), each containing two affected siblings, were studied. The disease segregation was compatible with autosomal recessive inheritance (Figure 1). There was no history of parkinsonism in the previous generations, nor was there evidence of parental consanguinity. The clinical phenotype consisted of juvenile-onset, progressive parkinsonism with additional pyramidal signs (increased tendon reflexes, spasticity and Babinski sign), and a prolonged course, thereby matching closely Davison's syndrome. Levodopa therapy yielded variable extent of benefit on the parkinsonism in the different patients. The more important clinical features are summarized in the Table 1, while the detailed case-reports are provided in the supplemental appendix E-1.

The relevant ethical authorities approved the study and written informed consent was obtained from all subjects. Genomic DNA was isolated from peripheral blood using standard protocols. The involvement of known genes causing early-onset autosomal recessive typical (*parkin*, *PINK1*, *DJ-1*) or atypical parkinsonism (*ATP13A2)*, as well as those causing Niemann-Pick disease type C1 and C2 [*NPC1*, *NPC2*] and the neuronal ceroid lipofuscinosis-3 [*CLN3*], were excluded by haplotype analysis and direct gene testing (genomic sequencing of all exons for all genes; gene dosage for *parkin*, *PINK1*, *DJ-1* (data not shown). All exons and exon-intron boundaries of the *FBXO7* gene were PCR-amplified from genomic DNA. cDNA studies were also performed in samples from control subjects and members of the Dutch family. PCR primers, protocols, and sequencing methods are reported in the supplemental appendix E-2. The novel

sequence variants detected in patients were tested in ethnically matched healthy controls, using direct sequencing.

Table 1 Clinical features in patients with *FBXO7* mutations

Patient code	**BO-53**	**BO-56**	**NIJ-002**	**NIJ-006**
Gender	female	male	female	male
Onset age (y.rs)	10	13	18	19
Symptoms at onset	arm tremor, writing difficulty, trunk stiffness, unsteadiness	hand tremor, slowness of movements, unsteadiness	tremor, nervousness	slowness of movements, social withdrawing
Signs at examination:				
Bradykinesia	+	+	+	+
Rigidity	+	+	+	+
Resting tremor	+	+	-	+
Action tremor	+	+	+	+
Postural instability	+	+	+	+
Dystonic features	+	+	-	-
Hyperactive tendon reflexes	+	+	+	+
Babinski sign	+	+	+	+
Other signs	dysarthria, dysphagia, urinary incontinence, fecal incontinence	slow saccades, reduced upgaze, dysarthria, dysphagia	slow saccades, reduced upgaze	dysphagia, reduced upgaze
Dementia	-	-	-	-
Levodopa response	+	+	+	+
Levodopa-induced side effects:				
Motor fluctuations	+	+	+	+
Dyskinesias	+	+	+	+
Behavioural disturbances	+	+	+	+
Performed instrumental investigations:				
Unremarkable:	Brain, EMG/ENG, Muscle biopsy	MRI, IBZM-SPECT, EMG/ENG, Muscle biopsy	Brain, IBZM-SPECT, EMG/ENG	MRI
Abnormal:			DaTSCAN-SPECT, TMS	

+ present; - absent

TMS = transcranial magnetic stimulation for the study of the motor pathways

EMG/ENG = electromyography/electroneurography

IBZM-SPECT = [^{123}I]iodobenzamide single photon emission computed tomography

DaTSCAN-SPECT = [^{123}I]ioflupane single photon emission computed tomography

Two Fbxo7 protein isoforms are known to be expressed from the usage of different open reading frame (ORF) start codons located on alternative 5'-exons (termed exon 1A and 1B) (Figure 2). Here, *FBXO7* variants are named according to the longest mRNA and protein isoforms (GenBank accession

number NM_012179.3; NP_036311.3) (Figure 2), and numbered at nucleotide level from the "A" of the ATG-translation initiation codon.

ACKNOWLEDGMENTS

We thank all patients and relatives for their contributions, M.J.R. Janssen (Radboud University Nijmegen Medical Center) for help with neuroimages, and Tom de Vries-Lentsch, Erasmus MC, Rotterdam, for artwork. This study was supported by the "Internationaal Parkinson Fonds" – Netherlands, the Erasmus MC Rotterdam (Erasmus Fellowship), and the Netherlands Organization for Scientific Research (NWO, VIDI grant) to V.B.

SUPPORTING INFORMATION

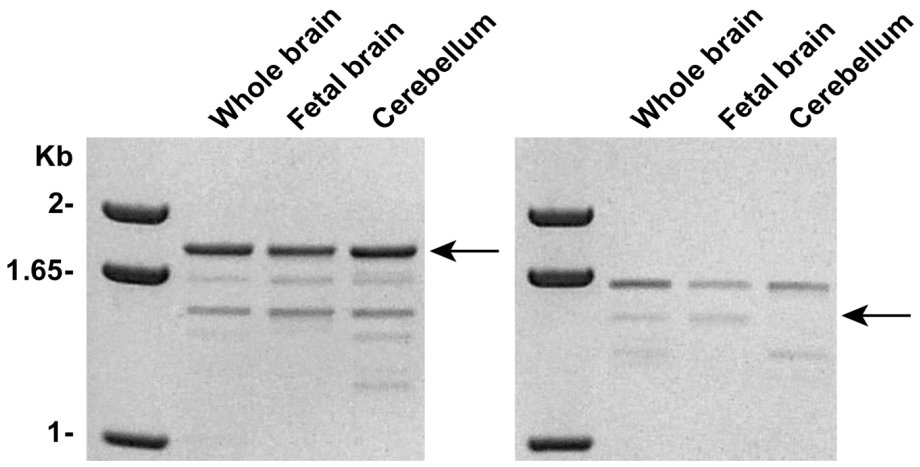

Supplemental Figure E-1 Agarose gel analysis of *FBXO7* transcripts amplified from RT-PCR material.

For amplification of the two previously known *FBXO7* isoforms, a forward primer specific for exon 1A (experiment shown in the left panel) and a different forward primer specific for exon 1B (right panel) were used; a reverse primer specific for exon 9 was used in both experiments. The expected sizes of the isoforms annotated in Genbank are indicated by the arrows. Evidence is shown for the expression of multiple *FBXO7* transcripts from whole adult human brain, fetal brain and cerebellum, including at least two novel isoforms resolved by sequencing analysis (isoform 3 and 4, confront Figure 2 in the article).

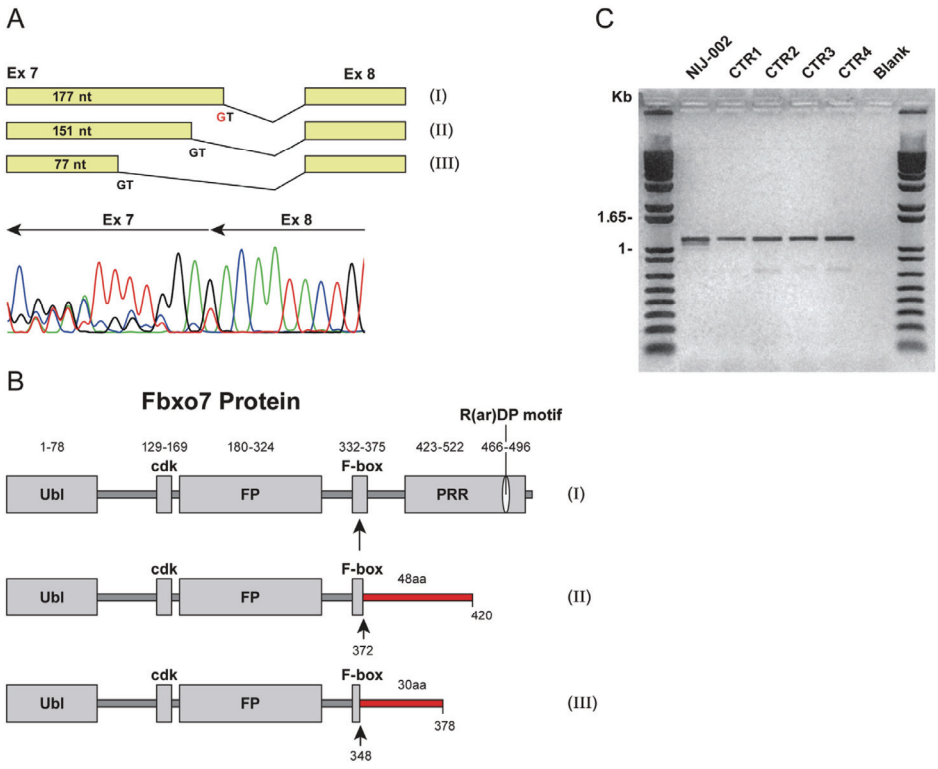

Supplemental Figure E-2.

(A) Analysis of the *FBXO7* cDNA in the patient NIJ-002.

The electropherogram (reverse-complemented) shows the normal splicing of exon 7 to exon 8, and two additional aberrant splicing species due to the IVS7+1 mutation, and resulting from usage of cryptic GT splice donor sites located within exon 7. The same scenario is schematically represented: (I) normal splicing between exon 7 and exon 8 (the IVS7+1G mutation is marked in red); (II-III) aberrant splice variants.

(B) Predicted effect of the two aberrant transcript isoforms (II-III) on the Fbxo7 protein.

Both transcript isoforms are predicted to dramatically affect the C-terminal region of the protein including the whole PRR domain and part of the F-box domain, as they introduce frameshift and encode an aberrant peptide (depicted in red) of 48 and 30 amino acids, before a premature Stop codon.

(C) Agarose gel analysis of an *FBXO7* cDNA fragment encompassing exon 3 to 9, showing a band of the expected size in normal individuals, and additional shorter bands in the NIJ-2 patient, who carries the IVS7+1 mutation.

Supplemental Appendix E-1: case reports

Patient BO-53

She was born as a result of a complicated delivery and suffered from night terror disorder (*pavor nocturnus)* till the age of 7 years. At the age of 10 she developed writing difficulties, trunk rigidity with retropulsion and tendency to falling, and tremor of the upper limbs, particularly the left arm. Subsequently, she developed hypomimia, diffuse rigidity, dysarthria, drooling and dysphagia causing severe loss of body weight. By the age of 17 she was confined to bed, unable to walk autonomously and talk. She developed severe dorsal scoliosis, and urinary and fecal incontinence. Neurological examination at age 17 showed an amimic face with open mouth and drooling, dysarthria, generalized rigidity, more evident proximally and in the cervical region, with dystonic posture in extension, cogwheeling, a coarse tremor of the upper and lower limbs, hyperreflexia, and bilateral Babinski sign; she was unable to stand or walk unaided; when aided, scissoring gait was present. Erythematous skin phenomena were present in her face (also present in her affected sibling). Currently, at the age of 38, the patient lies in bed all the time, is unable of talking and eating independently. She has developed severe restrictive pulmonary insufficiency and obstructive apneas during sleep and daytime, and arterial hypertension. Treatment with levodopa and pergolide were soon discontinued due to intolerable gastric side effects, but administration of single doses of levodopa 200mg + benserazide decreased the rigidity and akinesia, but caused hyperkinesias and agitation; botulinum toxin ameliorated the cervical dystonia. Normal laboratory and instrumental examinations included: EEG, CSF, brain CT and MRI (age 17), EMG and NCV, fundus oculi and campimetric testing; serum copper and ceruloplasmin; arylsulphatase A, galactosidase, oligo and muco-polysaccharides assays, exosaminidase, mitochondrial enzymes. A muscle biopsy was unremarkable, and lysosomal inclusions were not detected in monocytes by electron microscopy.

Patient BO-56

He was born after a normal pregnancy and delivery. His cognitive and motor development was slow, with delay in reaching milestones, especially concerning language, and he required speech therapy support. Around the age of 13, he developed tremor of the right hand, and subsequently slowing of writing, global slowing of movements, especially of speech and walking, associated with unsteadiness. He developed facial hypomimia and dysarthria with swallowing

difficulties, could not walk without assistance because of a tendency to fall backwards. Psychiatric evaluation suspected an IQ lower than normal. Equinus feet deformity required Achilles tenotomy at the age 18. Due to severe dysphagia he necessitates semiliquid diet since age 18. Neurological examination at age 15 showed facial hypomimia, dysarthria, open mouth, axial rigidity in extension more marked on the right, postural and action tremor, deep tendon hyperreflexia with bilateral Babinski sign, tendency to falling with absent postural reflexes, slow gait possible only with assistance. At the age of 17, he was examined by Prof. C.D. Marsden, who noted slow saccades with reduced upgaze and jerky pursuit, hypophonia and slow tongue movements, as well as akinesia with inability to initiate gait and complete loss of postural reflexes, resting and postural tremor of the arms especially on the right, retrocollis and dystonic hands and feet. He was at that time confined to a wheel chair and was unable to talk. A resting tremor of the right hand at 5-6 Hz with a dystonic component was recorded. Administration of pergolide 0.25 mg every 2-3 hours improved his akinesia and rigidity (he could walk unaided and talk) but caused peak-dose severe hyperkinesias and behavioural disturbances. The same happened with equivalent levodopa or pramipexole doses. Botulinum toxin ameliorated the cervical dystonia. The patient died suddenly at age 29 because of aspiration of food material. No autopsy data are available. Brain CT and MRI (at ages 16 and 20) were unremarkable (see Fig.1 in the article), and brain [123I]iodobenzamide (IBZM) SPECT at age 20 documented normal striatal tracer binding. Normal laboratory and instrumental examinations included: serum copper and ceruloplamin, CSF, EMG and NCV, fundus oculi, brainstem evoked responses, and muscle biopsy. Biopsy of rectal mucosa revealed normal neurons of the submucosal plexus.

Patient NIJ-002

Symptoms started with tremor and nervousness at the age of 18 years. At about age 25 she was prescribed amantadine 100 mg twice a day because of deterioration of motor function and festination. Later on, she started suffering from periods of freezing. At age 34, our examination revealed a symmetrical hypokinetic-rigid syndrome (Hoehn-Yahr stage 3 “on” and 4 “off”) with mild bilateral action tremor of the hands, masked face, bradykinesia, rigidity in upper and lower extremities, a shuffling and stooped gait with absent arm swing, postural instability and increased risk of falling. The tendon reflexes were hyperactive with sustained ankle clonus and bilateral Babinski sign. We found restricted upward gaze with slow saccades, which improved with levodopa.

There was no ataxia, or autonomic disturbance. Cognitive function and memory were normal. Investigations performed at age 34 included: the Groninger Intelligence Test (GIT) and Wechsler Memory Scale-Revised: IQ 110-115 (normal). Brain and spinal MRI and brain IBZM-SPECT were unremarkable, while DaTSCAN-SPECT showed a dramatic bilateral loss of striatal binding (see Fig.1 in the article). ENG yielded normal peripheral conduction velocities. However, transcranial magnetic stimulation (TMS) showed abnormal cortical motor conduction time to *M. Vastus Medialis*: right 20 msec, left 19 msec (normal value: 11.5 ± 2 msec). The analysis of CSF monoamines showed decreased HVA levels (57 nmol/l, normal range 87-372), normal MHPG and 5-HIAA; normal neopterine, but elevated biopterine (145 nmol/l, normal range 5-21) that normalized with levodopa therapy (5 nmol/l). The patient was treated with Sinemet 125 t.i.d. and greatly improved. However, after 3 months she developed visual hallucinations, disinhibited and socially inappropriate behavior with loss of insight. Rivastigmine 3 mg t.i.d. was effective, but seemed to increase parkinsonism. Quetiapine 25 mg t.i.d. was effective, but body weight increased about 5 kg. With Sinemet 62.5 t.i.d. and clozapine 12.5 mg in the morning, both behavior and disability became acceptable. At about age 36, wearing-off symptoms and disabling freezing appeared, just as dyskinesia, particularly dystonic myoclonic yerks in the perioral region and the platysma. Polyminimyoclonus was not seen.

Patient NIJ-006

He stuttered from childhood and was treated for behavioral problems since age 17. Bradykinesia and loss of initiative and social withdrawing started about age 19. At age 24 he complained of dysphagia, micrographia, freezing, retropulsion and tremor. Elsewhere a symmetric hypokinetic-rigid syndrome was detected with generalized bradykinesia, severe rigidity, action tremor and supranuclear ophthalmoplegia. The tendon reflexes were hyperactive and the Babinski sign was present. Cerebellar or autonomic dysfunction was absent. WAIS IQ verbal score was 113, and performal score was 86. Brain MRI was unremarkable. Madopar 125 t.i.d. combined with pergolide 0.75 mg t.i.d. clearly improved motor function but caused severe response fluctuations and behavioral side effects (disinhibition and violent conduct). He resided in psychiatric institutions since age 26. At the age of 38, our examination showed severe parkinsonism (Hoehn-Yahr stage 4) with resting and action tremor in off-periods, and severely hyperkinesias during onperiods, causing great difficulty with walking because of postural instability and frequent falls. Vertical gaze movements were impaired

during off-periods, but they improved in on-conditions. Tendon reflexes were hyperactive with extensor plantar reflexes. Intelligence seemed normal. Due to his unpredictable behavior, further instrumental examinations could not be performed.

Supplemental Appendix E-2: genetic methods

Primers used for the amplification of *FBXO7* fragments from genomic DNA

Exon	Forward Primer 5' →3'	Reverse Primer 5' →3'	Annealing T (total 35 cycles)	Size (bp)
1	TAACCTAAGGCTTCTC AGAGC	CATTTCCAACTTGAAATC TAACC	70°→60 (-1°/cycle), then 60°	1044
2	TTCATCACTTAGTTCT TCTAGG	GATAATTATCCTGACTG GAACAG	70°→60 (-1°/cycle), then 60°	500
3	ATGATGTACTTTGACT TTCAGC	GCAACTTGAGAGCAGGA ACC	70°→60 (-1°/cycle), then 60°	405
4	TGGCAATGTTAATGAT TTGATGC	TCACAACTGTATCATGAT AGCC	70°→60 (-1°/cycle), then 60°	394
5	AGGAGCTAGGAAATG CAAGC	AAACCACATTGTCTTCAA TATGC	70°→60 (-1°/cycle), then 60°	307
6	CACTGTACTTCTTCCA TGAGG	CAGTCAGATGTCATACT CACC	70°→60 (-1°/cycle), then 60°	337
7	GTTGTAGATGATGCAT ACTTGG	TATATGAAGCTTAGAGT CAGTC	70°→60 (-1°/cycle), then 60°	475
8	AAACCCACTGTTTAAT GCAGG	GATTGAGTCTAAAGTAA AAGTTG	70°→60 (-1°/cycle), then 60°	106
9	CTATAGATCTTTACTA TGAAAGC	CTGCCTATGCTATGTTC TCTG	68°→58 (-1°/cycle), then 58°	888

Additional internal primers used for the sequencing reactions

Primer name	Primer sequence 5' →3'
1seqF	TCCGGTAGTCGCCAGTCC
1seqR	CTGCAGCCCACAGATGACG
9seqF	CGGTTTGTGATGCTCCTGC
9seqR	ATAACACTCGAGATCAGCACC

Primers pairs used for the amplification of *FBXO7* cDNA fragments

Fragment	Forward Primer 5' →3'	Reverse Primer 5' →3'	Annealing T (total 35 cycles)	Size (bp)
Exon 1A to exon 9	TCGCCAGTCCGGGGTCGTC	ATAACACTCGAGATCAGCACC	68°→58 (-1°/cycle), then 58°	1764
Exon 1B to exon 9	TCCGGCTCCTGGAGAACATG	ATAACACTCGAGATCAGCACC	68°→58 (-1°/cycle), then 58°	1438
Exon 3 to exon 9	CCATGCTCTGTAGTGAATCG	ATAACACTCGAGATCAGCACC	68°→58 (-1°/cycle), then 58°	1157

Additional internal primers used for the cDNA sequencing reactions

Primer name	Primer sequence 5' →3'
2cDNAR	CTGTCGTCATTCCAAACACC
4cDNAR	CGCTCAACTTCCACTTCTCC
5cDNAF	TATTTGCAAAGAGAAACTAGGG
7cDNAF	CCCATTGGAACTGAAACTACG
8cDNAR	TCTTGAACTCTGACAGTATTG

PCR and sequencing conditions

Genomic DNA and RNA were isolated from peripheral blood using standard protocols. RNA from control human brain tissue (Clontech) was also used. The nine exons and intron-exon boundaries of the *FBXO7* gene, as well as fragments of *FBXO7* cDNA were amplified using PCR and above-mentioned primers. For sequencing of exons 1, exon 9, and of some cDNA fragments, internal primers were also used, as indicated above.

PCR reactions were performed in 10 µl containing 1.1 µl of 10x Roche PCR buffer with MgCl2, 25µM of each dNTP, 1µM forward primer, 1µM reverse primer, 0.5 units of FastStart taq Polymerase (Roche) and 50 ng genomic DNA or 1 µl total cDNA. For amplification of exon 1, and cDNA fragments, TaKaRa LA Taq polymerase and GC PCR buffer II were used (Takara Biomedicals).

Direct sequencing of both strands was performed using Big Dye Terminator chemistry ver.3.1 (Applied Biosystems). Fragments were loaded on an ABI3100 automated sequencer and analysed with DNA Sequencing Analysis (ver.3.7) and SeqScape (ver.2.1) software (Applied Biosystems).

REFERENCES

1. Davison C (1954) Pallido-pyramidal disease. J Neuropathol Exp Neurol 13: 50-59.
2. Moller JC, Oertel WH Other degenerative processes. In: Koller WC and Melamed E, editors. Parkinson's disease and related disorders, Part II - Handbook of Clinical Neurology, Vol. 84. Amsterdam: Elsevier; 2007: 445-457.
3. Sutton JP Other Adult-Onset Movement Disorders with a Genetic Basis. In: Pulst S-M, editor Genetics of Movement Disorders San Diego: Academic Press; 2003: 511-540.
4. Horowitz G, Greenberg J (1975) Pallido-pyramidal syndrome treated with levodopa. J Neurol Neurosurg Psychiatry 38: 238-240.
5. Tranchant C, Boulay C, Warter JM (1991) Le syndrome pallido-pyramidal: une entite meconnue. Rev Neurol (Paris) 147: 308-310.
6. Nisipeanu P, Kuritzky A, Korczyn AD (1994) Familial levodopa-responsive parkinsonian-pyramidal syndrome. Mov Disord 9: 673-675.
7. Pradat PF, Dupel-Pottier C, Lacomblez L, Salachas F, Meininger V, et al. (2001) Case report of pallido-pyramidal disease with supplementary motor area involvement. Mov Disord 16: 762-764.
8. Remy P, Hosseini H, Degos JD, Samson Y, Agid Y, et al. (1995) Striatal dopaminergic denervation in pallidopyramidal disease demonstrated by positron emission tomography. Ann Neurol 38: 954-956.
9. Kalita J, Misra UK, Das BK (2003) Sporadic variety of pallido-pyramidal syndrome. Neurol India 51: 383-384.
10. Rajendran P, Aleem MA, Chandrasekaran R, Raveendran S, Ramasubramanian D (2000) Familial Parkinsonian pyramidal syndrome. Neurol India 48: 297-298.
11. Srivastava T, Goyal V, Singh S, Shukla G, Behari M (2005) Pallido-pyramidal syndrome with blepharospasm and good response to levodopa. J Neurol 252: 1537-1538.
12. Panagariya A, Sharma B, Dev A (2007) Pallido-pyramidal syndrome: a rare entity. Indian J Med Sci 61: 156-157.
13. Shojaee S, Sina F, Banihosseini SS, Kazemi MH, Kalhor R, et al. (2008) Genome-wide linkage analysis of a Parkinsonian-pyramidal syndrome pedigree by 500 K SNP arrays. Am J Hum Genet 82: 1375-1384.
14. Bonifati V (2007) Genetics of parkinsonism. Parkinsonism Relat Disord 13 (Suppl 3): S233-S241.

15. Kirk R, Laman H, Knowles PP, Murray-Rust J, Lomonosov M, et al. (2008) Structure of a Conserved Dimerization Domain within the F-box Protein Fbxo7 and the PI31 Proteasome Inhibitor. J Biol Chem 283: 22325-22335.
16. Chang YF, Cheng CM, Chang LK, Jong YJ, Yuo CY (2006) The F-box protein Fbxo7 interacts with human inhibitor of apoptosis protein cIAP1 and promotes cIAP1 ubiquitination. Biochem Biophys Res Commun 342: 1022-1026.
17. Ho MS, Ou C, Chan YR, Chien CT, Pi H (2008) The utility F-box for protein destruction. Cell Mol Life Sci 65: 1977-2000.
18. Hsu JM, Lee YC, Yu CT, Huang CY (2004) Fbx7 functions in the SCF complex regulating Cdk1-cyclin B-phosphorylated hepatoma up-regulated protein (HURP) proteolysis by a proline-rich region. J Biol Chem 279: 32592-32602.
19. Laman H, Funes JM, Ye H, Henderson S, Galinanes-Garcia L, et al. (2005) Transforming activity of Fbxo7 is mediated specifically through regulation of cyclin D/cdk6. Embo J 24: 3104-3116.

3

Loss of Nuclear Activity of the FBXO7 Protein in Patients with Parkinsonian-Pyramidal Syndrome (PARK15)

Tianna Zhao, Esther De Graaff, Guido J. Breedveld, Agnese Loda, Lies-Anne Severijnen, Cokkie H. Wouters, Frans W. Verheijen, Marieke C. J. Dekker, Pasquale Montagna, Rob Willemsen, Ben A. Oostra, Vincenzo Bonifati

Published in PLoS ONE. 2011 Feb 11;6(2):e16983

ABSTRACT

Mutations in the *F-box only protein 7* gene (*FBXO7*) cause PARK15, an autosomal recessive neurodegenerative disease presenting with severe levodopa-responsive parkinsonism and pyramidal disturbances. Understanding the PARK15 pathogenesis might thus provide clues on the mechanisms of maintenance of brain dopaminergic neurons, the same which are lost in Parkinson's disease. The protein(s) encoded by *FBXO7* remain very poorly characterized. Here, we show that two protein isoforms are expressed from the *FBXO7* gene in normal human cells. The isoform 1 is more abundant, particularly in primary skin fibroblasts. Both isoforms are undetectable in cell lines from the PARK15 patient of an Italian family; the isoform 1 is undetectable and the isoform 2 is severely decreased in the patients from a Dutch PARK15 family. In human cell lines and mouse primary neurons, the endogenous or over-expressed, wild type FBXO7 isoform 1 displays mostly a diffuse nuclear localization. An intact N-terminus is needed for the nuclear FBXO7 localization, as N-terminal modification by PARK15-linked missense mutation, or N-terminus tag leads to cytoplasmic mislocalization. Furthermore, the N-terminus of wild type FBXO7 (but not of mutant FBXO7) is able to confer nuclear localization to profilin (a cytoplasmic protein). Our data also suggest that overexpressed mutant FBXO7 proteins (T22M, R378G and R498X) have decreased stability compared to their wild type counterpart. In human brain, FBXO7 immunoreactivity was highest in the nuclei of neurons throughout the cerebral cortex, intermediate in the globus pallidum and the substantia nigra, and lowest in the hippocampus and cerebellum. In conclusion, the common cellular abnormality found in the PARK15 patients from the Dutch and Italian families is the depletion of the FBXO7 isoform 1, which normally localizes in the cell nucleus. The activity of FBXO7 in the nucleus appears therefore crucial for the maintenance of brain neurons and the pathogenesis of PARK15.

INTRODUCTION

Parkinson's disease (PD), the second most common neurodegenerative disorder after Alzheimer's disease, is pathologically characterized by the progressive loss of dopaminergic neurons in the substantia nigra of the midbrain, and the formation of alpha-synuclein-containing protein aggregates, termed Lewy bodies, in surviving neurons [1]. In recent years, defective ubiquitin-proteasome system, mitochondrial dysfunction, oxidative stress, and autophagy impairment have all been suggested to play some roles in the PD pathogenesis, but the primary molecular mechanisms of this disease remain mostly unknown [2,3]. PD is a sporadic, idiopathic disorder in most patients, but the identification of genetic mutations causing rare Mendelian forms of parkinsonism has provided novel clues for understanding of the disease pathogenesis [3,4]. Some of these Mendelian parkinsonism, such as those caused by dominant mutations in the *alpha-synuclein* (PARK1) or *leucine-rich repeat kinase 2* (PARK8) gene, are more similar to the common, idiopathic PD form [5]. In other forms, such as those caused by recessive mutations in the *parkin* (PARK2), *PINK1* (PARK6), *DJ-1* (PARK7), and *ATP13A2* (PARK9), the phenotype is more often atypical due to younger-onset, presence of additional clinical signs (dementia, pyramidal signs), or absence of Lewy body-pathology [6,7,8]. However, despite these atypical phenotypes, understanding the mechanisms of the Mendelian parkinsonisms might provide important clues into the pathways leading to the degeneration of the dopaminergic neurons, which might also be involved in the common forms of PD. For example, the ATP13A2 protein has been recently identified as a potent modifier of the toxicity induced by alpha-synuclein in animal models of PD [9].

Recently, we characterized mutations in the *F-box only protein 7* (*FBXO7*) gene, encoding the F-box protein 7 (FBXO7), as the cause of PARK15, an autosomal recessive neurodegenerative disease presenting with juvenile, severe levodopa-responsive parkinsonism and additional pyramidal signs [10]. A homozygous *FBXO7* nonsense mutation (R498X) is present in an Italian family, while compound heterozygous mutations (IVS7+1G/T and a T22M mutation) are found in a Dutch family. Another homozygous mutation (R378G) was previously identified by others in an Iranian family [11].

FBXO7 is a member of the F-box-containing protein (FBP) family, characterized by a ~40-amino acids domain (the F-box) [12,13,14]. FBPs serve as molecular scaffolds in the formation of protein complexes, and have been implicated in a range of processes, such as cell cycle, genome stability, development, synapse formation, and circadian rhythms (reviewed in [15]). Through the interaction

between the F-box and the Skp1 protein, FBPs might become part of SCF (Skp1, Cullin1, F-box protein) ubiquitin ligase complexes, and play roles in ubiquitin-mediated proteasomal degradation [15]. However, FBPs might also be involved in ubiquitin-mediated, non-proteasomal pathways, and SCF-independent non-proteolytic functions [15].

Two *FBXO7* transcript variants are annotated in Genbank (accession number NM_012179.3 and NM_001033024.1), resulting from the usage of different open reading frame (ORF) start codons on alternatively spliced 5'-exons, and predicted to encode two FBXO7 protein isoforms of 522 and 443 amino acids (also referred to as isoform 1 and isoform 2). However, the experimental confirmation of the existence of these two protein isoforms has remained elusive. Nothing is known about the expression of the FBXO7 protein(s) in the human brain.

The FBXO7 isoform 1 is longer than isoform 2 because of the presence of an N-terminal ubiquitin-like (Ubl) domain (absent in the isoform 2), which is thought to interact with ubiquitin receptor proteins (Figure 1). The remaining domains are present in both isoforms, including an FP (FBXO7/PI31) domain, the F-box motif, and a C-terminal proline-rich region (PRR). The FP domain mediates the interaction of FBXO7 with the proteasome inhibitor protein PI31 [16]. The PRR appears crucial for the binding of FBXO7 to its reported substrates.

Very little is known about the function and the sub-cellular localization of these two FBXO7 proteins. FBXO7 has been reported to interact with the hepatoma up-regulated protein (HURP, a mitotic protein) [17], the inhibitor of apoptosis protein 1 (cIAP1) [18], and the proteasome inhibitor protein PI31 [16]. Last, FBXO7 was shown to possess SCF-independent transforming activity by enhancing the interaction of cyclin-dependent-kinase CDK6 with its targets [19]. Whether these or other still unknown FBXO7 interacting-proteins are important for the neuronal function of FBXO7 and for the mechanisms of neurodegeneration remains unknown. Here, we show the existence of two FBXO7 protein isoforms in normal human cells; we characterize their subcellular localization and their differential depletion in cell lines from the patients with PARK15; last, we characterize the expression of the FBXO7 proteins in the normal human brain.

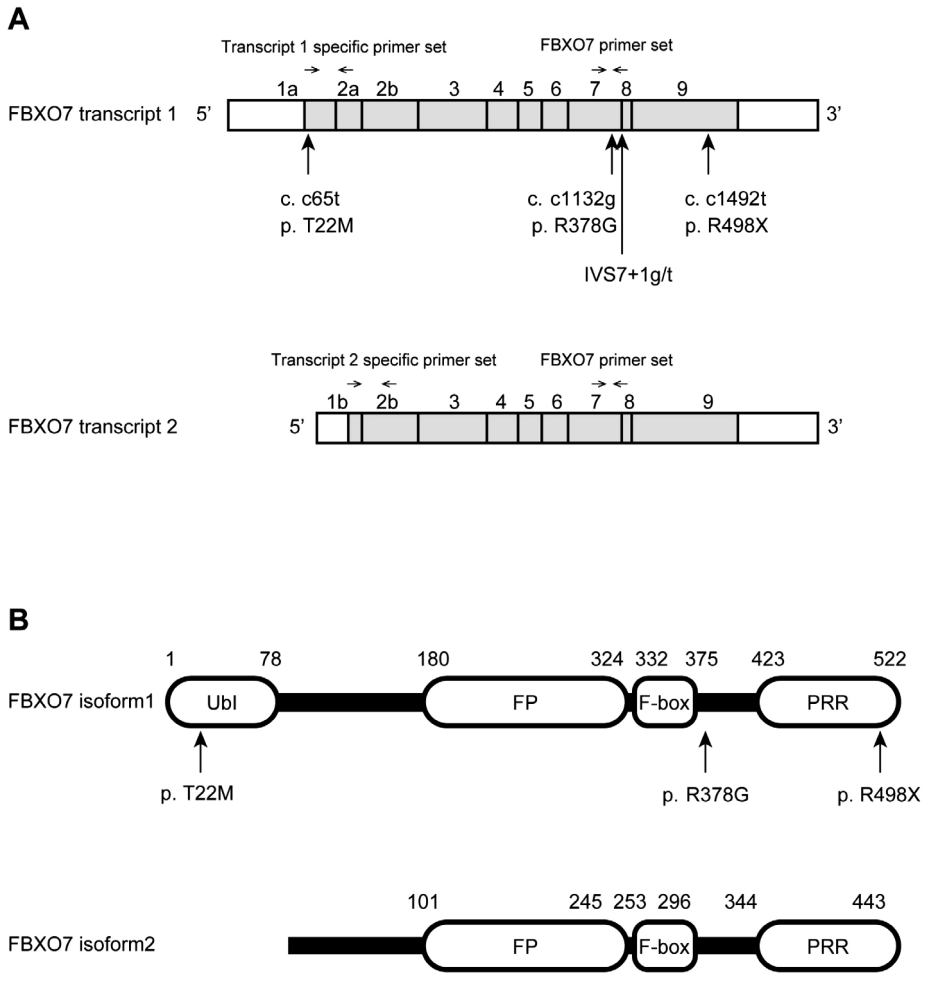

Figure 1 Schematic representation of the *FBXO7* transcripts and protein isoforms.
(A) The *FBXO7* transcripts with location of the mutations found in patients with PARK15. The location of the primers used in qPCR is indicated by arrows.
(B) Domain organization of the two FBXO7 protein isoforms.
Ubl: ubiquitin-like domain; FP: FBXO7/ PI31 domain; F-box: F-box motif; PRR: proline rich domain.

RESULTS

Expression of the FBXO7 proteins in families with PARK15

To study the expression of the endogenous FBXO7 proteins, we obtained Epstein-Barr virus (EBV)-transformed lymphoblastoid cell lines from members of the Italian and Dutch PARK15 families, and from unrelated normal controls. Fibroblast lines were also established from skin biopsies in one Dutch PARK15

patient and one unrelated control. Unfortunately, fibroblasts from the second Dutch PARK15 patient and from patients of the Italian PARK15 family were not available.

In lymphoblastoid cells from normal controls (Figures 2-3), and HEK 293T cells (Figure S1), our Western blot (WB) analysis using an antibody against FBXO7 revealed two bands of the expected molecular weight of the FBXO7 isoform 1 and isoform 2. The knock down (KD) of *FBXO7* gene in HEK 293T cells confirmed the specificity of the antibody for the FBXO7 proteins (Figure S1).

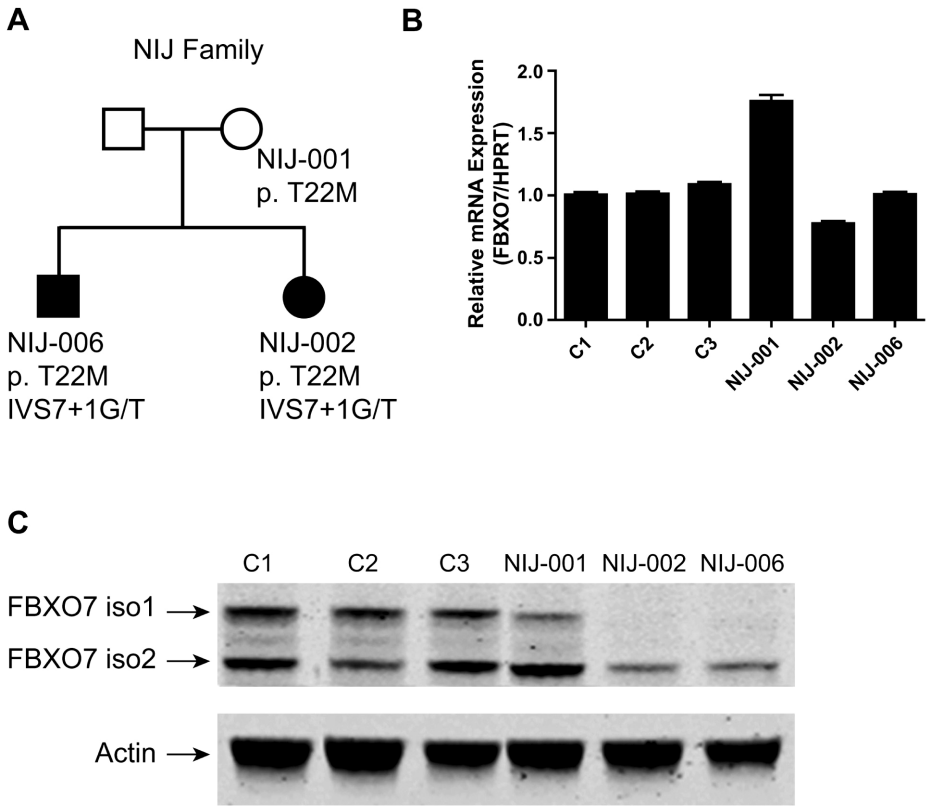

Figure 2 Expression of FBXO7 in the Dutch PARK15 family.
(A) Family pedigree and *FBXO7* genotypes.
(B) qPCR analysis of *FBXO7* mRNA (both transcript isoforms) in members of the PARK15 family and unrelated, healthy controls (C1-C3).
(C) Western blotting analysis. The two FBXO7 isoforms present in controls are altered in the mutation carriers. The isoform 1 is undetectable in the patients (NIJ-002 and NIJ-006) and decreased in the mother (NIJ-001), who also carries the mutation affecting this isoform (T22M). The isoform 2 is decreased in the patients and normal in the mother (see text for further details).

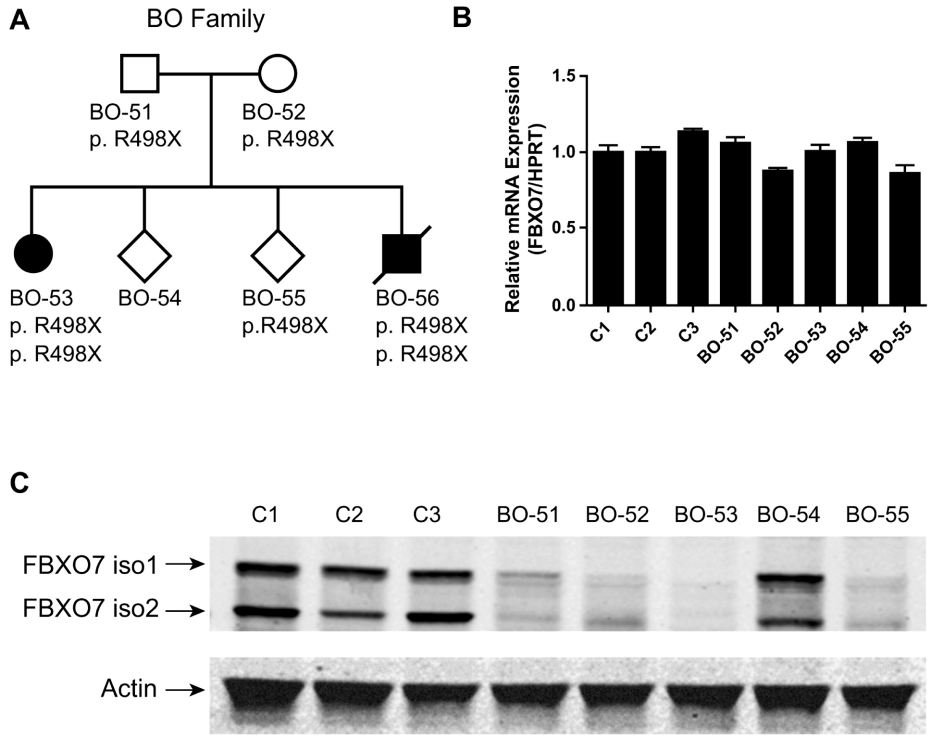

Figure 3 Expression of FBXO7 in the Italian PARK15 family.
(A) Family pedigree and *FBXO7* genotypes.
(B) qPCR analysis of *FBXO7* mRNA (both transcript isoforms) in members of the PARK15 family and unrelated, healthy controls (C1-C3).
(C) Western blotting analysis. The two FBXO7 isoforms present in controls are both undetectable in the PARK15 patient (BO-53), and markedly decreased in the heterozygous mutation carriers (BO-51, BO-52, BO-55). The BO-54 subject is not a carrier of the mutation and shows normal FBXO7 expression.

In the Dutch family, two siblings were affected by PARK15 and they carried compound heterozygous *FBXO7* mutations: the splice-site mutation IVS7+1G/T, which removes the invariable splice donor of intron 7 and is expected to disrupt the splicing of both the *FBXO7* transcript isoforms; and a substitution in exon 1A, c.C65T, predicted to lead to the missense change p.T22M, but only in the longer FBXO7 protein isoform 1 (Figure 2A). We previously documented the expression of both *FBXO7* alleles in these patients, by verifying the presence of the heterozygous c.C65T mutation in cDNA from blood cells [10]. We also showed multiple aberrantly spliced transcripts resulting from the activation of cryptic splice sites in exon 7, and encoding frame-shift proteins followed by premature truncation [10]. These are usually unstable and rapidly degraded by the cell.

In the Dutch PARK15 patients, the FBXO7 isoform 1 was undetectable in WB, while the isoform 2 was detected in lower amounts (Figure 2C). The unaffected mother (NIJ-001) who only carried the T22M mutation, showed lower amount of the isoform 1, and normal amount of isoform 2. These results are compatible with lack of FBXO7 protein expression from the allele containing the IVS7+1G/T mutation, and with only isoform 2 being expressed from the allele containing the T22M mutation. In other words, the T22M mutation leads to selective depletion of the isoform 1, the only isoform in which this mutation is incorporated.

To exclude effects of these mutations at mRNA level, or presence of other, unknown mutations in linkage disequilibrium, we performed quantitative PCR (qPCR) analysis of the total FBXO7 transcripts, as well as the isoform 1-specific and the isoform 2-specific transcripts separately. These experiments showed that the *FBXO7* mRNA levels in the Dutch patients were similar to those in unrelated controls (Figure 2B and Figure S3), suggesting that the main effect of these mutations is at the level of protein stability.

The two affected siblings in the Italian PARK15 family carry an *FBXO7* homozygous nonsense mutation in exon 9, predicted to affect both transcripts (c.C1492T, according to the longer *FBXO7* transcript, protein effect p.R498X) (Figure 3A). qPCR analysis showed similar *FBXO7* mRNA levels among unrelated healthy controls, R498X heterozygous and homozygous mutation carriers (Figure 3B and Figure S3), indicating that this truncating mutation escapes nonsense-mediated mRNA decay [20]. However, in WB analysis, the R498X heterozygous carriers displayed reduced levels of both the FBXO7 protein isoforms, while the FBXO7 proteins were both undetectable in the homozygous PARK15 patient (Figure 3C). Unfortunately, the second patient in this family died before cell lines could be obtained. Thus, in the case of this nonsense mutation, the main final effect is the depletion of both FBXO7 protein isoforms, likely due to protein instability. Since this mutation only removes the last 24 residues of FBXO7, the C-terminus appears therefore very important for the stability of this protein.

Subcellular localization of wild type and mutant FBXO7

To investigate the subcellular localization of FBXO7, we transiently transfected HEK 293T cells with plasmids overexpressing the wild type (WT) or mutant FBXO7 isoform 1. Forty-eight hours after transfection we analyzed the cells by immunofluorescence and confocal microscopy. In mock transfected HEK 293T cells, a main nuclear and much weaker cytosolic staining was observed (Figure 4A). *FBXO7* stable knock-down in these cells confirmed the specificity of the

staining, which represents therefore the endogenous FBXO7 protein (Figure S2). The overexpression of the WT FBXO7 isoform 1 in HEK 293T cells resulted in a mostly nuclear staining, a pattern shared by the R378G mutant (Figure 4B and Figure 4C). A much weaker signal was still diffusely detected in the cytoplasm.

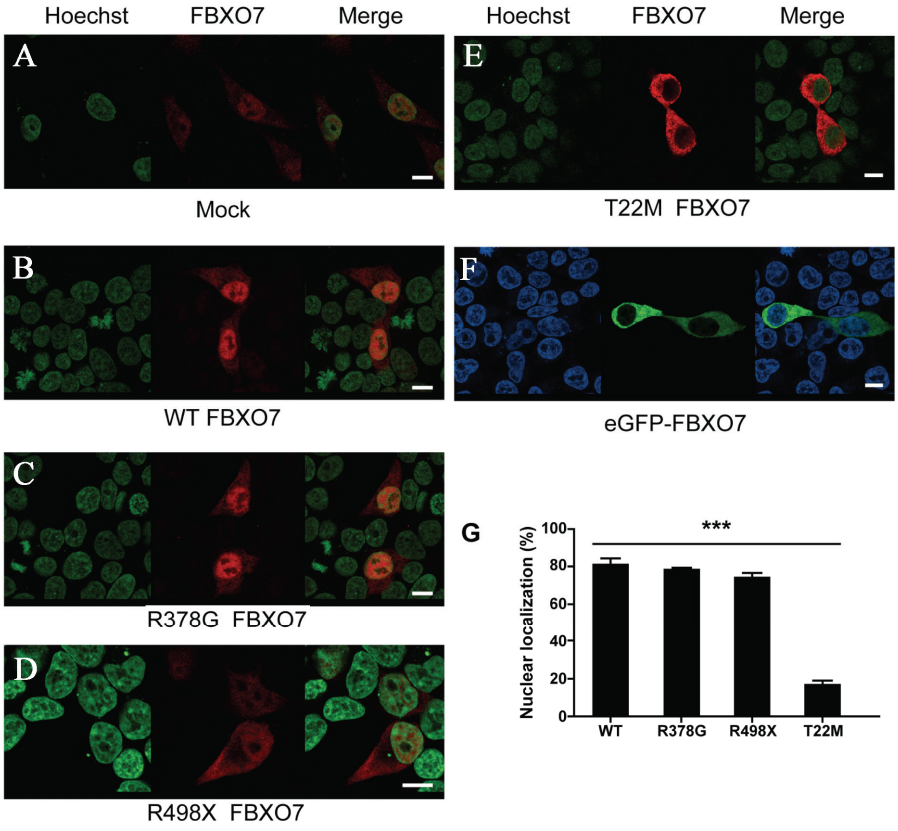

Figure 4 Localization of FBXO7 in HEK 293T cells.
Cells were transfected with empty vector (mock, A), wild type *FBXO7* (B), R378G mutant (C), R498X mutant (D), T22M mutant (E) and N-terminus-tagged *eGFP-FBXO7* (F). In panels A-E, the FBXO7 protein is visualized in red by using a mouse primary anti-FBXO7 antibody and a Cy3-coupled secondary anti-mouse antibody. In panel F, the FBXO7 protein is directly visualized by the green eGFP signal. The nucleus (Hoechst staining) is depicted in green, with the exception of panel F, where it is stained in blue (scale bars, 10 μm). (G) Quantification of the nuclear localization of FBXO7. At least 200 HEK 293T cells expressing FBXO7 were counted.
*** $p<0.01$ (chi-square test - T22M versus wild type and other FBXO7 variants)

To confirm the localization of endogenous wild type and mutant FBXO7, we performed immunofluorescence in fibroblasts from one Dutch PARK15 patient,

and one unrelated normal control (Figure 5). A pattern of mainly nuclear fluorescence (similar to that seen in HEK 293T cells in Figure 4A) was often observed in the control fibroblasts, but never in the patient fibroblasts (Figure 5). WB analysis confirmed the expression of two FBXO7 isoforms in normal fibroblasts (Figure 5D); compared with lymphoblasts, here the isoform 1 was much more abundant than isoform 2. In the fibroblasts from the Dutch PARK15 patient, the isoform 1 was undetectable by WB, while isoform 2 was detected, in agreement with the results of WB in lymphoblastoid cells from the same patient (Figure 2C). Taken together, the experiments in the patients fibroblasts show that the loss of isoform 1 (WB) is associated with the loss of immunoreactivity in the nucleus (seen in immunofluorescence). The weak cytosolic immunoreactivity is compatible with the residual expression of isoform 2 seen in this patient in WB.

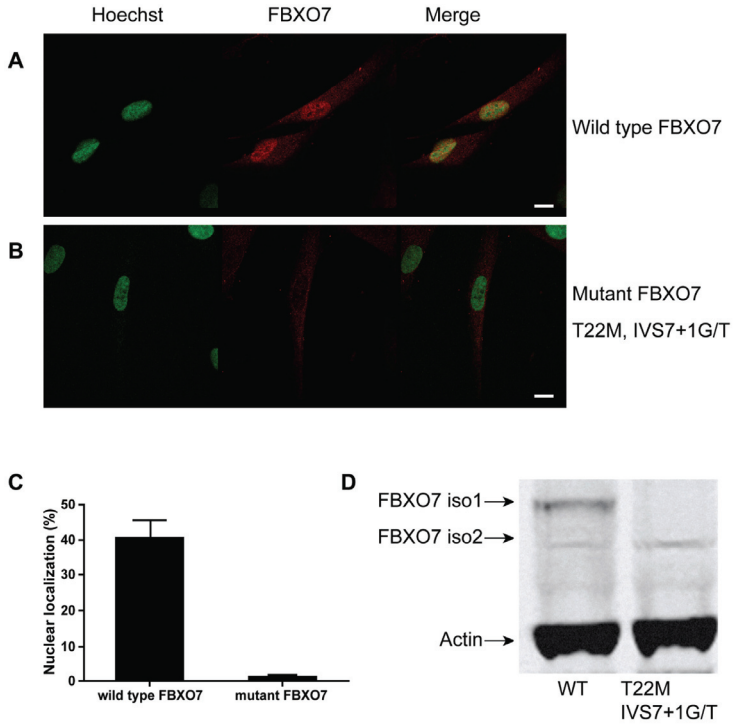

Figure 5 Expression of endogenous FBXO7 in human fibroblasts.
(A, B) For immunofluorescence, the FBXO7 protein is visualized in red by using a mouse primary anti-FBXO7 antibody and a Cy3-coupled secondary anti-mouse antibody. The nucleus (Hoechst staining) is depicted in green. (scale bars, 10 μm)
(A) normal control; (B) Dutch PARK15 patient with T22M and IVS7+1G/T mutations. (C) quantification of percentages of cells showing mainly nuclear localization of FBXO7. (D) Western blotting analysis of fibroblasts from a normal control and the Dutch PARK15 patient.

The FBXO7 R498X mutant displayed an abnormal pattern consisting of diffuse nuclear and cytosolic localization when overexpressed in HEK 293T cells (Figure 4D). Last, the T22M mutant showed the most striking aberrant pattern of mostly cytosolic localization (Figure 4E and Figure 4G). The T22M mutation is close to the N-terminus where it might impair a nuclear localization signal. To test this hypothesis, we overexpressed WT FBXO7 with an N-terminal tag (enhanced green fluorescent protein, eGFP). As expected, the N-terminal tagging totally blocked the nuclear localization of the protein (Figure 4F), mimicking the pattern of the T22M mutant. Furthermore, the first 40 amino acids of WT or T22M-mutant FBXO7 isoform 1 were cloned in front of the mCherry-labeled profilin, a well-known cytosolic protein. As a result, the WT FBXO7 N-terminal 40 amino acid peptide, but not the T22M-mutant, was able to change the localization of profilin from cytoplasm to nucleus (Figure 6).

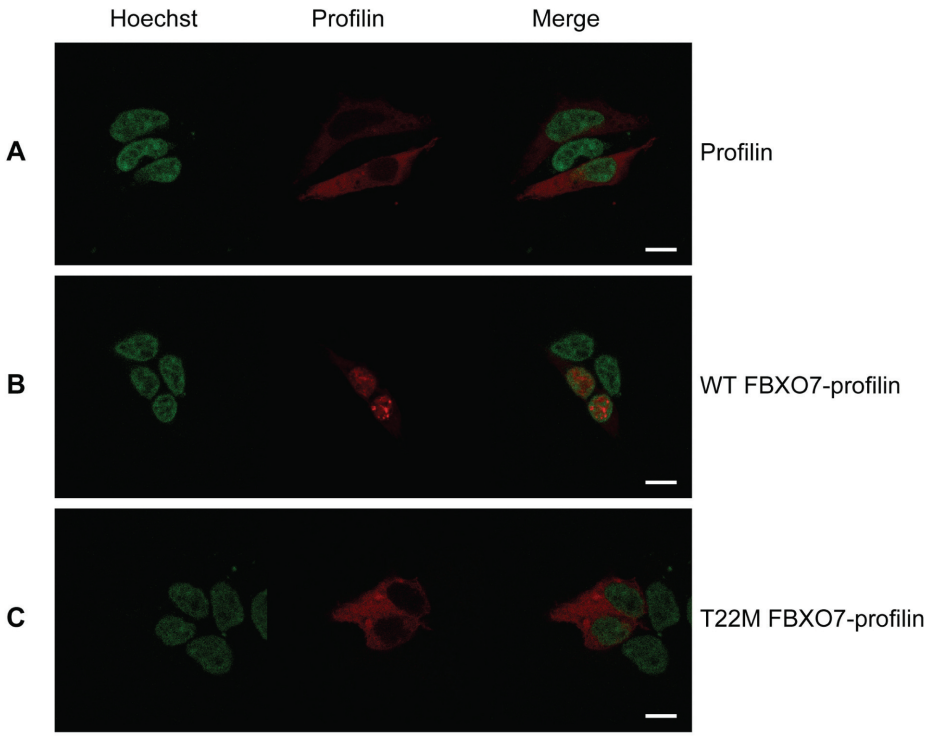

Figure 6 The N-terminus of FBXO7 confers nuclear localization to profiling.
In panel (A), Profilin, a well-known cytosolic protein, is visualized by the red mCherry signal; the nucleus is depicted in green (Hoechst staining). Expressing the first 40 amino acids of WT-FBXO7 isoform 1 in front of mCherry-labeled profilin changes the localization of profilin from the cytoplasm to the nucleus (B). The same FBXO7 N-terminal peptide carrying the T22M-mutation found in PARK15 patients is totally devoid of this capacity (C). (scale bars, 10 μm)

The localization pattern of WT- and mutant FBXO7 proteins in human neuroblastoma SH-SY5Y cells and mouse primary hippocampal neurons were similar to those described in HEK 293T cells (Figure 7A-I).

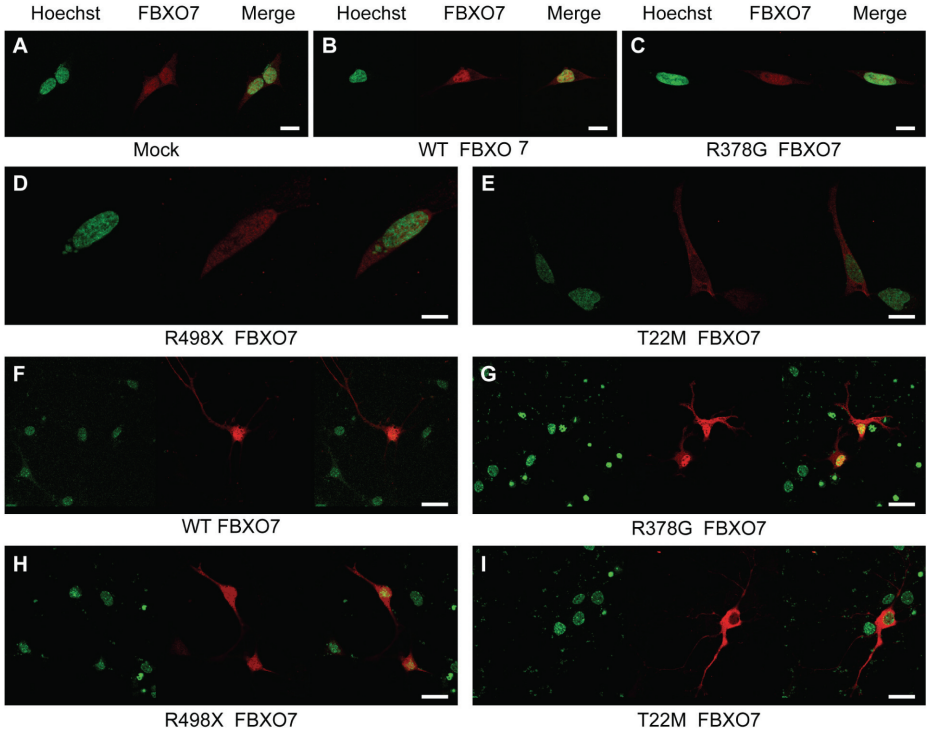

Figure 7 Localization of FBXO7 in SH-SY5Y cells and primary hippocampal neurons. Neuroblastoma SH-SY5Y cells (A-E) and mouse primary hippocampal neurons (F-I) were transfected with empty vector (mock, A), wild type FBXO7 (B, F), R378G mutant (C, G), R498X mutant (D, H), and T22M mutant (E, I) FBXO7. The FBXO7 protein is visualized in red by using a mouse primary anti-FBXO7 antibody and a Cy3-coupled secondary anti-mouse antibody. The nucleus (Hoechst staining) is depicted in green. (scale bars, 20 μm)

Stability of mutant FBXO7 *in vitro*

On the basis of the WB and qPCR observations on the cells from the PARK15 patients, we hypothesized that the missense and nonsense mutants (T22M and R498X) markedly decreased the stability of FBXO7.

To test this hypothesis, the WT and mutant *FBXO7* (T22M and R498X) were transfected in HEK 293T cells. The R378G mutant reported previously in an Iranian PARK15 family [11] was also tested. The overexpression of all these FBXO7 mutants yielded consistently and significantly decreased levels in WB

compared with their WT counterpart (Figure 8A-B). This is consistent with our observations in the patient cells and suggest that the FBXO7 mutants are rapidly degraded.

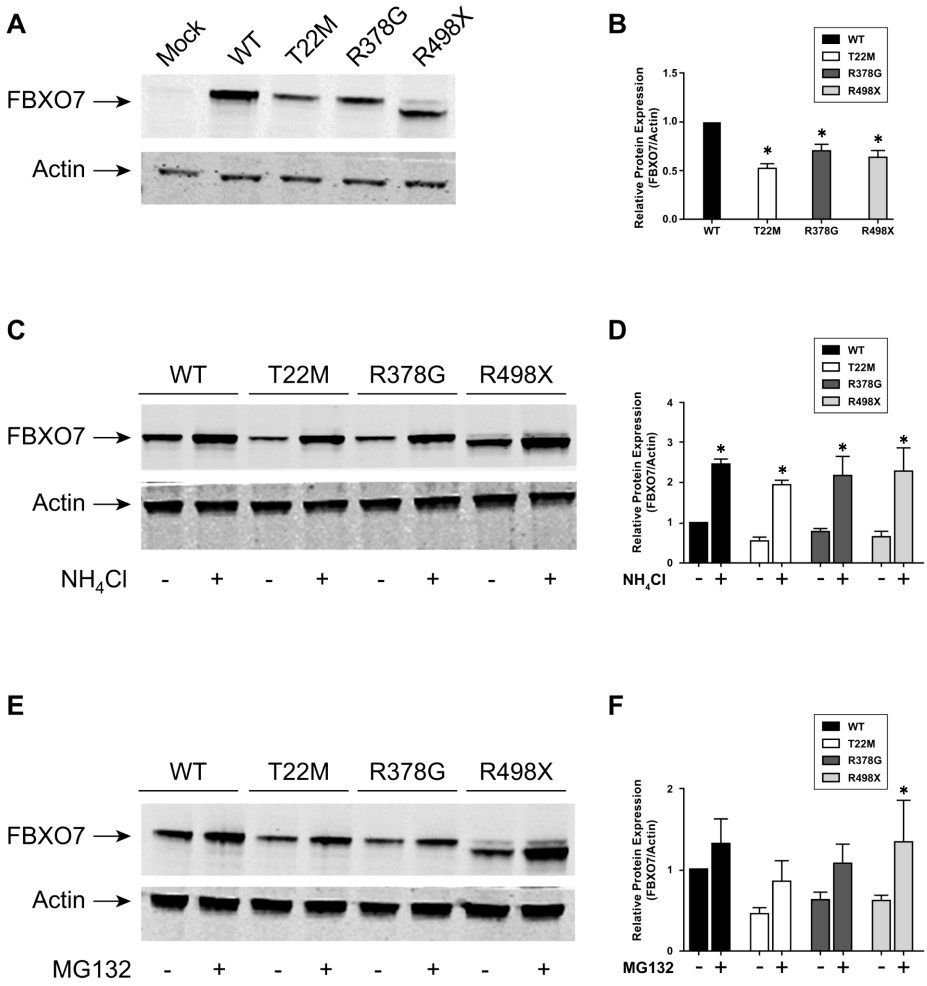

Figure 8 Overexpression of wild type and mutant FBXO7.
Overexpression of wild type and mutant FBXO7 proteins in HEK 293T cells (A), and effect of the treatment with the lysosomal inhibitor NH_4Cl (C) and the proteasomal inhibitor MG-132 (E). Actin is used as loading control. The quantification of the protein levels is shown in the right panels (B, D, and F). Asterisks in Figure 8B indicate statistical significant differences between indicated group and WT group, asterisks in Figure 8D indicate statistical significant differences between control and NH_4Cl groups, and asterisks in Figure 8F indicate statistical significant differences between control and MG132 groups.

To explore the degradation pathways of FBXO7, the lysosomal inhibitor NH_4Cl or the proteasome inhibitor MG-132 were added to the cells overexpressing WT and mutant FBXO7. Treatment with NH_4Cl strongly inhibited the degradation of FBXO7, increasing the steady-state protein expression by three to four fold (Figure 8C-D), which suggests that overexpressed FBXO7 is mainly degraded by the lysosomal pathway. The treatment with MG-132 leads to smaller increases in steady-state FBXO7 expression (Figure 8E-F), indicating a minor role of the proteasome degradation pathway. To control for the transfection efficiency, the WT and mutant *FBXO7* (T22M, R378G, and R498X) were transfected in HEK 293T cells together with the eGFP protein. Similar results were obtained (Figure S4).

FBXO7 proteins expression in the human brain

To characterize the expression of the FBXO7 proteins in the human brain, we studied the following brain regions by immunohistochemistry: frontal, temporal, and occipital cerebral cortex, hippocampus, globus pallidum, substantia nigra, and cerebellar cortex. The immunoreactivity was highest in the nuclei of neurons throughout the cerebral cortex, intermediate in neurons in the globus pallidum and the substantia nigra, and lowest in the hippocampus (Figure 9) and cerebellar cortex (not shown).

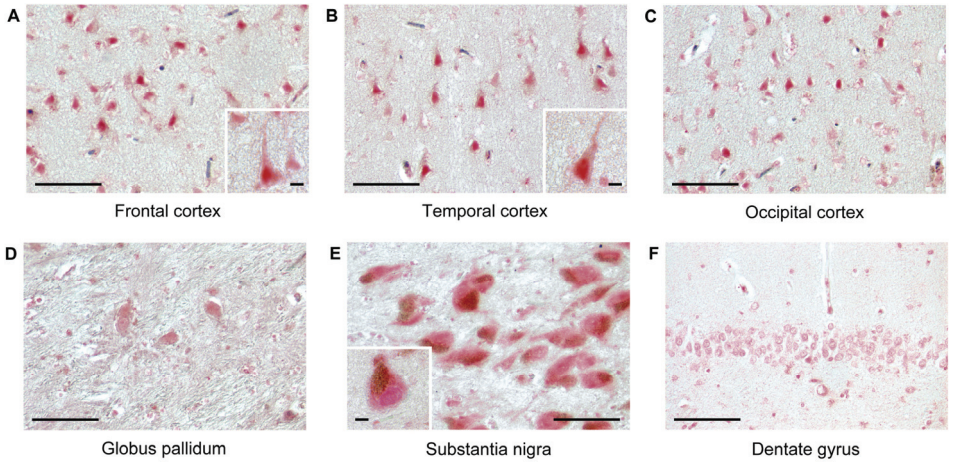

Figure 9 Expression of the FBXO7 protein in the normal human brain.
Brain sections are stained using anti-FBXO7 antibody (Abnova): frontal (A), temporal (B), and occipital (C) cortex; globus pallidum (D); substantia nigra (E); dentate gyrus of hippocampus (F). (scale bars, 100 μm)

DISCUSSION

Recessive *FBXO7* mutations are definitely established as the cause of PARK15, a novel form of juvenile neurodegenerative parkinsonism with additional pyramidal signs [10,11]. However, very little is known about the biology of the FBXO7 proteins. Even the existence of the two protein isoforms remained to be confirmed, the subcellular localization was poorly characterized, and the expression in the human brain unexplored. A localization of overexpressed FBXO7 to the cytoplasm and nucleus has been reported in previous studies which all used N-terminal tags to visualize FBXO7 (mostly isoform 1), and did not control for tag-related effects [16,18,19]. The N-terminal tagging was probably responsible for the observed cytosolic localization of FBXO7 in those studies. The localization of the over-expressed untagged FBXO7 or of the endogenous FBXO7 was not previously investigated. This uncertainty in the subcellular localization of the FBXO7 protein also complicates the interpretation of the biological plausibility of the reported interactions with other proteins. On the other hand, it is crucial to assess whether the FBXO7 disease-causing mutations affect protein stability, before these mutants are used in functional studies and conclusions are made about possible pathogenetic mechanisms.

A first important message of this study is that two FBXO7 protein isoforms are expressed in normal human cells. This contention is supported by the fact that the two FBXO7 immunoreactive bands are both undetectable in HEK 293T cells with stable *FBXO7* gene KD, and in the cells from the patients with PARK15 who carry a homozygous truncating mutation predicted to affect both the *FBXO7* transcripts. In keeping with this model, only the FBXO7 isoform 1 is markedly depleted in the Dutch patients, as one of the mutations present in those patients (T22M) is indeed only affecting the isoform 1, leaving the isoform 2 unaffected. Thus, the Dutch patients are still able to express the isoform 2 from this mutant allele, while the other allele (carrying the IVS7+1G/T splice mutation) disrupts the expression of both isoforms. Interestingly, the heterozygous mutation carriers of the Italian family, who display lower levels of both FBXO7 isoforms, remain healthy (Figure 3). On the contrary, the Dutch patients, who still express low levels of only the isoform 2, are affected (Figure 2). This strongly suggests that the depletion of the isoform 1 is the culprit for the pathogenesis of PARK15.

Furthermore, we show that the overexpressed, untagged FBXO7 isoform 1 and also the endogenous FBXO7 protein are mostly localized to the cell nucleus in two human cell models (HEK 293T and SH-SY5Y), as well as in mouse primary hippocampal neurons and human skin fibroblasts. We also show that an intact N-terminus is essential for proper nuclear localization of FBXO7 isoform 1.

Modifications in this region of FBXO7, including the missense T22M mutation or N-terminal tagging by eGFP, lead to mislocalization to the cytoplasm. These observations also support the contention that previous reports of cytoplasmic localization of FBXO7 are probably due to N-terminal tagging.

Canonical nuclear localization signals are not present in the N-terminus of FBXO7. However, nucleus localization signals might also consist of one or more short sequences of positively charged lysine or arginine residues, which are indeed present in the N-terminus of FBXO7 (Figure S5) [21,22]. The effects of N-terminal tagging would therefore be explained by the masking of these signals. How the T22M mutation prevents the nuclear localization of overexpressed FBXO7 is unclear, but the mutation might affect the interaction with other proteins which are crucial for the nuclear import of FBXO7. In support of this contention, we showed that the first 40 amino acids of FBXO7 isoform 1 are crucial for nuclear localization, as they efficiently direct profilin (a cytosolic protein) to the nucleus; however, the T22M mutation suppresses this effect. The C-terminus of the protein might also contain important motifs for nuclear import or export, as the overexpressed R498X mutant also displays an abnormal pattern of equally diffuse, cytosolic and nuclear localization.

Regarding the stability of the FBXO7 missense and truncated proteins encoded by the mutations causing PARK15, our data collectively suggest that the T22M, R378G and R498X mutants are all significantly unstable compared with the WT protein, at least in our overexpressing systems (Figure 8 and Figure S4). It is possible that the overexpressed FBXO7 mutants were insoluble and therefore not present in the cell lysate fraction. We therefore detected FBXO7 in insoluble fractions, but the amount of FBXO7 mutants was still lower than that of the WT counterpart (data not shown). Furthermore, formation of inclusions or membrane association of overexpressed FBXO7 was not observed. Last, we showed that the overexpressed WT and mutant FBXO7 are mainly degraded via the lysosomal pathway, with also a minor role of the proteasome pathway. Our data also suggest that the overexpressed R378G mutant is less stable than the WT FBXO7. The Iranian PARK15 patients might thus also suffer a severe depletion of the endogenous protein. It will be of interest to test this prediction in patients-derived cells, since we found that R378G does not significantly alter the nuclear localization in transfected cells. If sufficiently stable, this mutant protein could provide important clues about the nuclear function of FBXO7 that is lost in PARK15.

Last, we provide the initial characterization of the expression of the FBXO7 proteins in the normal human brain by immunohistochemistry. The nuclei of neurons throughout the cerebral cortex showed the strongest FBXO7 immunoreactivity, followed by the neurons in the subcortical diencephalic region, and the substantia nigra, while the lowest immunoreactivity was detected in the hippocampus and the cerebellar cortex (Figure 9 and data not shown).

Limited data on the expression of the *FBXO7* gene at mRNA level were reported in one of the studies that originally characterized this gene (named *FBX* therein) [14]. The FBXO7 mRNA appeared to be broadly expressed in human tissues, but enriched in bone marrow, liver, kidney, testis, and thyroid gland. Interestingly, a strong expression was also found in several regions of the human brain, such as the corpus callosum, caudate nucleus, substantia nigra, as well as in the spinal cord [14]. Furthermore, microarray data on the regional expression of the *FBXO7* gene in the human brain, are available in the ALLEN Human Brain Atlas website (http://www.brain-map.org, accessed on Dec. 1, 2010). In this Atlas, *FBXO7* expression levels are high in the cerebral cortex (particularly the frontal and parietal regions), the striatum, pallidum, thalamus, substantia nigra, red nucleus, and deep cerebellar nuclei, while low expression levels are documented in the hippocampus and the cerebellar cortex.

The *FBXO7* mRNA and proteins seem therefore highly expressed in the motor areas of the human brain, including both the extrapyramidal and the pyramidal systems, which fits with the clinical phenotype of parkinsonian-pyramidal disorder caused by the loss of the FBXO7 function in PARK15. Intriguingly, the widespread and abundant expression of the FBXO7 proteins in the frontal cerebral cortex suggests that additional, cognitive and behavioural disturbances of frontal type might be prominent in the phenotype. Interestingly, severe behavioural disturbances were noted in one of the Dutch PARK15 patients [10].

In conclusion, the common cellular abnormality found in the PARK15 patients from the Dutch and Italian families is the depletion of the FBXO7 isoform 1, which normally localizes mostly in the cell nucleus. The activity of FBXO7 in the nucleus appears therefore crucial for the maintenance of brain neurons and the pathogenesis of PARK15.

MATERIALS AND METHODS

Subjects

The Dutch and Italian families with *FBXO7* mutations have been described previously by some of us [10].

Ethics Statement

The study was approved by the Medical Ethical Committee (Medisch Ethische Toetsings Commissie, METC) of the Erasmus MC Rotterdam, and all participating subjects provided their informed consent.

Cell culture and transfection

Lymphoblastoid cell lines were obtained by Epstein-Barr virus (EBV) immortalization of peripheral blood cells obtained from patients and controls, according to standard protocols. The lymphoblastoid cells were cultured in RPMI 1640 medium (Gibco) supplemented with 15% fetal calf serum, 50 U/ml penicillin and 50 mg/ml streptomycin, in a humidified 5% CO_2 incubator. Human Embryonic Kidney (HEK) 293T cells, human neuroblastoma cells (SH-SY5Y), and human fibroblasts were grown in Dulbecco's modified Eagle's medium (DMEM) (Lonza). The HEK 293T cells were incubated in a humidified 5% CO_2 incubator, and the SH-SY5Y cells and fibroblasts were incubated in a humidified 10% CO_2 incubator. The HEK 293T cells were transiently transfected by polyethyleneimine (PEI, Polysciences Inc.). Lipofectamine™ LTX and PLUS™ Reagents (Invitrogen) transfection were used in SH-SY5Y cells according to the manufacturer's instructions. Furthermore, stable *FBXO7* knock down HEK 293T cells were generated using *FBXO7* shRNA (#TRCN 0000004339, Sigma); a non-targeting vector (shNT) (SHC002, Sigma) was used as control. Mouse primary hippocampal neurons were dissected and cultured as described previously [23]. After 20 days *in vitro*, the hippocampal neurons were transfected with constructs expressing wild type or mutant FBXO7 by using Lipofectamine 2000 (Invitrogen).

***FBXO7* constructs**

The full-length *FBXO7* cDNA (GenBank accession number NM_012179.3; NP_036311.3) was amplified by PCR using cDNA obtained from SH-SY5Y neuroblastoma cells as template. The PCR product was ligated into pcDNA™3.1/V5-His-TOPO (Invitrogen). After sequencing, the insert WT *FBXO7* was subcloned in frame into the mammalian expression plasmid pEGFP-C3 (BD biosciences), resulting in an N-terminal fusion protein eGFP-FBXO7. All primers used are given in the Supplementary Table S1. The untagged WT *FBXO7* was obtained using the QuikChange site-directed mutagenesis kit (Stratagene) by introducing a stop codon in front of the V5-His tag. All untagged *FBXO7* mutants (T22M, R378G, and R498X) were also prepared using the above-mentioned mutagenesis kit. The cDNA fragment encoding the first 40 amino acids of WT or T22M-mutant FBXO7 isoform 1 was amplified and subcloned in front of mCherry-labeled profilin (the mCherry-profilin construct was a gift from Josien

Levenga, Clinical Genetics Department, Erasmus MC). The complete cDNA open reading frame of all constructs was verified by direct sequencing.

Immunofluorescence

The HEK 293T and SH-SY5Y cells were seeded onto glass coverslips coated with 0.1% gelatin (Sigma-Aldrich), and transfected with untagged WT or mutant *FBXO7* constructs. The cells were fixed in 4% (w/v) paraformaldehyde in PBS for 10 minutes and permeabilized in 100% methanol for 20 minutes. The cells were then blocked with 3% bovine serum albumin (BSA, Sigma) in PBS (w/v) for 30 minutes, and probed at 4°C overnight with mouse polyclonal antibody raised against full-length FBXO7 (Abnova, 1/300). The samples were then incubated with Cy3-coupled secondary anti-mouse antibodies (Jackson ImmunoResearch, 1/200) for 1 hour. The cell nuclei were stained with Hoechst dye 33342 (Invitrogen), but the staining is shown in green color to increase image contrast. Cells were then mounted on slides with fluorescent mounting medium (DAKO). Fluorescence images were collected using a Leica SP5 confocal microscope (Leica Microsystems), and analyzed with the Leica Confocal Software.

Immunofluorescence of primary hippocampal neurons was performed 24 hours after transfection. The cells were fixed with 4% paraformaldehyde and permeabilized with staining buffer containing 50 mM Tris, 0.9% NaCl, 0.25% gelatin, and 0.5% Triton X-100, at pH 7.4. The subsequent antibody incubation was performed as described above.

Quantitative PCR (qPCR)

Total RNA was isolated by RNA Bee (TEL-TEST Inc.) from EBV-transformed lymphoblastoid cells and converted into first-strand cDNA using the iScript™ cDNA Synthesis Kit (Bio-Rad). qPCR was carried out using a KAPA SYBR® FAST qPCR Kit (Kapa Biosystems) in the ABI Prism 7300 Sequence Detection System (Applied Biosystems). Thermal cycling conditions in the ABI Prism 7300 Detection System were as follows: denaturing step (95°C for 3 minutes), followed by 35 cycles of denaturing (95°C for 5 seconds), annealing and extension (60°C for 30 seconds). Fluorescence detection and data analysis were performed by ABI Prism 7300 SDS software (version 1.3.1, Applied Biosystems). Experiments were performed in triplicate using hypoxanthine phosphoribosyl-transferase (HPRT) as the endogenous control for gene expression normalization.

The primers used for the qPCR studies, including one assay for the total *FBXO7* transcripts (isoform 1 and isoform 2), one assay specific for the isoform 1, and another assay specific for the isoform 2, are given in Supplementary Table S2.

Western Blotting

The cells were washed with cold phosphate buffer (PBS) and harvested in lysis buffer containing 20mM Tris-HCl at pH 8.0, 150mM NaCl, 1mM $NaVO_4$, 50mM NaF, 1% Triton X-100, and a protease inhibitor cocktail (Roche Molecular Biochemicals). The cells were lysed for 30 minutes on ice before centrifugation (15000 *g* for 10 minutes at 4°C), and then the total protein concentration of the supernatant was determined by using the bicinchoninic acid (BCA™) protein assay kit (Pierce) according to the manufacturer's instructions. The protein samples (40 micrograms) were separated by 6%-12% Criterion™ XT 4-12% Bis-Tris Gel (Bio-Rad), and then transferred to nitrocellulose membranes. Membranes were blocked with 5% low-fat milk powder (Fluka) in 1×PBS containing 0.1% Tween20 (PBST) for 1 hour at room temperature and incubated overnight at 4°C with mouse polyclonal antibody against full length FBXO7 (Abnova, 1/3000) and mouse monoclonal against actin (Abcam, 1/2500) or against eGFP (Roche, 1/2000). After washing 3 times with PBST, the membranes were incubated in the dark for 1 hour with PBST containing donkey anti-mouse secondary antibodies (800nm, LI-COR Biosciences Lincoln, 1/5000 dilution). After washing, the membranes were scanned using the Odyssey ™ Infrared Imager (Li-COR Biosciences). The integrated intensities of the protein bands were quantified by the Odyssey software.

Proteasome and lysosomal-mediated degradation of FBXO7 mutants

The HEK 293T cells were seeded onto 6-well plates and transfected with 1.5 µg *FBXO7* constructs; empty vector pcDNA3 (Invitrogen, Carlsbad, CA, U.S.A.) was used as mock control. To test for the proteasomal degradation of the FBXO7 protein, 40 hours after transfection the cultured medium was replaced with DMEM containing either 42 µM MG-132 (Sigma-Aldrich) or vehicle control DMSO. After 6 hours incubation, the cells were harvested and analyzed by WB. The lysosomal degradation pathway was tested by adding 30mM NH_4Cl to the cell culture 28 hours after transfection. The cells were incubated with NH_4Cl for 20 hours and harvested for WB analysis.

FBXO7 protein studies in human brain tissue

Human brain tissues were obtained from The Netherlands Brain Bank, Netherlands Institute for Neuroscience, Amsterdam. All material has been collected from donors from whom a written informed consent for brain autopsy

and the use of the material and clinical information for research purposes had been obtained by the Netherlands Brain Bank. For immunohistochemistry, paraffin-embedded sections (7 μm) were analyzed from the brain of two non-parkinsonian, non-demented male donors (age at death 76 and 81 years-old). The following regions were studied: frontal, temporal, and occipital cerebral cortex, globus pallidum, hippocampus, substantia nigra, and cerebellum. Briefly, dewaxed sections were pretreated for antigen retrieval using pressure cooking in 0.1 M sodium citrate buffer (pH 6) for 5 min. Subsequently, sections were incubated overnight with antibodies against FBXO7 (Abnova, 1:100) at 4^{o} C. The broad spectrum poly–AP powervision reagent (immunoLogic) was used for 1 hour at room temperature for visualization. Enzyme detection was performed by using 1% new fuchsin, 1% sodiumnitrite, 0.03% naphtol AS-MX phosphate (Sigma), and 0.025% levamisol (Acros) for 20 minutes at room temperature. The sections were not counterstained but directly mounted in aquamount for examination under a light microscope.

Data analysis and statistics

Quantitative data are expressed as means ± SEM based on at least three independent experiments. Statistical analyses were performed using contingency tables.

ACKNOWLEDGEMENTS

We thank the family members for their participation, Dr. Mark Nellist and Dr. Andre Hoogeveen (Dept. Clinical Genetics, Erasmus MC, Rotterdam) for their helpful advices, and Tom de Vries Lentsch for artwork.

SUPPORTING INFORMATION

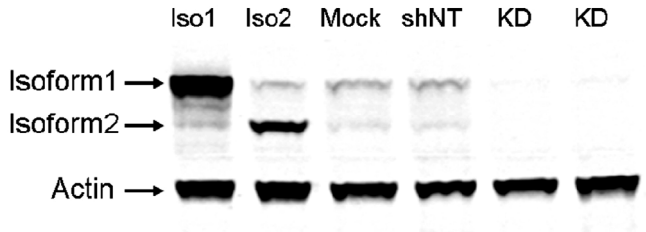

Figure S1 Validation of the specificity of the FBXO7 antibody by Western blotting in stable *FBXO7* gene knock down HEK 293T cells.
The FBXO7 protein is visualized by using a mouse anti-FBXO7 antibody (Abnova). Cells overexpressing the FBXO7 isoform 1 or isoform 2 are also shown as a reference. Actin is immunostained as loading control.
Iso1: cells transfected with FBXO7 isoform 1 expression construct
Iso2: cells transfected with FBXO7 isoform 2 expression construct
Mock: untransfected cells (endogenous FBXO7 proteins)
shNT: non-targeting shRNA
KD: *FBXO7* knock down shRNA

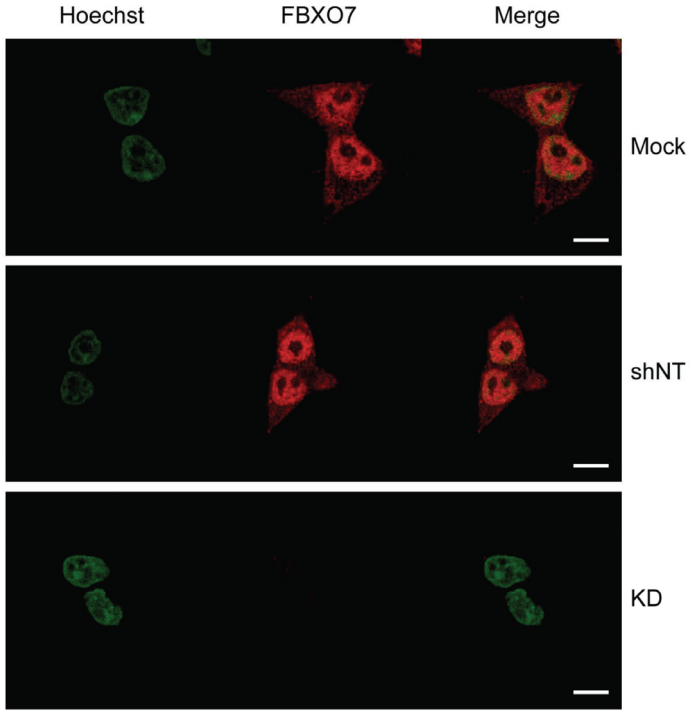

Figure S2 Validation of the specificity of the FBXO7 antibody by immunofluorescence in stable *FBXO7* gene knock down HEK 293T cells.
The endogenous FBXO7 protein is visualized in red by using a mouse primary anti-FBXO7 antibody (Abnova) and a Cy3-coupled secondary anti-mouse antibody. The nucleus (Hoechst staining) is depicted in green. (scale bars, 10 mm)
Mock: untransfected cells; shNT: non-targeting shRNA; KD: *FBXO7* knock down shRNA.

A – target transcript: *FBXO7* isoform 1; reference transcript: *HPRT*

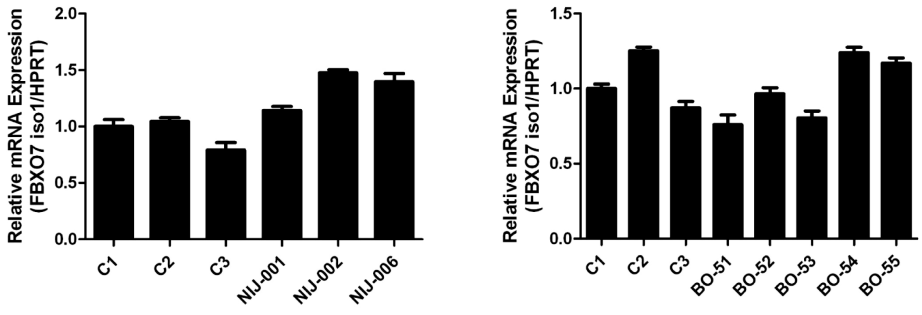

B – target transcript: *FBXO7* isoform 2; reference transcript: *HPRT*

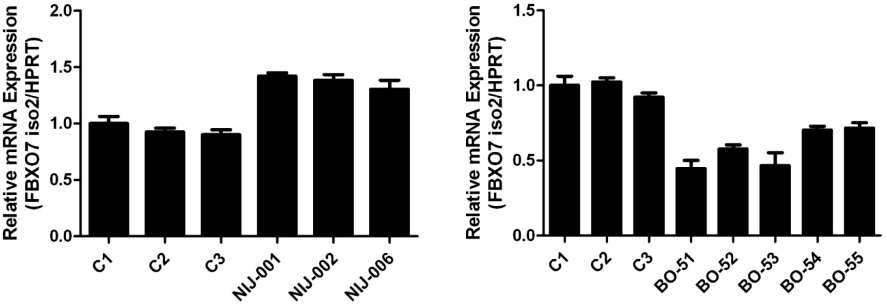

C – target transcript: *FBXO7* isoform 1; reference transcript: *FBXO7* isoform 2

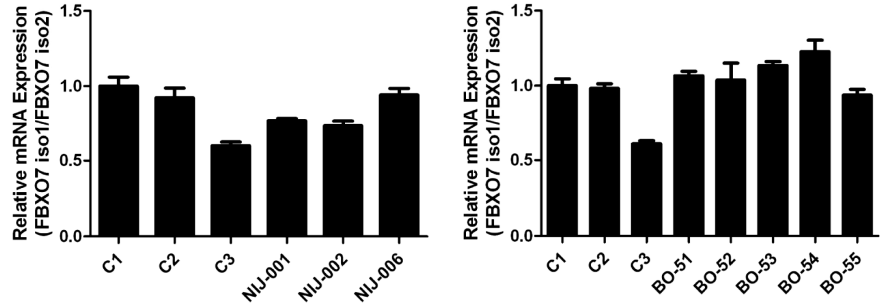

Figure S3 qPCR analysis of *FBXO7* isoform-specific transcripts in members of the PARK15 families and unrelated healthy controls (C1-C3).

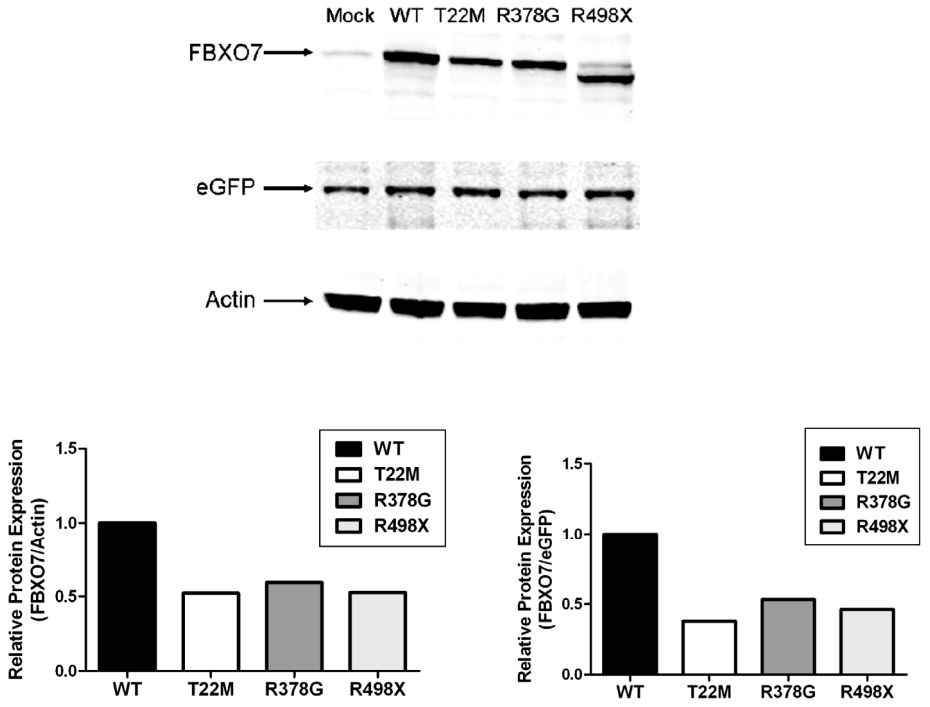

Figure S4 Overexpression of wild type and mutant FBXO7.
Wild type and mutant FBXO7 isoform 1 proteins are co-transfected with eGFP in HEK 293T cells. The eGFP is used as control of transfection efficiency, while actin is used as loading control. The quantification of the protein levels is shown as FBXO7/actin and FBXO7/eGFP ratios (Odyssey software).

mrlrvrllkrtwplevpeteptlghlrshlrqsllctwgyssntrftitlnykdpltgdeetlasygivsgd
liclilqddipapnipsstdsehsslqnneqpslatssnqtsmqdeqpsdsfqgqaaqsgvwnd
dsmlgpsqnfeaesiqdnahmaegtgfypsepmlcsesvegqvphsletlyqsadcsdanda
livlihllmlesgyipqgteakalsmpekwklsgvyklqymhplcegssatltcvplgnlivvnatlki
nneirsvkrlqllpesfickeklgenvaniykdlqklsrlfkdqlvypllaftrqalnlpdvfglvvlplelk
lrifrlldvrsvlslsavcrdlftasndpllwrflylrdfrdntvrvqdtdwkelyrkrhiqrkespkgrfv
mllpssthtipfypnplhprpfpssrlppgiiggeydqrptlpyvgdpisslipgpgetpsqfpplrpr
fdpvgplpgpnpilpgrggpndrfpfrpsrgrptdgrlsfm

Figure S5 Positively charged amino acids in the FBXO7 protein.
The positively charged amino acids in the FBXO7 protein are highlighted in yellow. Note the abundance at N-terminus.

Table S1 Primers used for molecular cloning.

Constructs	Forward primer (5'-3')	Reverse primer (5'-3')
FBXO7-V5-His	TCGCCAGTCCGGGGTCGTC	AAGCTTCATGAATGACAGCCGGCCATC
eGFP-FBXO7	CAGGAGAAGCTTAGGCTGCGGGTGCG	CGCCCGGGCTTCATGAATGACAGC
WT FBXO7	GCCGGCTGTCATTCATGTAGCTTAAGGGCAATTCTGC	GCAGAATTGCCCTTAAGCTACATGAATGACAGCCGGC
T22M FBXO7	CCCGAGACGGAGCCGATGCTGGGGCATTTGCGC	GCGCAAATGCCCCAGCATCGGCTCCGTCTCGGG
R378G FBXO7	GGAGGTTTTTATATCTGGGTGATTTTCGAGAC	GTCTCGAAAATCACCCAGATATAAAAACCTCC
R498X FBXO7	CCTAACCCCATCTTGCCAGGGTGAGGCGGCCC	GGGCCGCCTCACCCTGGCAAGATGGGGTTAGG
FBXO7-profilin	GCCAGCTAGCATGAGGCTGCGG	GCAGGCTAGCGTGTACCCCCAG

Table S2 Primers used for qPCR.

Gene	Forward primer (5'-3')	Position	Reverse primer (5'-3')	Position
FBXO7 transcript 1	AGTCCCTGCTGTGCACCTG	Exon 1a	CGCTGGAATGTCATCTTGAAGA	Exon 2a
FBXO7 transcript 2	AACATGGCCCGGCCTC	Exon 1b	TTCTGGAGTGAAGAATGCTCTGAA	Exon 2b
FBXO 7 Transcript 1 and 2	GTCTGCGGTTTGTCGTGACC	Exon 7	TCTTGAACTCTGACAGTATTG	Exon 8
HPRT	TGACACTGGCAAAACAATGCA		GGTCCTTTTCACCAGCAAGCT	

REFERENCES

1. Tolosa E, Wenning G, Poewe W (2006) The diagnosis of Parkinson's disease. Lancet Neurol 5: 75-86.
2. Gupta A, Dawson VL, Dawson TM (2008) What causes cell death in Parkinson's disease? Ann Neurol 64 Suppl 2: S3-15.
3. Gasser T (2009) Molecular pathogenesis of Parkinson disease: insights from genetic studies. Expert Rev Mol Med 11: e22.
4. Bonifati V (2007) Genetics of parkinsonism. Parkinsonism Relat Disord 13 (Suppl 3): S233-S241.
5. Healy DG, Falchi M, O'Sullivan SS, Bonifati V, Durr A, et al. (2008) Phenotype, genotype, and worldwide genetic penetrance of LRRK2-associated Parkinson's disease: a case-control study. Lancet Neurol 7: 583-590.
6. Ahlskog JE (2009) Parkin and PINK1 parkinsonism may represent nigral mitochondrial cytopathies distinct from Lewy body Parkinson's disease. Parkinsonism Relat Disord 15: 721-727.
7. Bonifati V (2010) PARK7, DJ1. In: Kompoliti K, and Verhagen Metman L (eds) Encyclopedia of Movement Disorders Oxford: Academic Press 3: 392-395.
8. Ramirez A, Heimbach A, Grundemann J, Stiller B, Hampshire D, et al. (2006) Hereditary parkinsonism with dementia is caused by mutations in ATP13A2, encoding a lysosomal type 5 P-type ATPase. Nat Genet 38: 1184-1191.
9. Gitler AD, Chesi A, Geddie ML, Strathearn KE, Hamamichi S, et al. (2009) Alpha-synuclein is part of a diverse and highly conserved interaction network that includes PARK9 and manganese toxicity. Nat Genet 41: 308-315.
10. Di Fonzo A, Dekker MC, Montagna P, Baruzzi A, Yonova EH, et al. (2009) FBXO7 mutations cause autosomal recessive, early-onset parkinsonian-pyramidal syndrome. Neurology 72: 240-245.
11. Shojaee S, Sina F, Banihosseini SS, Kazemi MH, Kalhor R, et al. (2008) Genome-wide linkage analysis of a Parkinsonian-pyramidal syndrome pedigree by 500 K SNP arrays. Am J Hum Genet 82: 1375-1384.
12. Cenciarelli C, Chiaur DS, Guardavaccaro D, Parks W, Vidal M, et al. (1999) Identification of a family of human F-box proteins. Curr Biol 9: 1177-1179.
13. Winston JT, Koepp DM, Zhu C, Elledge SJ, Harper JW (1999) A family of mammalian F-box proteins. Curr Biol 9: 1180-1182.

14. Ilyin GP, Rialland M, Pigeon C, Guguen-Guillouzo C (2000) cDNA cloning and expression analysis of new members of the mammalian F-box protein family. Genomics 67: 40-47.
15. Ho MS, Ou C, Chan YR, Chien CT, Pi H (2008) The utility F-box for protein destruction. Cell Mol Life Sci 65: 1977-2000.
16. Kirk R, Laman H, Knowles PP, Murray-Rust J, Lomonosov M, et al. (2008) Structure of a Conserved Dimerization Domain within the F-box Protein Fbxo7 and the PI31 Proteasome Inhibitor. J Biol Chem 283: 22325-22335.
17. Hsu JM, Lee YC, Yu CT, Huang CY (2004) Fbx7 functions in the SCF complex regulating Cdk1-cyclin B-phosphorylated hepatoma up-regulated protein (HURP) proteolysis by a proline-rich region. J Biol Chem 279: 32592-32602.
18. Chang YF, Cheng CM, Chang LK, Jong YJ, Yuo CY (2006) The F-box protein Fbxo7 interacts with human inhibitor of apoptosis protein cIAP1 and promotes cIAP1 ubiquitination. Biochem Biophys Res Commun 342: 1022-1026.
19. Laman H, Funes JM, Ye H, Henderson S, Galinanes-Garcia L, et al. (2005) Transforming activity of Fbxo7 is mediated specifically through regulation of cyclin D/cdk6. Embo J 24: 3104-3116.
20. Holbrook JA, Neu-Yilik G, Hentze MW, Kulozik AE (2004) Nonsense-mediated decay approaches the clinic. Nat Genet 36: 801-808.
21. Boulikas T (1994) Putative nuclear localization signals (NLS) in protein transcription factors. J Cell Biochem 55: 32-58.
22. French CA, Tambini CE, Thacker J (2003) Identification of functional domains in the RAD51L2 (RAD51C) protein and its requirement for gene conversion. J Biol Chem 278: 45445-45450.
23. Levenga J, Buijsen RA, Rife M, Moine H, Nelson DL, et al. (2009) Ultrastructural analysis of the functional domains in FMRP using primary hippocampal mouse neurons. Neurobiol Dis 35: 241-250.

4

Dopaminergic neuronal loss and dopamine-dependent locomotor defects in Fbxo7-deficient zebrafish

Tianna Zhao, Herma Zondervan-van der Linde, Lies-Anne Severijnen, Ben A. Oostra, Rob Willemsen, Vincenzo Bonifati

Submitted to PLoS ONE

ABSTRACT

Recessive mutations in the *F-box only protein* 7 (*FBXO7*) gene cause PARK15, a Mendelian form of early-onset, levodopa-responsive parkinsonism with severe loss of nigrostriatal dopaminergic neurons. The function of the protein encoded by *FBXO7*, and the pathogenesis of PARK15 remain unknown. No animal models of this disease exist. Here, we report the generation of a vertebrate model of PARK15 in zebrafish. We first show that the zebrafish Fbxo7 homolog protein (zFbxo7) is expressed abundantly in the normal zebrafish brain. Next, we used two *zFbxo7*-specific morpholinos to knock down the zFbxo7 expression. The injection of either of these *zFbxo7*-specific morpholinos in the fish embryos induced a marked decrease in the zFbxo7 protein expression, and developmental defects. Furthermore, whole-mount *in situ* mRNA hybridization showed abnormal patterning and significant decrease in the number of diencephalic *tyrosine hydroxylase*-expressing neurons, corresponding to the human nigrostriatal dopaminergic neurons. The *dopamine transporter*-expressing neurons were much more severely depleted, suggesting dopaminergic dysfunctions earlier and larger than those due to neuronal loss. Last, the zFbxo7 morphants displayed severe locomotor disturbances (bradykinesia), which were dramatically improved by the dopaminergic agonist apomorphine. The severity of these abnormalities correlated with the severity of zFbxo7 protein deficiency. The co-injection of *p53*-specific morpholinos did not modify the effects of the *zFbxo7*-specific morpholinos. In conclusion, this novel vertebrate model reproduces pathologic and behavioral hallmarks of human parkinsonism (dopaminergic neuronal loss and dopamine-dependent bradykinesia), representing therefore a valid tool for investigating the mechanisms of dopaminergic neuronal death, and screening for modifier genes and therapeutic compounds.

INTRODUCTION

Parkinson's disease (PD), the second most common neurodegenerative disorder after Alzheimer's disease, is characterized by the progressive loss of nigrostriatal dopaminergic neurons, and the formation of alpha-synuclein-containing protein aggregates, termed Lewy bodies, in surviving neurons [1]. The molecular mechanisms underlying PD remain poorly understood, but the recent identification of rare inherited forms of parkinsonism has opened novel research avenues into the disease pathogenesis [2,3]. Mutations in the *alpha-synuclein* (PARK1), *leucine-rich repeat kinase 2* (PARK8), and *vacuolar protein sorting 35* (VPS35) genes cause autosomal dominant forms, while mutations in the *parkin* (PARK2), *PINK1* (PARK6), *DJ-1* (PARK7), *ATP13A2* (PARK9), and *FBXO7* (PARK15) genes cause autosomal recessive forms of parkinsonism [3,4]. Whether the mutations in the different forms of monogenic parkinsonisms converge on the same or different cellular pathways remains currently unclear. However, understanding the mechanisms of these Mendelian parkinsonisms might provide important clues into the pathways leading to the degeneration of the dopaminergic neurons, which might also be involved in the common forms of PD. For example, there are evidences of functional links between the alpha-synuclein and the ATP13A2 pathways [5,6]. Our group characterized mutations in the *F-box only protein 7* (*FBXO7*) gene, encoding the F-box protein 7 (FBXO7), as the cause of PARK15 [7]. PARK15 patients display dramatic loss of nigrostriatal dopaminergic neurons, and they suffer from juvenile parkinsonism, with varying degrees of pyramidal disturbances. Of note, the parkinsonism displays a good response to levodopa therapy, indicating the relative integrity of the striatal neuronal circuitry acting downstream to the nigrostriatal dopaminergic defect [7,8].

FBXO7 is a member of the F-box-containing protein (FBP) family, characterized by a ~40-amino acids domain (the F-box). FBPs might become part of SCF (Skp1, Cullin1, F-box protein) ubiquitin ligase complexes, and play roles in ubiquitin-mediated proteasomal degradation [9]. We recently reported that two protein isoforms are expressed from the *FBXO7* gene, and that PARK15 patients display a severe depletion of the longer isoform, which normally localizes in the cell nucleus. The activity of FBXO7 in the nucleus appears therefore crucial for the maintenance of brain neurons in humans and the pathogenesis of PARK15 [10]. However, the precise function of the FBXO7 proteins remains largely unknown, and animal models of PARK15 have not been reported so far. Understanding why the loss of the function of this protein leads

to PARK15 might illuminate the mechanisms of selective dopaminergic neuronal death, which could also be important for PD in general.

There is a growing interest in the use of zebrafish (*Danio rerio*) for modeling neurodegenerative diseases in vertebrates [11,12]. High degrees of evolutionary conservation are present between zebrafish and human homologue proteins and pathways involved in neurodegenerative diseases. Furthermore, zebrafish offers advantages compared with other vertebrate models, including a rapid and external embryonic development, and availability of rapid and efficient tools for genetic manipulation [11,12].

Here, we report the generation of a first vertebrate animal model of PARK15 by morpholino (MO)-mediated knock-down of the *FBXO7* homologue gene in the zebrafish (*zFbxo7*). The morphants display dopaminergic neuronal loss and dopamine-dependent locomotor defects, thereby reproducing pathologic and behavioral hallmarks of the human disease. This is a novel important tool for investigating the mechanisms of selective dopaminergic neuronal death, and for the implementation of high-throughput screening of modifier genes or compounds.

RESULTS

Characterization of the *zFbxo7* gene in zebrafish

The human *FBXO7* gene **(***hFBXO7*), expresses two transcripts (ENST00000266087 and ENST00000382058), resulting from the usage of alternatively spliced 5'-exons, and encoding two FBXO7 protein isoforms of 522 and 443 amino acids (also referred to as isoform 1 and isoform 2), only differing at the N-terminus [10]. In the zebrafish genome, a single homologue to *hFBXO7*, here termed ***zFbxo7,*** is annotated (ENSDART00000082132). Its 1452-nucleotide transcript is predicted to encode a protein of 483 amino acids, which displays the same domain organization as the human longer FBXO7 isoform 1, and shows an overall 40% amino acid identity, rising to 65% identity and 78% similarity in the F-box domain (Figure 1A). The high level of sequence identity and similarity suggests functional conservation between zebrafish and human Fbxo7 proteins.

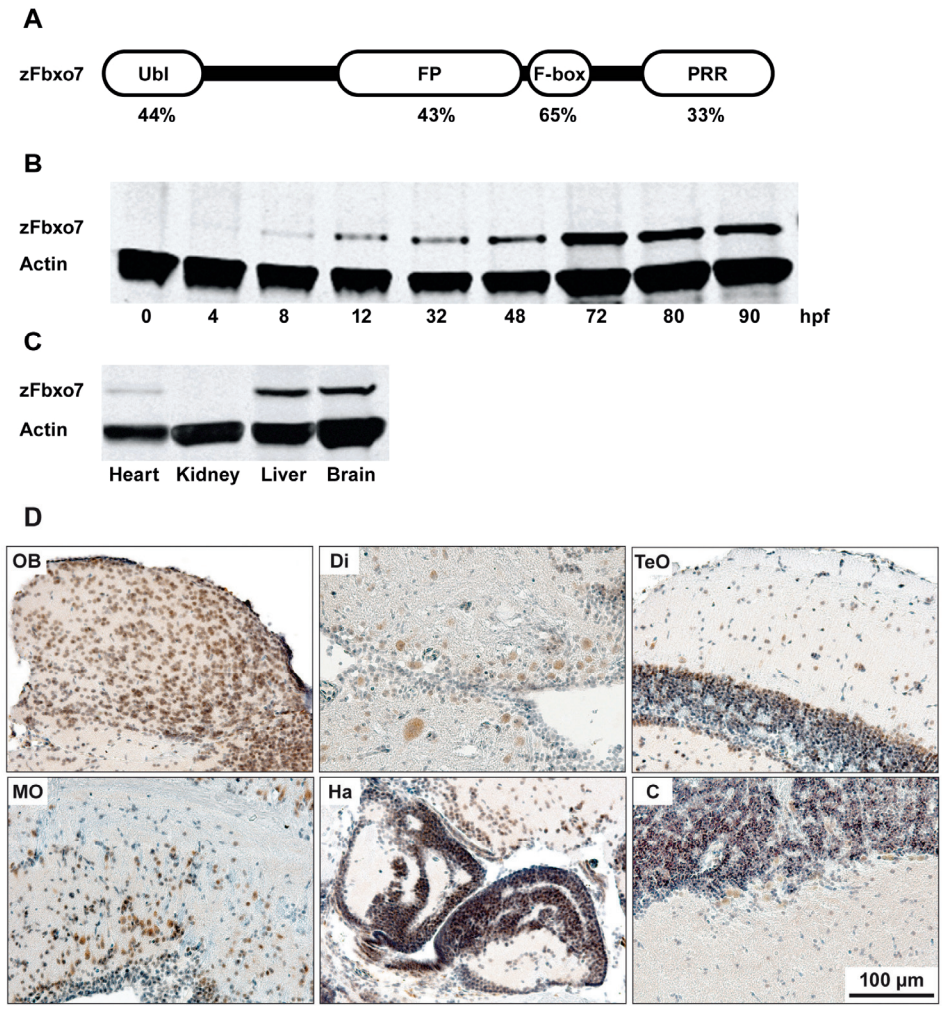

Figure 1 Characterization of the zFbxo7 protein in zebrafish.

(A) Schematic representation of the zFbxo7 functional domains. The values underneath each domain indicate the amino acids identity between zFbxo7 and hFBXO7 (isoform1). Ubl: ubiquitin-like domain; FP: FBXO7/ PI31 domain; F-box: F-box motif; PRR: proline rich domain.

(B) Western blot analysis of the zFbxo7 protein expression at different developmental stages.

(C) Western blot analysis of zFbxo7 protein expression in different tissues of eight-month-old adult zebrafish. Actin was used as reference protein.

(D) Immunostaining of the zFbxo7 protein in eight-month-old zebrafish brain areas. The zFbxo7 immunoreactivity is shown in brown, while the cell nuclei are counterstained in blue using hematoxylin. The following areas are shown: olfactory bulb (OB), diencephalon (Di), optic tectum (TeO), medulla oblongata (MO), habenula (Ha), and cerebellum (C). Scale bars: 100 µm.

To confirm our *in silico* analyses, we amplified and sequenced the *zFbxo7* cDNA from the tupfel long fin (TL) zebrafish. This revealed that the *zFbxo7* transcript is the product of 10 exons, as also annotated in Ensembl. Compared with the sequence annotated in Ensembl (ENSDART00000082132) we only detected one polymorphic variant, a heterozygous insertion of two CAG triplets at position +448 from the A of the ATG start codon, leading to in-frame incorporation of two additional residues in a glutamine stretch.

zFbxo7 protein expression throughout embryonic development and in adult tissues

The pattern of zFbxo7 protein expression was studied by Western blot (WB), using a mouse polyclonal antibody raised against full-length human FBXO7, which was previously validated by us for the human FBXO7 proteins in both WB and immunohistochemistry [10]. A single band corresponding to the predicted size of the zebrafish zFbxo7 protein was detectable at 12 hours post fertilization (hpf), which gradually increased in abundance during pharyngula, hatching stages, reaching a peak at the larvae stage (72 hpf) (Figure 1B). In 8-month-old adult wild type (WT) zebrafish, the zFbxo7 protein was abundantly expressed in the brain and liver, and hardly detected in the heart and kidney (Figure 1C). We further characterized the expression of the zFbxo7 protein in the brain by immunohistochemistry using the same antibody. The zFbxo7 immunoreactivity was ubiquitously present, more prominent in neurons of the olfactory bulb and diencephalon, intermediate in cerebellum and medulla oblongata, and weaker in the optic tectum and habenula (Figure 1D).

Knock down of zFbxo7 results in developmental defects

Two non-overlapping zFbxo7 MOs were designed, one targeting the ATG translation initiation site (ATG-start-codon-targeting MO, ATG-MO) and the other targeting the exon2/intron2 splice site (splice-site-targeting MO, SP-MO) of *zFbxo7*, respectively. The MOs were injected into the embryo yolk at one-cell or two-cell stage. No gross morphological abnormalities were observed at 24 hpf and 48 hpf in the MOs injected embryos, compared to non-injected ones (data not shown). A range of morphological phenotypes was observed at 72 hpf, including curly tails, heart edema, and heart malformations (Figure 2A). These phenotypes were similar in the morphants treated with ATG-MO and in those treated with SP-MO. The morphants were then divided in two groups, according to the severity of their phenotypes. Lethality was also quantified. The percentages of mild and severe phenotypes and of lethality associated with the

injection of the ATG-MO and the SP-MO (N=300 morphants for each of the two MO), are shown in the Figure 2B. Injection of the ATG-MO resulted in 17% lethality, 42% mild phenotype (ie. characterized by heart edema and slightly curly tail, ATG-MO-Mild), and 29% severe phenotype (ie. severe heart deformation and severe curly tail, ATG-MO-Severe). The morphants injected with SP-MO showed 12% lethality, 15% mild phenotype (SP-MO-Mild) and 67% severe phenotype (SP-MO-Severe).

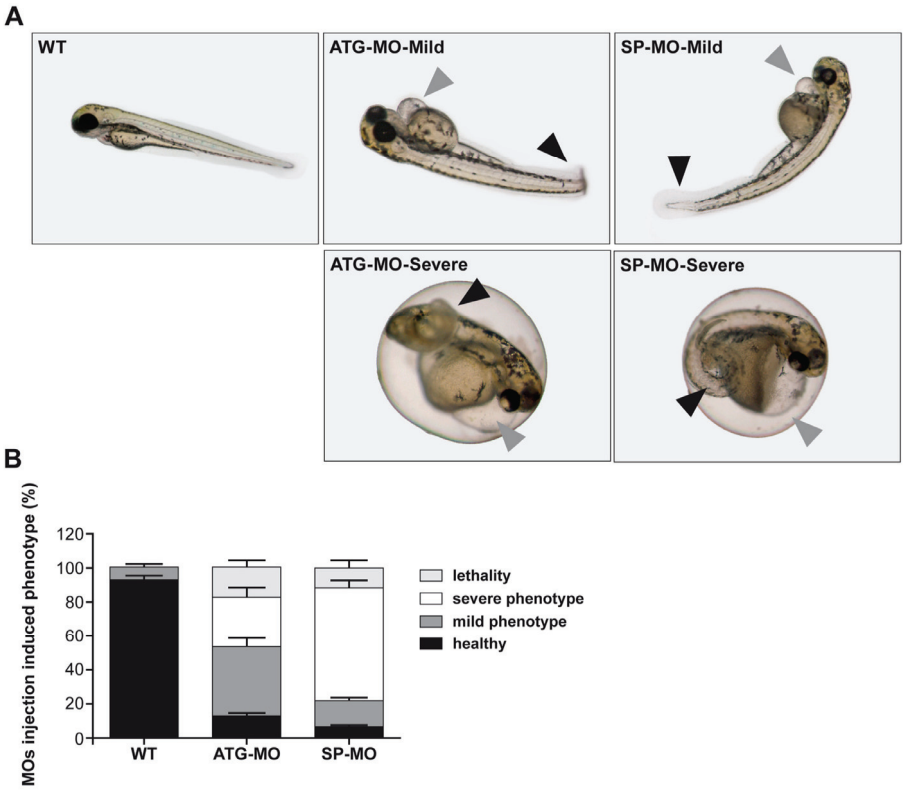

Figure 2 *zFbxo7* knock down results in developmental defects.
(A) Representative images of zebrafish wild type and morphants. Injection of ATG-MO or SP-MO induced a range of phenotypes, which were grouped in mild and severe, including curly tails (black arrowheads), heart edema and heart malformations (grey arrowheads).
(B) Percentages of healthy phenotype, mild phenotype abnormalities, severe phenotype abnormalities and lethality among uninjected control (WT) and MOs-injected morphants.

zFbxo7 knock down results in decreased zFbxo7 protein expression

The efficiency of knock-down was monitored by measuring the zFbxo7 protein levels using western blot. Markedly and significantly decreased expression

levels were observed after the injection of either MOs (Figure 3). Of note, the morphants displaying severe phenotypes showed more severe zFbxo7 protein depletion (to ~16% of normal protein levels in the ATG-MO morphants, and to ~10% of normal levels in SP-MO morphants), compared with those displaying mild phenotypes (~53% of normal protein levels in the ATG-MO morphants, and ~35% of normal levels in SP-MO morphants) (Figure 3B). This correlation between severity of protein depletion and severity of phenotype was present for both *zFbxo7*-targeting MO strategies. The lowest levels of zFbxo7 protein expression were seen in SP-MO-Severe morphants (Figure 3).

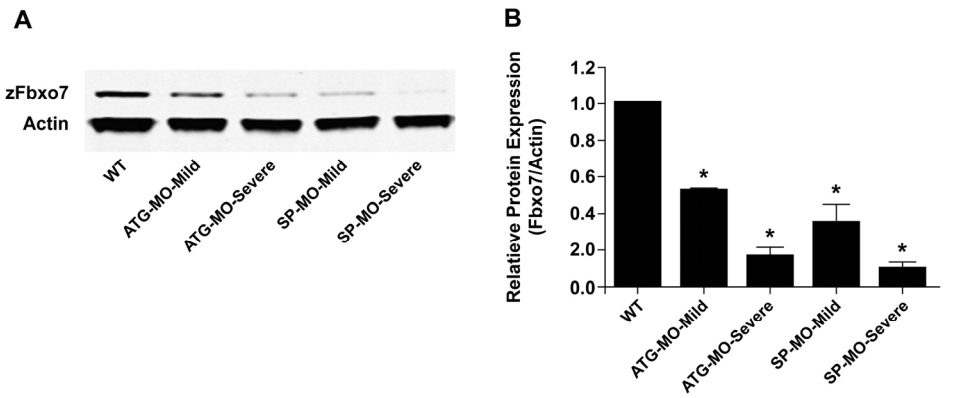

Figure 3 *zFbxo7* knock down results in decreased zFbxo7 protein expression.
(A) Western blot of the zFbxo7 protein at 72 hpf in uninjected control (WT) and MOs-injected morphants which showed mild or severe phenotype abnormalities.
(B) Quantification of the zFbxo7 protein levels is shown in panel A (Odyssey software). Data were collected from three independent experiments, $P<0.01$.

zFbxo7 knock down leads to abnormal patterning and dopaminergic neuronal cell loss

To investigate the effect of the zFbxo7 knock down on the development of the brain dopaminergic neurons, we studied the expression of the *tyrosine hydroxylase* (*th*), and the *dopamine transporter* (*slc6a3*, *dat*) mRNA, using whole mount *in situ* hybridization (WISH). Eighty morphants were analyzed in each experiment. In the zFbxo7 morphants, the patterning of the th^+/dat^+ diencephalic dopaminergic neurons was disturbed (neurons were organized in more compact groups) compared to wild type animals (Figure 4A and 4C). Furthermore, a significant reduction (40%) in the number of th^+ neurons was seen, but only in the SP-MO-severe morphants compared with WT zebrafish (Figure 4A and 4B). On the contrary, the number of dat^+ neurons was significantly reduced in both

the ATG-MO and SP-MO morphants, and more dramatically in the morphants with more severe phenotypes (ATG-MO-Severe and SP-MO-Severe) where the *dat*$^{+}$ neurons were hardly detectable (Figure 4C and 4D).

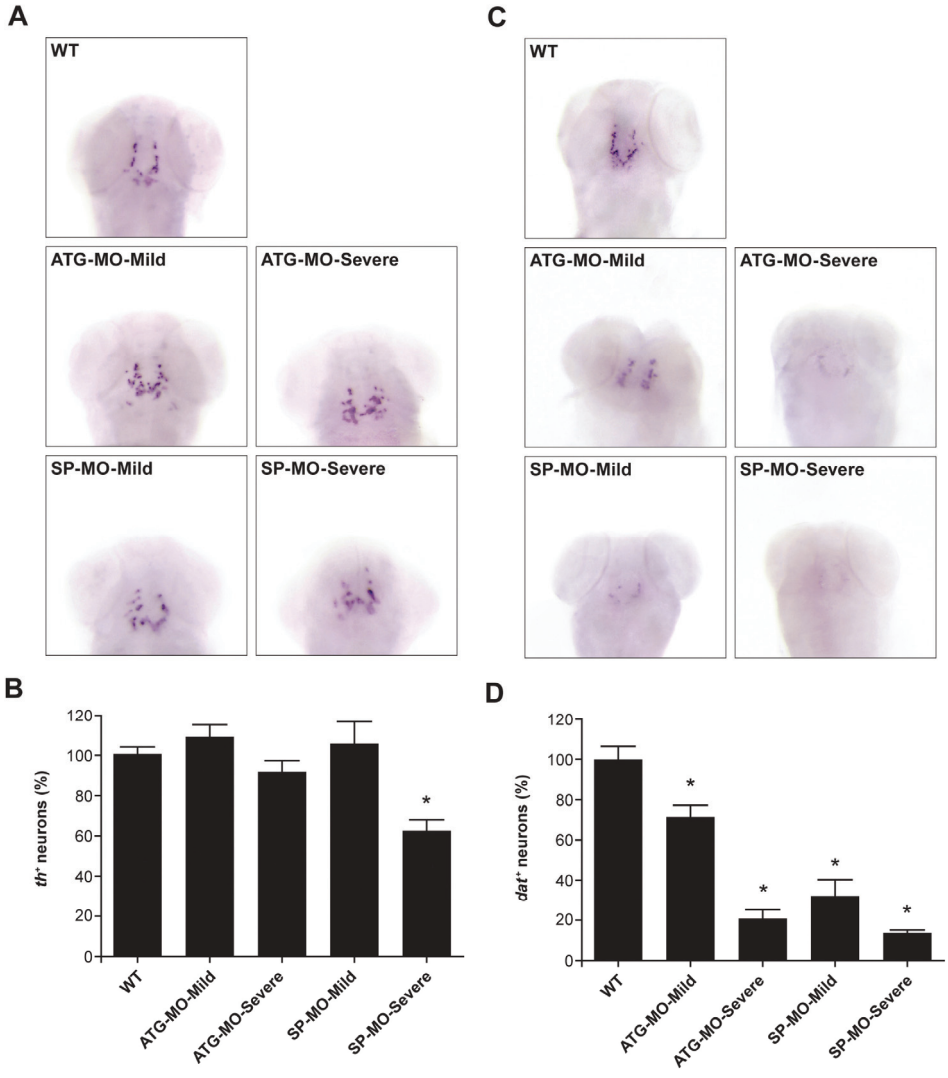

Figure 4 *zFbxo7* knock down results in dopaminergic neuronal cell loss.
The brain catecholaminergic neurons were visualized by whole-mount *in situ* hybridization using antisense RNA probes specific for *tyrosine hydroxylase* (panel A) or *dopamine transporter* (panel C). Number of neurons were counted manually and normalized to the counts in wild type zebrafish (panels B and D). * P<0.01

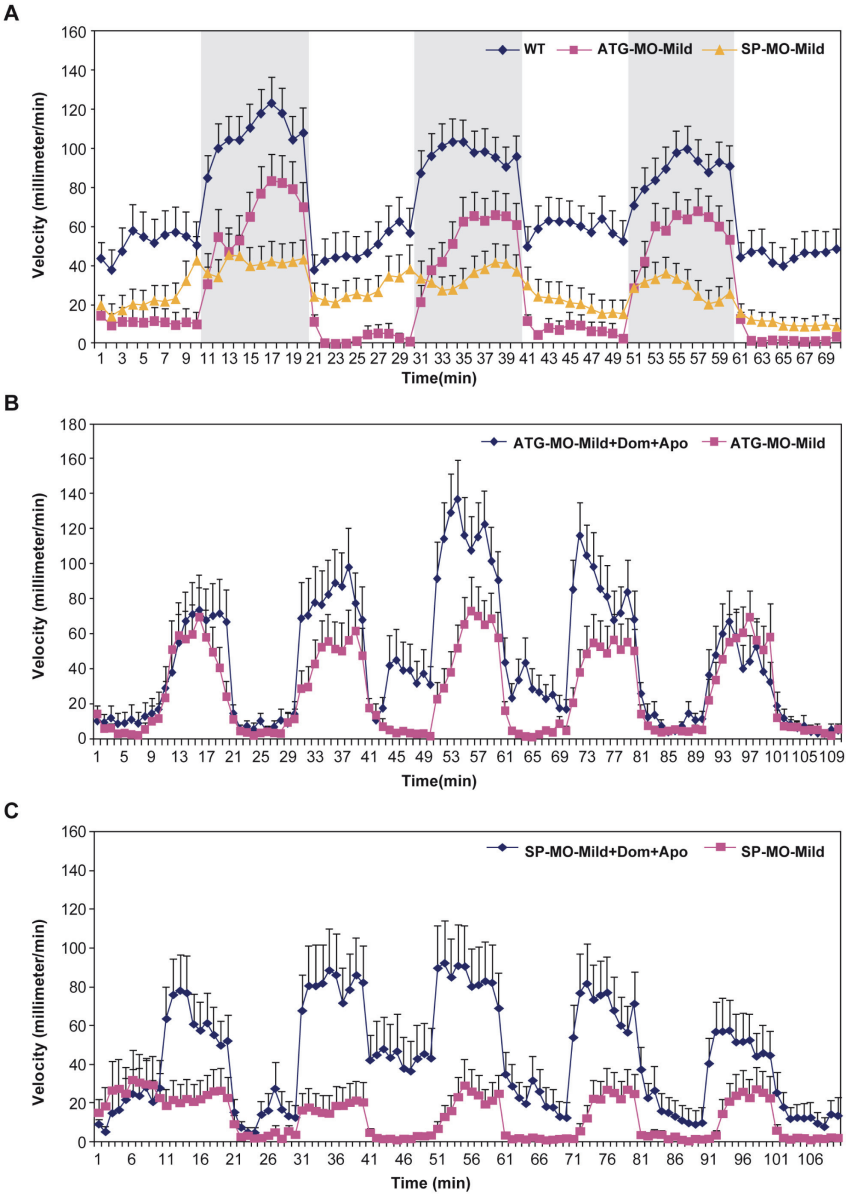

Figure 5 *zFbxo7* knock down results in locomotor defects, which are improved by apomorphine.

The movements of WT zebrafish, ATG-MO-Mild and SP-MO-Mild morphants were recorded during three cycles of 10-minutes light / 10-minutes darkness (periods of darkness are shown in grey). Compared with WT, morphants showed significantly decreased velocity in both light and dark phases (P<0.01, panel A), which were significantly improved by treatment with apomorphine (P<0.01 in the dark phase, panels B and C).

Dom: domperidone. Apo: apomorphine.

***zFbxo7* knock down results in locomotor defects, which are improved by apomorphine**

ATG-MO-Severe and SP-MO-Severe morphants showed hardly any motor activities. Further locomotor analyses were therefore focused on the ATG-MO-Mild and SP-MO-Mild morphants. In order to assess the locomotor behavior, the swimming velocity was automatically measured in wild type zebrafish and morphants at 96 hpf, during cycles of light/darkness. Both the ATG-MO-Mild and SP-MO-Mild morphants displayed significantly decreased swimming velocity, compared to wild type zebrafish (Figure 5A).

In order to assess whether these locomotor defects are dependent by the dopamine deficiency in the brain (and not by general developmental delay), we studied the effects of apomorphine, a potent, direct dopamine agonist, also used in the treatment of PD patients. In order to prevent unwanted effects of apomorphine on the peripheral (extra-cerebral) dopamine receptors, we first exposed the animals to domperidone, a dopamine-receptor peripheral antagonist that does not cross the blood-brain barrier. Domperidone is also widely used in humans to prevent the peripheral side effects of apomorphine and other dopamine agonists (vomiting, hypotension).

We first show that no locomotor effects are detectable after placing either wild type zebrafish or morphants in water containing domperidone alone, at a concentration of up to 3µM (Supplementary Material, Figure S2B and S2C). We then exposed wild type and morphants to water containing 3µM domperidone and 3µM apomorphine. While no effects were detectable in the wild type animals, the swimming defects in the morphants were markedly and significantly improved, their performances reaching levels similar to those of the wild type animals (Figure 5B and 5C).

Off-target effects due to MO-induced p53 activation are not detected

To prevent off-target MOs effects due to activation of p53 expression, a specific *p53*-targeting MO was co-injected with *zFbxo7*-specific MOs (Figure 6A). The frequency of healthy phenotype, mild phenotype abnormalities, severe phenotype abnormalities, and lethality, among uninjected controls, single-injected morphants, and morphants co-injected with *p53*-targeting MO, was unchanged (Figure 6B). These results indicate that the observed phenotypes are not due to off-target effects mediated by the induction of p53 expression.

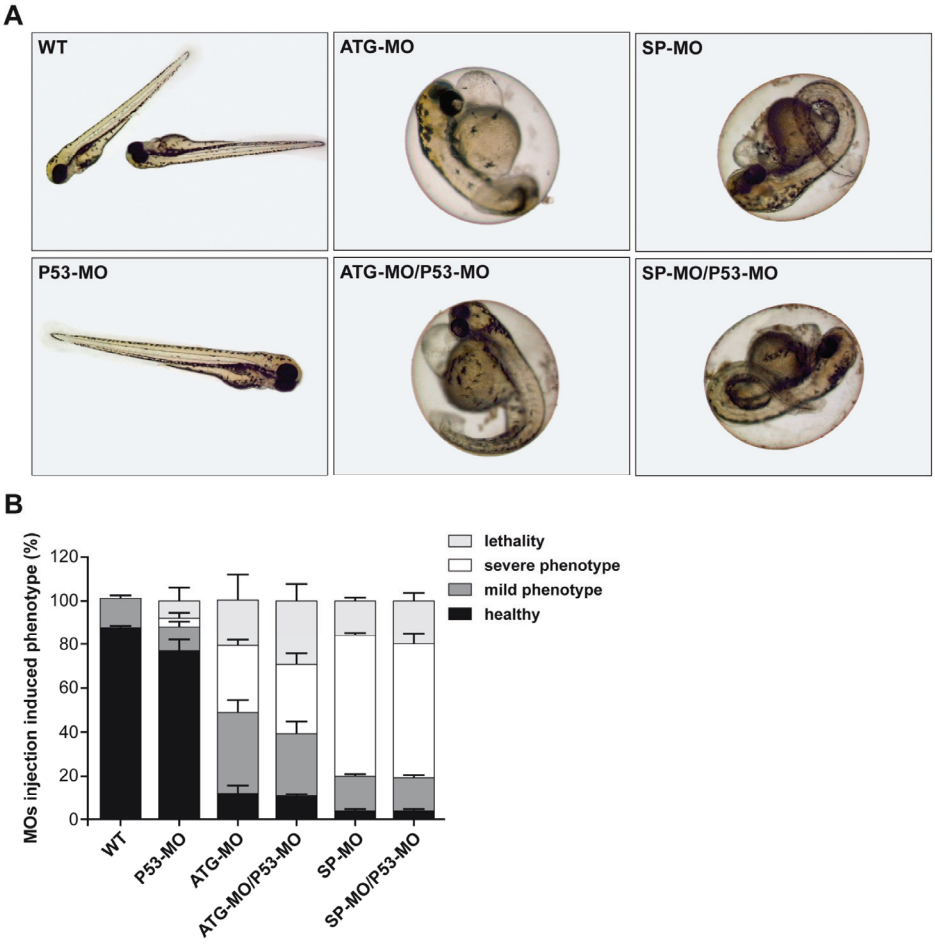

Figure 6 Off-target effects due to MO-induced p53 activation are not detected.
(A) Representative images of zebrafish embryos treated with single MO injection (ATG-MO, SP-MO or P53-MO) or co-injection (ATG-MO/P53-MO or SP-MO/P53-MO).
(B) Percentage of healthy phenotype, mild phenotype abnormalities, severe phenotype abnormalities and lethality among uninjected control (WT), single injected morphants and co-injected morphants.

Rescue of the phenotypes associated with *zFbxo7* MOs injection

In order to rescue the phenotypes associated to *zFbxo7* MOs injection, human *FBXO7* (*hFBXO7)* mRNA was prepared, and the quality confirmed by *in vitro* translation (Supplementary Material, Figure S1A). The hFBXO7 protein is ~5 kDa larger than the zFbxo7 protein, and therefore, these two proteins can be easily distinguished by Western blot. However, when co-injected together with *zFbxo7* MOs, the *hFBXO7* mRNA failed to rescue the morphological phenotypes

induced by *zFbxo7* MOs (data not shown). The analysis of the temporal pattern of expression showed strong levels of the exogenous hFBXO7 protein at 8 hpf, which quickly wore off and disappeared at 48 hpf (Supplementary Material, Figure S1B). On the contrary, the levels of the endogenous zFbxo7 protein were almost undetectable before 12 hpf, and increased gradually until 72 hpf (Figure 1B). The discrepancy between the time course of expression of the exogenous hFBXO7 and the endogenous zFbxo7 protein (which could be due to the usage of different promoters) is likely the explanation of the lack of rescuing effects.

DISCUSSION

PARK15 is an autosomal recessive disease, caused by the loss of function of the proteins encoded by the *FBXO7* gene [7], and in particular, by the loss of the function of the longer FBXO7 isoform (isoform 1), which localizes in the cell nucleus [10]. However, how the loss of this function leads to neurodegeneration with massive, early death of the nigrostriatal dopaminergic neurons remains unknown. Here, we establish the first zebrafish model of PARK15, by transient knock down of the *zFbxo7* expression using MOs. We show that two different, non-overlapping *zFbxo7* MOs are able to efficiently knock down the zFbxo7 protein expression, resulting in developmental defects, abnormalities at the level of the patterning and number of the brain dopamine neurons, and locomotor defects. These last defects are dramatically improved by the dopamine agonist apomorphine.

Tyrosine hydroxylase (Th), the rate-limiting enzyme in the synthesis of dopamine and other catecholamines, is expressed by all the catecholaminergic neurons (dopaminergic, noradrenergic and adrenergic) [13,14]. On the contrary, the dopamine transporter (Dat) is a specific dopaminergic neuronal marker [15,16]. In wild type zebrafish, diencephalic clusters of th^{+}/dat^{+} dopaminergic neurons are present, which project to the ventral telencephalon, and are equivalent of the human nigrostriatal dopaminergic neurons (Figure 4A and 4C) [17,18].

Th or Dat staining at the level of mRNA (WISH) or protein (immuno-histochemistry) are widely used to assess the number of dopaminergic neurons in animal models of PD, including the zebrafish (reviewed in [11,12]). Zebrafish knock down models have been previously generated targeting the homologues of other PD-causing genes, including *PARKIN* [19,20], *PINK1* [21,22,23], *DJ-1* [24,25], and *LRRK2* [26,27], while the *alpha-synuclein gene* has no homologue in zebrafish [28]. Overall, the results of these studies have not been very

consistent, depending in part from the different knock out strategies and efficiencies. Also, off-target effects were not entirely excluded in some studies reporting the most severe phenotypes [21]. Of note, none of the previous models has shown robust evidence of dopaminergic neuronal loss, together with, dopamine-dependent behavioral abnormalities. Instead, the zFbxo7 knock down model described here yields abnormalities at the level of both patterning and number of the brain dopamine neurons, as well as dopamine-dependent locomotor defects.

We show that the depletion of zFbxo7 alters the patterning of the th^+/dat^+ diencephalic dopaminergic neurons (Figure 4A and 4C), suggesting an important role for the zFbxo7 protein in the development of the brain dopaminergic systems. A similar disturbance of dopaminergic neuronal patterning, without neuronal loss, has been reported after the knock down of the zebrafish homologue of human *PINK1* [23].

We also show that the number of th^+ neurons is significantly reduced (by 40%), in the morphants with most severe phenotypes, and using the SP-MO morpholinos (Figure 4A and 4B). Similar loss of th^+ neurons (~40%) was previously reported in one knock down model of the zebrafish *PINK1* homologue [21], though off-target effects were not excluded, and subsequent studies did not report that phenotype [22,23,29]. A milder (~20%) loss of th^+ neurons was reported in one knock down model of the zebrafish *PARKIN* homologue, in absence of behavioral abnormalities [19], while neither loss of th^+ neurons nor behavioral phenotypes were reported in a second study using a different knock down strategy for the *PARKIN* zebrafish homologue [20]. Loss of th^+ neurons was not reported in two knock down studies of the zebrafish *DJ-1* homologue [24,25], while they were detected in only one of two knock down studies of the zebrafish *LRRK2* homologue [26,27].

Of note, the *dat* expression was not investigated in most of these previous studies, which only used *th* expression to assess the integrity of the dopaminergic neurons. Intriguingly, we found that the number of dat^+ neurons was reduced much more than the number of the th^+ neurons, in both the ATG- and SP-MOs morphants, and even more dramatically in the morphants with more severe phenotypes (Figure 4C and 4D). This discrepancy between the reduction in the th^+ and dat^+ neurons might indicate, in part, a selective loss of dopaminergic neurons, within the larger compartment of the catecholaminergic

neurons. However, this pattern more likely indicates the presence of surviving *th*$^{+}$ dopaminergic neurons with down-regulated *dat* expression. The same pattern (reduced DAT in preserved DA neurons) is seen *in vivo* in humans with genetic forms of PD by PET imaging in the earlier stages of dopaminergic neuronal degeneration. This represents a compensatory neuronal reaction aimed to maintain sufficient synaptic dopamine levels by down-regulating the DAT-mediated presynaptic reuptake of the neurotransmitter [30].

As a behavioral correlate, there are marked locomotor defects in the morphants injected with both *zFbxo7* MOs, and more importantly, these defects are dramatically improved by a direct, centrally-acting dopamine agonist, apomorphine. Of note, we prevented the effects of apomorphine on the peripheral dopamine receptors by co-administering domperidone, a dopamine-receptor antagonist that does not cross the blood-brain barrier. In these conditions, the observed effects are due to the action of apomorphine on dopamine receptors within the brain. The dopamine-dependence of the locomotor defects (bradykinesia) is a hallmark of PARK15 and PD in general, and it indicates the presence of presynaptic lesions at the level of the nigrostriatal dopaminergic neurons, in the context of preserved post-synaptic dopamine receptor and downstream brain circuitry. This hallmark feature is thus reproduced in the zebrafish *fbxo7* model.

The specificity of MO-mediated gene knock down is an important issue in zebrafish models. In this study, we used two non-overlapping MOs, targeting the ATG start codon and the intron2/exon2 splice site of *zFbxo7*, respectively. Both of them resulted in efficient zFbxo7 depletion (measured by western blot), and qualitatively similar neuronal phenotypes. This is the first evidence that the effects are due to the specific knock down of the zFbxo7 protein. Furthermore, the degree of zFbxo7 protein depletion correlated with the severity of embryonic development defects, of neuronal abnormalities and of the locomotor phenotypes. This is a second argument in support that the observed phenotypes are specifically due to the depletion of the zFbxo7 protein. It is well-known that the injection of MO might induce apoptosis by activating the expression of the *p53* transcription (general MO toxicity) [31,32]. Therefore, we also excluded that the observed phenotypes were caused by the activation of p53, by co-injecting *p53*-targeting MOs.

Another way to support specificity of effects would be rescuing these phenotypes by using the mRNA of the specific gene of interest. Unfortunately, here *hFBXO7* failed to rescue the morphological phenotypes induced by *zFbxo7* MOs. However, a detailed analysis of the temporal pattern of expression disclosed a clear discrepancy between the time course of expression of the exogenous hFBXO7 and the endogenous zFbxo7 protein. Moreover, it is very difficult to reproduce the cell-specific expression pattern of endogenous proteins by overexpressing exogenous proteins. The timing and localization of Fbxo7 expression might therefore be critical to its function, and the early and short-lasting expression of the *hFBXO7* mRNA is likely the explanation of the lack of rescuing effects. Lack of rescue of truly-specific effects is a well-known phenomenon in zebrafish MO-mediated modeling [11,12].

In conclusion, this novel vertebrate model reproduces pathologic and behavioral hallmarks of human parkinsonism (dopaminergic neuronal loss and dopamine-dependent bradykinesia), representing therefore a valid tool for investigating the mechanisms leading to selective dopaminergic neuronal death, screening for modifier genes or libraries of potential therapeutic compounds.

MATERIALS AND METHODS

Zebrafish maintenance

The use of zebrafish embryos for this study was approved by the Institutional Review Board for experimental animals of the Erasmus MC, Rotterdam. All procedures and conditions were in accordance with Dutch animal welfare legislation. Wild type tupfel long fin zebrafish were used for all experiments. Embryos were collected after natural spawning and raised in embryo medium containing methylene blue at 28°C under standard conditions [33].

Genetic analysis of the zebrafish *FBXO7* orthologue

The sequences of the *zFbxo7* transcript and protein (ENSDART00000082132, ENSDARP00000076569) were retrieved from Ensembl, and the zFbxo7 protein was blasted to the human FBXO7 proteins, isoform 1 (ENSP00000266087) and isoform 2 (ENSP00000371490). Total RNA was isolated from 72 hpf tupfel long fin zebrafish as described before [10], and complementary DNA was synthesized using the iScript™ cDNA Synthesis Kit (Bio-Rad) according to the manufacturer's instructions. The coding region of *zFbxo7* was amplified and sequenced (PCR primers are shown in the Supplementary Material, Table 1), and aligned to the sequence deposited in Ensembl (ENSDART00000082132).

Table 1 PCR primers used for the amplification of the *zFbxo7* cDNA.

Exon	Forward primer (5'→3')	Reverse primer (5'→3')
1, 2, 3	ACTGCGTTACTTTGACGTTTCTG	TGCTGCTGCTGCTGATCC
4	CGTCGTCTCTGGTGATCTG	CTCCAGCAGAGGGTGGACA
5, 6	TGCTCTGCTGTGAGGCTG	CAAACGCAGCAGCAGCTCA
7, 8, 9	CCTGACGAGTATGTGACAGC	TGGCCGAGGAAGGATGAC
10	TCGATCTCTCGTCTCGCT	GAGGAGAAGCAGGCTTGAC

Western blot

Zebrafish embryos at different developmental stages, as well as different organs of eight-month-old adult zebrafish were collected, and the proteins extracted by homogenization with buffer containing 10 mM HEPES, 300 mM KCl, 3 mM $MgCl_2 \cdot 6H_2O$, 100 uM $CaCl_2 \cdot 2H_2O$, 0.45% Triton X-100 and 0.05 % Tween-20, pH 7.6. Thirty µg of total protein were separated in 6%-12% Criterion™ XT 4-12% Bis-Tris Gel (Bio-Rad), and blotted with nitrocellulose membrane as previously described [10]. The primary antibodies used were: mouse polyclonal antibody raised against full-length human FBXO7 (Abnova, 1/3000), and mouse monoclonal anti-β-Actin (Sigma, 1/10000). After incubation with secondary antibody, the membrane was scanned with the Odyssey TM Infrared Imager (Li-COR Biosciences). The integrated intensities of the zFbxo7 protein bands were quantified by the Odyssey software, using Actin as loading control.

Immunohistochemistry

The brain of eight-month-old zebrafish was dissected and fixed in 4% phosphate-buffered paraformaldehyde (PFA) overnight. Paraffin embedded sections (6µm) were prepared for immunostaining. Briefly, dewaxed sections were pretreated for antigen retrieval by microwave heating in 0.1 M sodium citrate buffer (pH 6). Immunostaining was performed with mouse polyclonal antibody raised against full-length human FBXO7 (Abnova, 1/40) followed by indirect immunoperoxidase labeling and hematoxylin counterstain.

Morpholino and mRNA microinjections

Anti-sense morpholinos (MOs) were purchased from Gene Tools LLC (Philomath OR). Two MOs were designed to target *zFbxo7*: one was targeting the *zFbxo7* translation initiation site (**ATG-MO**, 5'-GAG CTT CAT TCT GTG CTT CCA GAA A-3'), and another for the *zFbxo7* exon2/intron2 splice site (**SP-MO**, 5'-GAT GAA GGT GCT CAG ACT GAC CGG A-3'). A previously described MO

targeting the translation initiation site of *p53* (**P53-MO**, 5'-GCG CCA TTG CTT TGC AAG AAT TG-3') was also used [32].

All MOs were dissolved in double distilled H_2O and diluted with Danieau solution (58mM NaCl, 0.7mM KCl, 0.4mM $MgSO_4$, 0.6 mM $Ca(NO_3)_2$, 5.0 mM HEPES pH 7.6), containing 1% phenol red as indicator. The amounts of ATG-MO and SP-MO were optimized for maximal knock-down efficiency and minimal toxicity (data not shown), and 4 ng of ATG-MO and 8 ng of SP-MO were selected for the following experiments. These MO were injected into the embryos yolk at one-cell or two-cell stage to knock down the expression of *zFbxo7*. In separate experiments, the P53-MO was co-injected with *zFbxo7*-specific MO (6 ng with ATG-MO or 8 ng with SP-MO), to prevent off-target effects due to activation of p53 expression.

Full length human *FBXO7* cDNA (*hFBXO7*) amplified by RT-PCR from peripheral mononuclear blood cells [10] was ligated into the pCR2.1-TOPO vector (Invitrogen), and subcloned at the site of *EcoR*I in pCS2+ vector [34]. The fidelity of *hFBXO7*-pCS2 was verified by direct sequencing. Using *Not*I-linearized h*FBXO7*-pCS2 as template, *hFBXO7* mRNA was generated with the mMessage mMachine SP6 kit (Ambion). To test the quality of h*FBXO7* mRNA, the *in vitro* translation was performed using Rabbit Reticulocyte Lysate System (Promega). For rescue experiments, *hFBXO7* mRNA was co-injected with *zFbxo7* MOs at one cell stage. In all the experiments, the morphology of morphants was observed at 24, 48, and 72 hpf by two investigators in blind conditions.

Whole mount *in situ* hybridization

Briefly, a digoxigenin-labelled antisense RNA probe specific for the *tyrosine hydroxylase* (*th*) transcript was synthesized from linearized pCRII-TOPO-*th* plasmid and transcribed by T7 RNA polymerase (Roche). The plasmid containing the *dopamine transporter* (*dat*, *slc6a3*) transcript was a kind gift from Dr. Edward A. Burton, Department of Neurology, University of Pittsburgh School of Medicine, Pittsburgh, PA, (USA) [35], and the corresponding RNA probe was generated by T3 RNA polymerase (Roche). Embryos were fixed overnight at 72 hpf in 4% PFA, and bleached with 10% H_2O_2 to remove pigmentation. Embryos were then transferred to 100% methanol for dehydration at -20°C for at least 24h and then the hybridization procedure was followed as previous described [36]. After staining with NBT/BCIP solution (Roche), labeled embryos were washed

with PBST (0.1% Tween 20 in PBS) in dark and mounted with 80% glycerol. The images of *th*$^{+}$ and *dat*$^{+}$ neurons were acquired and quantified by two investigators in blind fashion, under an Olympus microscope. The results are shown as percentages of the labeled neurons present in uninjected wild type embryos, staged and treated in parallel with the *zFbxo7* knock-down morphants.

Locomotor activity studies

For behavioral studies, wild type and morphant larvae were harvested at 96 hpf, and placed in 96-well plates (one larva per well) containing 150 ul of embryo medium at 28°C. The larvae were allowed to acclimatize for 15 min before starting the behavioral monitoring. DanioVision (Noldus) was used for tracking movement during three cycles of 10-min white light-on (light) and 10-min light-off (darkness). All digital tracks were analyzed by Ethovision XT software (Noldus) for velocity, and a minimum movement distance of 0.2-mm was used to filter out system noise.

For the assessment of the dopamine-dependence of the locomotor defects, morphants were first kept for one hour in water containing 3μM domperidone, an orally active compound that blocks the peripheral dopamine receptors, but does not cross the blood-brain barrier. At this concentration, domperidone induced no behavioral effects in wild type or in morphants. After the pre-treatment with domperidone, the larvae were placed in water containing 3μM apomorphine (a potent dopamine receptor full agonist), and the swimming activity was tracked during five cycles of light-on/light-off.

Data analysis

Quantitative data are expressed as means ± SEM, and each treatment group was normalized to the wild type control group. All experiments were done in triplicates, and the statistical analyses were performed using one-way ANOVA or T-test, as appropriate, with the SPSS package. The data were considered statistically significant at $P<0.01$.

ACKNOWLEDGEMENTS

We thank Dr. Edward A. Burton, Department of Neurology, University of Pittsburgh School of Medicine, Pittsburgh, PA (USA), for providing the plasmid with the zebrafish *dat*; the aquarium staff at EDC (Erasmus laboratory animal center) for the zebrafish maintenance; and Tom de Vries Lentsch (Erasmus MC) for the artwork.

CONFLICT OF INTEREST STATEMENT.

None declared.

FUNDING

This work was supported by grants from the Netherlands Organization for Scientific Research (NWO, VIDI grant n.4600268033), and the Internationaal Parkinson Fonds (The Netherlands) to VB.

SUPPORTING INFORMATION

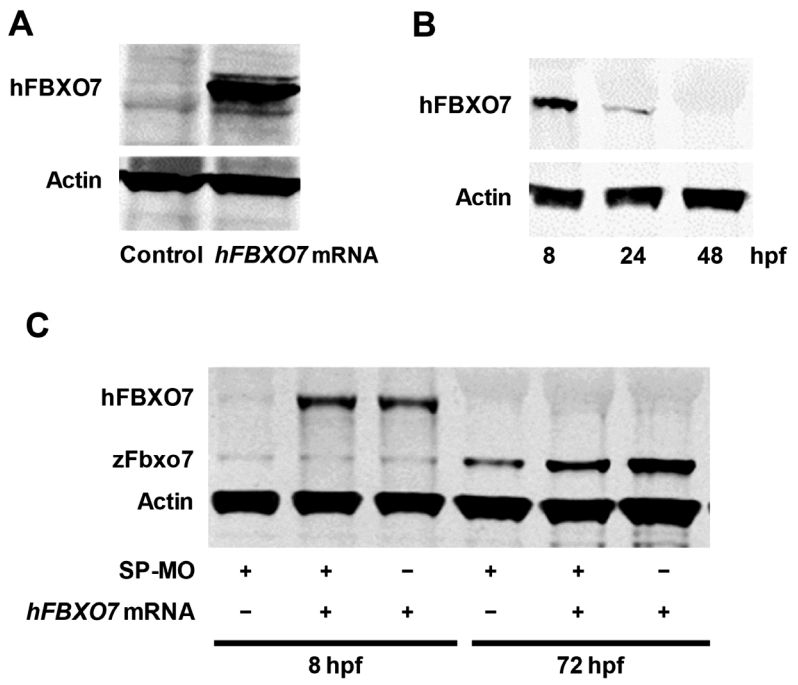

Figure S1 Expression of endogenous zFbxo7 and exogenous hFBXO7 occurs in different time points during the zebrafish development.

(A) Western blot analysis after *in vitro* protein translation of the *hFBXO7* mRNA. A band of the expected size of the hFbxo7 protein was detected, validating the *hFBXO7* mRNA as a rescuing template mRNA. An empty lane (Control) shows the reaction product after omitting the *hFBXO7* mRNA template.

(B) Time course of the expression of exogenous hFBXO7 *in vivo* in wild type embryos.

The *hFBXO7* mRNA was injected into one-cell stage embryos, and the expression of hFBXO7 was probed at 8, 24 and 48 hpf by Western blot. The expression of hFBXO7 was already markedly lower at 24 hpf, and was undetectable at 48 hpf.

(C) The expression of exogenous hFBXO7 and endogenous zFbxo7 *in vivo* in zebrafish embryos with or without co-injection of SP-MO. The *hFBXO7* mRNA and/or SP-MO were injected into one-cell stage embryos, and the expression of proteins was probed at 8 and 72 hpf by Western blot. The expression of the endogenous zFbxo7 was maximal at 72 hpf, when the exogenous hFBXO7 was undetectable.

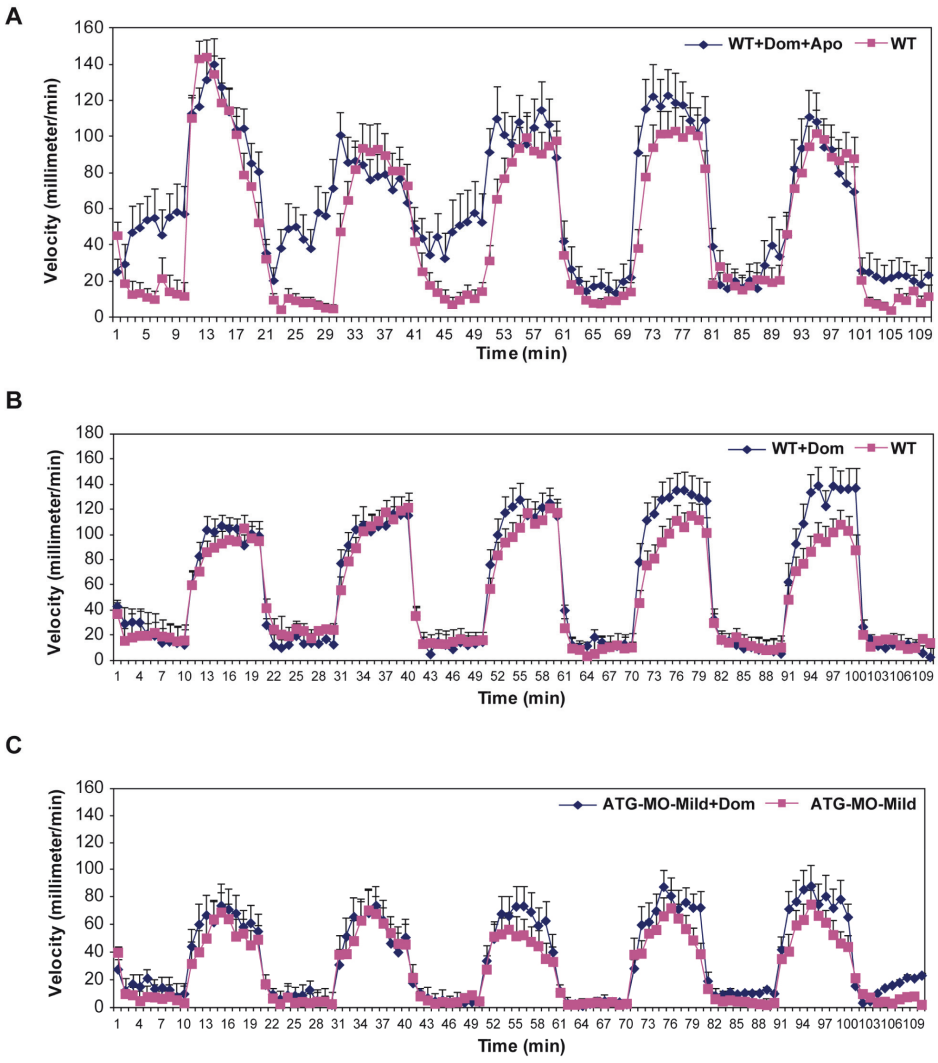

Figure S2 Locomotor behavior is not affected by domperidone.

The automated analysis of locomotion shows that the treatment with domperidone together with apomorphine (A) or domperidone alone (B) induced no detectable effects on the wild type zebrafish. Furthermore, domperidone alone induced no detectable locomotor effects in the ATG-MO-injected morphants (C).

Dom: domperidone. Apo: apomorphine.

REFERENCES

1. Tolosa E, Wenning G, Poewe W (2006) The diagnosis of Parkinson's disease. Lancet Neurol 5: 75-86.
2. Cookson MR, Bandmann O (2010) Parkinson's disease: insights from pathways. Hum Mol Genet 19: R21-27.
3. Corti O, Lesage S, Brice A (2011) What genetics tells us about the causes and mechanisms of Parkinson's disease. Physiol Rev 91: 1161-1218.
4. Bonifati V (2012) Autosomal recessive parkinsonism. Parkinsonism Relat Disord 18 Suppl 1: S4-6.
5. Gitler AD, Chesi A, Geddie ML, Strathearn KE, Hamamichi S, et al. (2009) Alpha-synuclein is part of a diverse and highly conserved interaction network that includes PARK9 and manganese toxicity. Nat Genet 41: 308-315.
6. Usenovic M, Knight AL, Ray A, Wong V, Brown KR, et al. (2012) Identification of novel ATP13A2 interactors and their role in alpha-synuclein misfolding and toxicity. Hum Mol Genet E-Pub ahead of print, May 29.
7. Di Fonzo A, Dekker MC, Montagna P, Baruzzi A, Yonova EH, et al. (2009) FBXO7 mutations cause autosomal recessive, early-onset parkinsonian-pyramidal syndrome. Neurology 72: 240-245.
8. Paisan-Ruiz C, Guevara R, Federoff M, Hanagasi H, Sina F, et al. (2010) Early-onset L-dopa-responsive parkinsonism with pyramidal signs due to ATP13A2, PLA2G6, FBXO7 and spatacsin mutations. Mov Disord 25: 1791-1800.
9. Ho MS, Ou C, Chan YR, Chien CT, Pi H (2008) The utility F-box for protein destruction. Cell Mol Life Sci 65: 1977-2000.
10. Zhao T, De Graaff E, Breedveld GJ, Loda A, Severijnen LA, et al. (2011) Loss of nuclear activity of the FBXO7 protein in patients with parkinsonian-pyramidal syndrome (PARK15). PLoS One 6: e16983.
11. Bandmann O, Burton EA (2010) Genetic zebrafish models of neurodegenerative diseases. Neurobiol Dis 40: 58-65.
12. Kabashi E, Brustein E, Champagne N, Drapeau P (2011) Zebrafish models for the functional genomics of neurogenetic disorders. Biochim Biophys Acta 1812: 335-345.
13. Ibanez CF (2008) Catecholaminergic neuron survival: getting hooked on GDNF. Nat Neurosci 11: 735-736.
14. Holzschuh J, Ryu S, Aberger F, Driever W (2001) Dopamine transporter expression distinguishes dopaminergic neurons from other

catecholaminergic neurons in the developing zebrafish embryo. Mech Dev 101: 237-243.
15. Hersch SM, Yi H, Heilman CJ, Edwards RH, Levey AI (1997) Subcellular localization and molecular topology of the dopamine transporter in the striatum and substantia nigra. J Comp Neurol 388: 211-227.
16. Ciliax BJ, Heilman C, Demchyshyn LL, Pristupa ZB, Ince E, et al. (1995) The dopamine transporter: immunochemical characterization and localization in brain. J Neurosci 15: 1714-1723.
17. Rink E, Wullimann MF (2001) The teleostean (zebrafish) dopaminergic system ascending to the subpallium (striatum) is located in the basal diencephalon (posterior tuberculum). Brain Res 889: 316-330.
18. Rink E, Wullimann MF (2002) Development of the catecholaminergic system in the early zebrafish brain: an immunohistochemical study. Brain Res Dev Brain Res 137: 89-100.
19. Flinn L, Mortiboys H, Volkmann K, Koster RW, Ingham PW, et al. (2009) Complex I deficiency and dopaminergic neuronal cell loss in parkin-deficient zebrafish (Danio rerio). Brain 132: 1613-1623.
20. Fett ME, Pilsl A, Paquet D, van Bebber F, Haass C, et al. (2010) Parkin is protective against proteotoxic stress in a transgenic zebrafish model. PLoS One 5: e11783.
21. Anichtchik O, Diekmann H, Fleming A, Roach A, Goldsmith P, et al. (2008) Loss of PINK1 function affects development and results in neurodegeneration in zebrafish. J Neurosci 28: 8199-8207.
22. Sallinen V, Kolehmainen J, Priyadarshini M, Toleikyte G, Chen YC, et al. (2010) Dopaminergic cell damage and vulnerability to MPTP in Pink1 knockdown zebrafish. Neurobiol Dis 40: 93-101.
23. Xi Y, Ryan J, Noble S, Yu M, Yilbas AE, et al. (2010) Impaired dopaminergic neuron development and locomotor function in zebrafish with loss of pink1 function. Eur J Neurosci 31: 623-633.
24. Bretaud S, Allen C, Ingham PW, Bandmann O (2007) p53-dependent neuronal cell death in a DJ-1-deficient zebrafish model of Parkinson's disease. J Neurochem 100: 1626-1635.
25. Baulac S, Lu H, Strahle J, Yang T, Goldberg MS, et al. (2009) Increased DJ-1 expression under oxidative stress and in Alzheimer's disease brains. Mol Neurodegener 4: 12.
26. Sheng D, Qu D, Kwok KH, Ng SS, Lim AY, et al. (2010) Deletion of the WD40 domain of LRRK2 in Zebrafish causes Parkinsonism-like loss of neurons and locomotive defect. PLoS Genet 6: e1000914.

27. Ren G, Xin S, Li S, Zhong H, Lin S (2011) Disruption of LRRK2 does not cause specific loss of dopaminergic neurons in zebrafish. PLoS One 6: e20630.
28. Milanese C, Sager JJ, Bai Q, Farrell TC, Cannon JR, et al. (2012) Hypokinesia and reduced dopamine levels in zebrafish lacking beta- and gamma1-synucleins. J Biol Chem 287: 2971-2983.
29. Matsui H, Taniguchi Y, Inoue H, Kobayashi Y, Sakaki Y, et al. (2010) Loss of PINK1 in medaka fish (Oryzias latipes) causes late-onset decrease in spontaneous movement. Neurosci Res 66: 151-161.
30. Adams JR, van Netten H, Schulzer M, Mak E, McKenzie J, et al. (2005) PET in LRRK2 mutations: comparison to sporadic Parkinson's disease and evidence for presymptomatic compensation. Brain 128: 2777-2785.
31. Eisen JS, Smith JC (2008) Controlling morpholino experiments: don't stop making antisense. Development 135: 1735-1743.
32. Robu ME, Larson JD, Nasevicius A, Beiraghi S, Brenner C, et al. (2007) p53 activation by knockdown technologies. PLoS Genet 3: e78.
33. Kimmel CB, Ballard WW, Kimmel SR, Ullmann B, Schilling TF (1995) Stages of embryonic development of the zebrafish. Dev Dyn 203: 253-310.
34. Turner DL, Weintraub H (1994) Expression of achaete-scute homolog 3 in Xenopus embryos converts ectodermal cells to a neural fate. Genes Dev 8: 1434-1447.
35. Bai Q, Burton EA (2009) Cis-acting elements responsible for dopaminergic neuron-specific expression of zebrafish slc6a3 (dopamine transporter) in vivo are located remote from the transcriptional start site. Neuroscience 164: 1138-1151.
36. Thisse C, Thisse B (2008) High-resolution in situ hybridization to whole-mount zebrafish embryos. Nat Protoc 3: 59-69.

5

The expression of the FBXO7 proteins in the normal human brain and in Parkinson's disease

Tianna Zhao, Lies-Anne Severijnen, Marcel van der Weiden, Ping Pin Zheng, Ben A. Oostra, Rob Willemsen, Johan M. Kros, Vincenzo Bonifati

To be submitted

ABSTRACT

Mutations in the gene encoding the F-box only protein 7 (FBXO7) cause PARK15, a rare autosomal recessive form of juvenile parkinsonism. The brain pathology in the PARK15 patients remains unexplored, and whether Lewy bodies are present is unknown. However, PARK15 patients display good response to levodopa and they suffer from severe loss of dopaminergic nigrostriatal neurons as shown by *in vivo* imaging. These features resemble those of patients with classical, late-onset Parkinson's disease. Understanding the pathogenesis of PARK15 might therefore illuminate the mechanisms of selective dopaminergic neuronal death, which could also be important for Parkinson's disease in general.

Two protein isoforms, of mostly unknown function, are expressed from the *FBXO7* gene. The pattern of expression of these proteins in the human brain remains poorly characterized. Furthermore, the expression of the FBXO7 proteins in the brain of the patients with late-onset Parkinson's disease was never explored before. Here, we studied the expression of the FBXO7 proteins in the brain of normal human subjects and of Parkinson's disease patients using immunohistochemistry and a polyclonal antibody raised against full-length FBXO7.

We observed widespread neuronal FBXO7 immunoreactivity throughout all the brain regions analysed. The highest levels of expression were detected in the cerebral cortex, putamen and cerebellum. Semiquantitative analysis showed no gross difference in the level of immunoreactivity between normal controls and Parkinson's disease patients. Of note, FBXO7 immunoreactivity was detected in some Lewy bodies and Lewy neurites, where it was co-localized with α-synuclein by double fluorescence staining. The FBXO7 immunoreactivity was mostly concentrated in the halo of Lewy bodies, but occasionally it was present in the entire inclusions. These findings suggest a role for the FBXO7 proteins in the pathogenesis of Lewy-body pathology in the common forms of synucleinopathies.

KEYWORDS: FBXO7, PARK15, Parkinson's disease, Lewy body, pathology

INTRODUCTION

Parkinson's disease (PD) is one of the most common neurodegenerative disorders, and it affects 1-2% of the population above the age of 60 years-old [1]. The cardinal clinical features of the disease are resting tremor, bradykinesia, muscular rigidity, and postural instability [2,3]. The pathogenesis of PD remains poorly understood, and, as a consequence, no treatment is available to stop or even slow the disease progression. From the pathological standpoint, PD is mainly characterized by the selective loss of dopaminergic neurons in the substantia nigra, and by the presence of Lewy bodies (LBs) or Lewy neurites (LNs) in the surviving neurons [4]. LBs are round cytoplasmic inclusion bodies, while LNs present as spindle-like or thread-like inclusion bodies within neuronal processes. Aggregated forms of the α-synuclein protein are the main component of these inclusions [5,6], and indeed, the presence of α-synuclein immunoreactive inclusions (together with dopaminergic neuronal loss) has become the gold standard criterion for the neuropathological diagnosis of PD and diffuse Lewy body disease (DLB). Furthermore, α-synuclein is also the major component of the glial cytoplasmic inclusions, the pathological hallmark of multiple system atrophy (MSA). The term "α-synucleinopathy" is currently adopted to indicate the whole spectrum of neurodegenerative diseases, characterized by misfolding and aggregation of α-synuclein [7,8].

There is increasingly evidence that genetic risk factors contribute to the etiology of PD. Mutations in several genes have been identified as the cause of human parkinsonism, inherited as autosomal dominant or autosomal recessive trait (reviewed in [9]). Mutations in the *F-box only 7* gene cause PARK15, a rare autosomal recessive form of juvenile parkinsonism. The brain pathology of PARK15 remains unexplored, and whether Lewy bodies are present is currently unknown. Intriguingly, the PARK15 patients display good response to levodopa and they suffer from severe loss of dopaminergic nigrostriatal neurons as shown by neuroimaging *in vivo* [10]. These features resemble those of the patients with the classical, late-onset form of PD. Understanding the pathogenesis of PARK15 might therefore illuminate the mechanisms of selective dopaminergic neuronal death, which could also be important for PD.

Two protein isoforms, of mostly unknown function, are expressed from the *FBXO7* gene. The pattern of expression of these proteins in the human brain remains poorly characterized. Furthermore, the expression of the FBXO7 proteins in the brain of the patients with late-onset PD was never explored

before. Here, we studied the expression of the FBXO7 proteins in the brain of normal human subjects and of PD patients.

RESULTS

FBXO7 antibody specificity

Two FBXO7 protein isoforms of 522 and 443 amino acids, only differing at their N-terminus (also referred to as isoform 1 and isoform 2), are encoded by the human *FBXO7* gene as a result of the usage of alternatively spliced 5'-exons (transcripts ENST00000266087 and ENST00000382058 [11]. A mouse polyclonal antibody (Abnova, B01P) raised against the full-length human FBXO7 longer protein isoform (522 amino acids) was used in this study. In order to assess the specificity of this antibody, we generated stable *FBXO7* knock down (*FBXO7*-KD) cells using shRNA targeting a sequence present in both the *FBXO7* transcripts. Cells treated with a non-targeting shRNA (shNT) served as negative control.

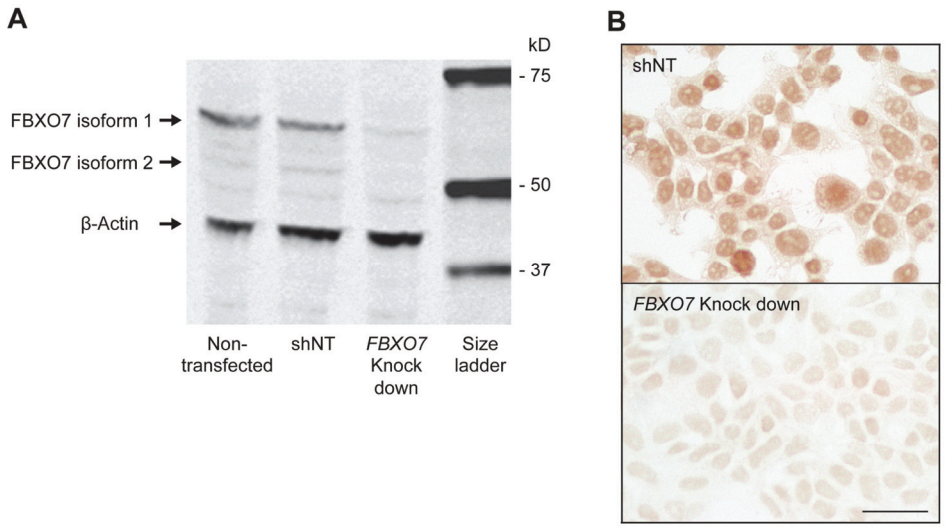

Figure 1 Specificity of the FBXO7 antibody.

(A) Western blotting using the FBXO7 antibody yields two bands of the predicted molecular weight, corresponding to the two endogenous isoforms of FBXO7 proteins in non-transfected HEK 293T cells, and in cells transfected with non-targeting *shRNA* (shNT). The intensity of these two bands is drastically decreased after treatment with *FBXO7*-targeting shRNA (KD). β-Actin is used as loading control.

(B) Immunocytochemistry using the same FBXO7 antibody reveals strong immunoreactivity in HEK 293T cells transfected with non-targeting *shRNA* (shNT). The immunoreactivity is drastically reduced after treatment of cells with *FBXO7*-targeting *shRNA* (KD). (Scale bar: 30 μm)

Two normal FBXO7 isoforms of the expected molecular weight were detected by Western blotting in the control (shNT) cells, while the expression of both proteins was markedly depleted in the *FBXO7*-KD cells (Figure 1A). Furthermore, FBXO7 immunoreactivity was detected using immunocytochemistry in the control cells but not in the *FBXO7*-KD cells (Figure 1B), further supporting the contention that the B01P antibody is able to specifically detect the endogenous FBXO7 proteins in human cell lines.

Table 1 Clinical and pathological details.

Cases	Gender	Age of Death (y.rs)	Braak Stage LB pathology	Brain (g)	Weight	Diagnosis
1	female	61	nd*	1312		Control
2	female	81	nd*	1052		Control
3	female	88	1	1186		Control
4	male	62	nd*	1352		Control
5	male	80	1	1350		Control
6	female	85	0	1257		Control
7	female	73	nd*	1447		Control
8	male	81	0	1348		Control
9	male	76	nd*	1514		Control
10	female	59	4	1465		PD
11	female	72	6	1122		PD
12	female	81	5	1330		PD
13	female	83	nd*	1059		PD
14	female	88	6	1190		PD
15	male	61	6	1756		PD
16	male	71	6	1552		PD
17	male	81	6	1481		PD
18	male	83	4	1217		PD
19	male	87	4	1403		PD
20	female	87	6	1195		PD
21	male	77	5	1380		PD
22	male	84	5	1198		PD

* nd: not determined.

Expression of FBXO7 in the normal and PD brain

To characterize the expression of the FBXO7 proteins in the normal human brain and in PD, we stained different brain regions from nine normal brain donors (controls) and thirteen PD patients (Tables 1 and 2, Figure 2). The FBXO7 immunoreactivity disappeared when the primary antibody was omitted (data not shown).

Table 2 FBXO7 immunoreactivity in normal human brain regions and in PD.

Brain region	Controls	PD patients
Frontal cortex	++ / +++	++ / +++
Parietal cortex	++	++
Temporal cortex	++ / +++	++ / +++
Occipital cortex	++ / +++	++ / +++
Hippocampus	+ / ++	+ / ++
Putamen	++ / +++	++ / +++
Substantia nigra	+ / ++	+ / ++
Locus coeruleus	+ / ++	+ / ++
Cerebellum	++ / +++	++ / +++

+: weak immunoreactivity

++: moderate immunoreactivity

+++: strong immunoreactivity

The FBXO7 immunoreactivity was widely detected throughout the brain regions analysed: intense expression was detected in the neocortex (all areas), putamen, and cerebellum, while more moderate levels were seen in the hippocampus, substantia nigra, and locus coeruleus (Figure 2). Strong FBXO7 expression was observed in the pyramidal cells of the cerebral cortex (Figure 2A-C, black arrows), while weaker expression was seen in hippocampal neurons (Figure 2D, arrowhead) and in Purkinje cells (Figure 2E, white arrow). While the FBXO7 immunoreactivity was generally present in both nucleus and cytoplasm, the nuclear localization often prevailed in the pyramidal cells of the neocortex. Furthermore, FBXO7 immunoreactivity was also present in the nuclei of astrocytes and oligodendroglial cells. Last, the distribution and intensity of the FBXO7 immunoreactivity in the brain of the PD patients showed no gross differences in comparison with that of the normal brains (Table 2).

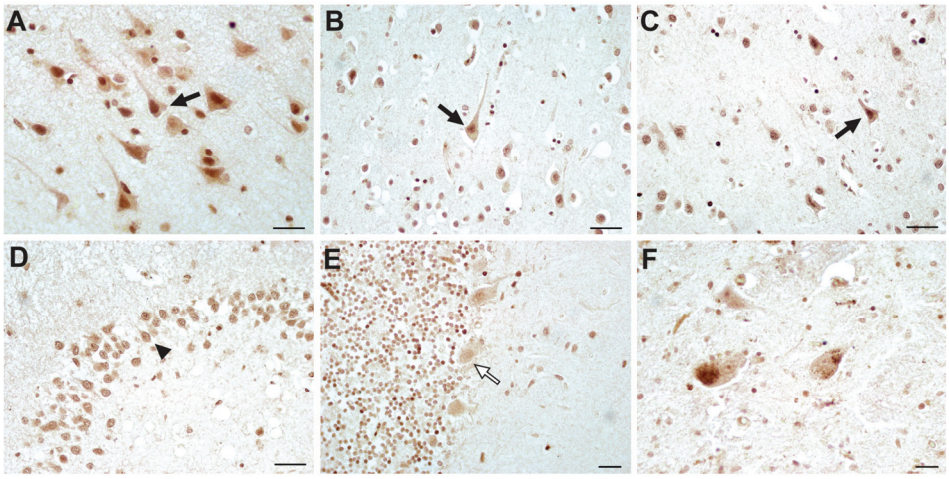

Figure 2 Expression of FBXO7 proteins in the normal human brain.
FBXO7 immunoreactivity is widely detected in different regions; shown are frontal cortex (A), parietal cortex (B), occipital cortex (C), dentate gyrus (D), cerebellum (E) and substantia nigra (F). Strong immunoreactivity is seen in the pyramidal neurons in the cerebral cortex (black arrows); weaker immunoreactivity is present in the hippocampal neurons (arrowhead) and the Purkinje neurons (white arrow). (Scale bar: 30 μm)

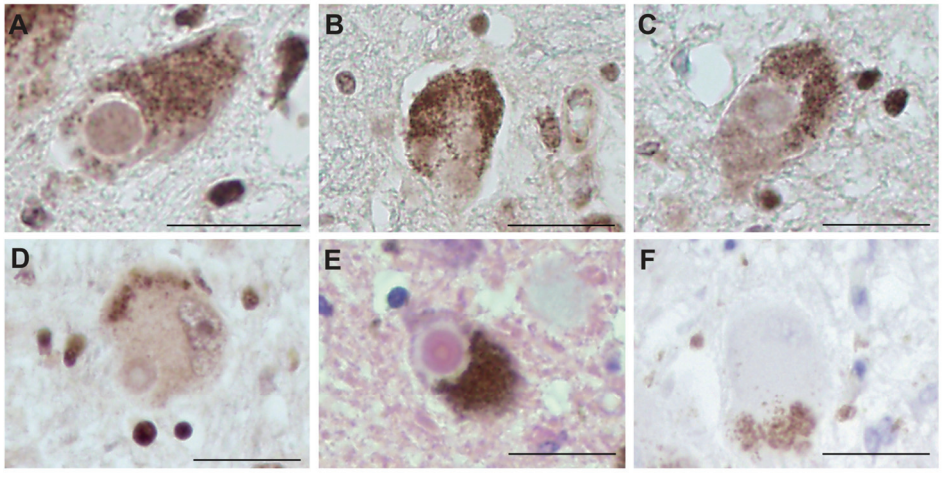

Figure 3 FBXO7 immunoreactivity in Lewy bodies.
FBXO7 immunoreactivity is detected in the majority of brainstem LBs, either in a diffuse pattern (A-B) or in a peripheral ring-like pattern (C-D). The classical morphology of the LBs is also shown by hematoxylin-eosin staining (E). No FBXO7 immunoreactivity is seen if the primary antibody is omitted (F). (Scale bar: 30 μm)

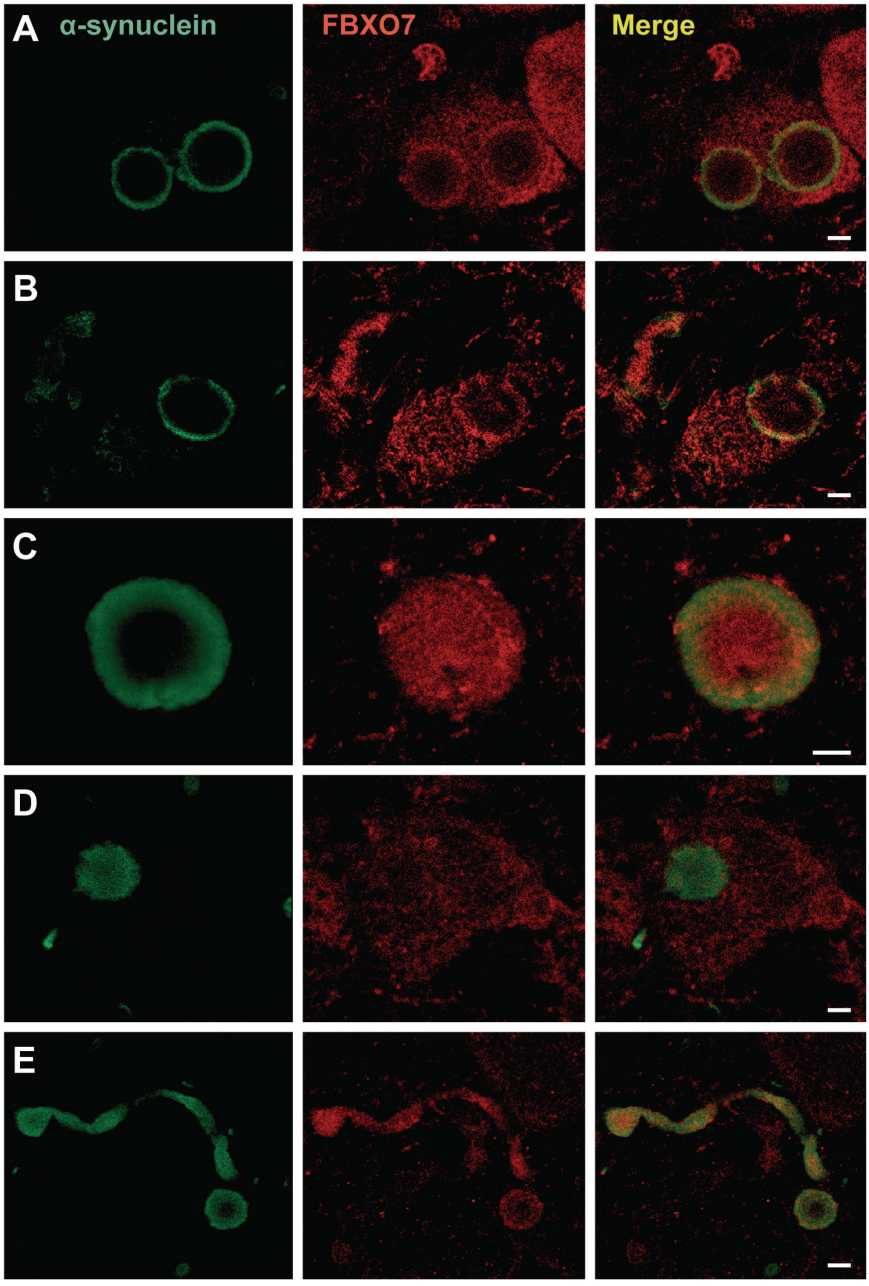

Figure 4 Co-localization of FBXO7 and α-synuclein in LBs and LNs.
Double immunofluorescence reveals the co-localization of FBXO7 and α-synuclein immunoreactivity. In some inclusions, the co-localization is detected in the periphery of LBs (locus coeruleus, A; substantia nigra, B); other inclusions show a more diffuse pattern of co-localization (C), whereas some LBs do not show FBXO7 immunoreactivity (D). The co-localization of FBXO7 and α-synuclein immunoreactivity is also detected in LNs (E). (Scale bar: 5 μm)

Localization of FXBO7 in the Lewy bodies and Lewy neurites

To investigate whether the FBXO7 proteins are present in the pathological inclusions which characterize PD, we studied the FBXO7 immunoreactivity of LBs using brain immunohistochemistry. We focused on the classic, brainstem type LBs, because these LBs are necessary for the pathological diagnosis of PD, and were therefore present in all the 13 PD brains available for this study (Figure 3).

We detected FBXO7 immunoreactivity in the LBs in the substantia nigra and in the locus coeruleus (Figure 3A-D). The immunoreactivity was more frequently localized to the periphery of LB (Figure 3C and 3D), but sometimes it was diffused to the whole inclusion (Figure 3A and 3B). Again, immunoreactivity was not seen when the primary antibody was omitted (Figure 3F).

The main component of LBs and LNs is the α-synuclein protein [12]. Therefore, in order to confirm the localization of FBXO7 in LBs and LNs, we performed double immunofluorescence and confocal microscopy using α-synuclein and FBXO7 antibodies. Co-localization of α-synuclein and FBXO7 was found (Figure 4). In particular, ~53% of the LBs displayed a peripheral ring-like pattern of FBXO7 immunoreactivity (Figure 4A-B), while ~32% of the LBs showed a diffuse pattern of immunoreactivity (Figure 4C), and ~14% of the LBs displayed no FBXO7 immunoreactivity (Figure 4D).

DISCUSSION

PARK15 is a Mendelian form of parkinsonism caused by recessive mutations in the *FBXO7* gene. We previously described the depletion of FBXO7 protein expression in the PARK15 patients, and the loss of the normal function of this gene is therefore underlying the pathogenesis of this form [10,13]. Two protein isoforms, of mostly unknown function, are expressed from the *FBXO7* gene [11]. The pattern of expression of these proteins in the human brain remains poorly characterized. Furthermore, the expression of the FBXO7 proteins in the brain of the patients with late-onset Parkinson's disease was never explored before.

This study aimed at the characterization of the expression of the FBXO7 proteins in the normal human brain and in the patients with the classical, late-onset PD form. A particular question is whether the FBXO7 proteins are detectable in the LBs and LNs, the hallmark pathological lesions of PD. Our findings show that the FBXO7 immunoreactivity is present in the different

regions of the normal human brain and this pattern is not altered in the PD brain. Furthermore, the FBXO7 immunoreactivity is present in the LBs and LNs, suggesting a role for FBXO7 in the pathogenesis of the common forms of synucleinopathies.

Some preliminary data concerning the FBXO7 immunoreactivity in the normal human brain were reported recently by us [11]. Here, we perform a systematic investigation of a higher number of brain areas, using brain tissue from nine normal donors and thirteen PD donors. The possible inter-individual variability in FBXO7 immunoreactivity is therefore minimized.

In keeping with the results of our previous study [11], the FBXO7 immunoreactivity was widely expressed in all the regions analysed from the normal brain, including the different areas of the cerebral cortex, the hippocampus, the putamen, the substantia nigra, the locus coeruleus, and the cerebellum. Moreover, the immunostaining in normal human brain showed ubiquitous distribution of the FBXO7 protein in all major neuronal groups throughout the brain, including dopaminergic neurons, pyramidal neurons, stellate neurons, granule and Purkinje neurons. Furthermore, no gross differences were observed when the FBXO7 immunoreactivity was compared between control and PD brains. The protein encoded by *leucine-rich repeat kinase 2* (*LRRK2*), another PD-causing gene, showed also a similar expression in control and PD brains, including *LRRK2*-mutant (Gly2019Ser) cases [14].

Brain tissue from patients with disease-causing *PARK15* mutations has not become available for autopsy study, yet. The brain pathology of PARK15 remains therefore unexplored. In particular, it is currently unknown whether Lewy bodies are present in this form of Mendelian, recessive parkinsonism. A different question is whether the FBXO7 proteins are contained in the LBs and LNs, the pathologic hallmark of the common forms of late-onset PD. Here, we identified abundant FBXO7 immunoreactivity in the LBs and LNs lesions of patients with the common form of PD. We show that ~85% of all the α-synuclein positive LBs display FBXO7 immunoreactivity (N=90). In addition, we show FBXO7 immunoreactivity in LNs. To our knowledge, this is the first study showing an involvement of the FBXO7 proteins in PD. Intriguingly, immunoreactivity for the proteins encoded by other PD-related genes, such as *LRRK2* and *PTEN-induced putative kinase 1 (PINK1)*, has also been detected in the periphery of LBs with a ring-like pattern [14,15]. The FBXO7

immunoreactivity in the α-synuclein-positive LBs and LNs suggests a possible important role for the FBXO7 proteins in the formation of these inclusions, and in the pathogenesis of the common forms of synucleinopathies, such as PD and diffuse Lewy body disease.

This study has some limitations. First, only one FBXO7 antibody was available for study. Though we provided strong evidence for the specificity of this antibody for the human FBXO7 proteins, it is important to confirm our findings in future studies using different antibodies. Second, we analysed several brain regions, and included brain tissue from a number of normal and PD donors. However, the distribution of the FBXO7 immunoreactivity remains to be investigated in other, related neurodegenerative conditions, including other synucleinopathies (diffuse Lewy body disease, MSA) and tauopathies (progressive supranuclear palsy, corticobasal degeneration, frontotemporal dementia, Alzheimer's disease). Third, and perhaps most importantly, this study is descriptive, and it does not address the mechanisms underlying the involvement of the FBXO7 proteins in the synucleinopathies.

FBXO7 is a member of the F-box-containing protein (FBP) family, characterized by a ~40-amino acids domain (the F-box) [16]. FBPs might become part of SCF (Skp1, Cullin1, F-box protein) ubiquitin ligase complexes, and play roles in ubiquitin-mediated proteasomal degradation. It will be important to investigate whether the FBXO7 protein is involved in the ubiquitination of α-synuclein or other LB proteins, and for the degradation of these proteins. Preliminary observations in our laboratory (unpublished) suggest that FBXO7 knock down in non-neuronal cells has no gross effects on the steady-state level of the α-synuclein or the parkin proteins. However, much more work is warranted using both cell system and animal models, in order to clarify the normal functions of the FBXO7 proteins in neurons, the mechanisms leading to neurodegeneration in PARK15, and the possible interplay with the pathways involved in other inherited forms of parkinsonism and the common PD form.

MATERIALS AND METHODS

Brain tissues

Brain tissues including 13 patients affected by idiopathic Parkinson's disease and 9 age-matched controls were obtained from The Netherlands Brain Bank, Netherlands Institute for Neuroscience, Amsterdam. All material has been collected from donors from whom a written informed consent for brain autopsy

and the use of the material and clinical information for research purposes had been obtained by the Netherlands Brain Bank.

Cell culture and Western blotting

Human embryonic kidney (HEK) 293T cells were grown in Dulbecco's modified Eagle's medium (DMEM) according to standard protocols. The stable *FBXO7* knock down HEK 293T cells were generated using *FBXO7* shRNA (#TRCN 0000004339, Sigma). A non-targeting *shRNA* (shNT, SHC002, Sigma) was used as control.

For Western botting, cultured cells were harvested as previous described [11]. Briefly, forty micrograms of protein was loaded onto 6-12% CriterionTM XT 4-12% Bis-Tris Gel (Bio-Rad), and transferred to nitrocellulose membranes. The membrane was then incubated with FBXO7 purified mouse polyclonal antibody (B01P) against the full-length FBXO7 longer isoform (isoform 1, 522 amino acids) (Abnova, 1/500), and mouse monoclonal against β-Actin (Sigma, 1/2000). After washing with phosphate buffered saline with Tween 20 (PBST), the membranes were incubated in the dark for 1 hour with anti-mouse secondary antibody, and scanned using the Odyssey TM Infrared Imager (Li-COR Biosciences).

Immunohistochemistry and immunocytochemistry

Sections (5-µm-thick) were prepared from formalin fixed, paraffin embedded brain tissue. The endogenous peroxidase activity was blocked using 0.6% H_2O_2 and 0.125% $NaNO_3$ in phosphate buffered saline (PBS). The sections were then incubated overnight at 4°C with primary antibody against full-length human FBXO7 (Abnova, 1/100), and subsequently with BrightVision horseradish peroxidase-linked secondary antibody (Immunologic, 1/1) for one hour at room temperature. After washing with PBS, the immunoreactivity was visualized by freshly prepared Liquid DAB Substrate Chromogen solution (DAKO). Last, the sections were dehydrated through graded ethanol, cleared with xylene, and mounted with Entellan medium (Electron Microscopy Sciences). To detect brainstem-type Lewy bodies, sections from substantia nigra and locus coeruleus were subjected to standard hematoxylin and eosin staining, and then immunostaining was performed on serial sections. For immunocytochemistry, HEK293T cells were seeded on slides, permeabilized, incubated with anti-FBXO7 antibody and then processed for DAB immunostaining.

Double fluorescence staining

Double staining of the FBXO7 and α-Synuclein proteins was performed in the region of substantia nigra and locus coeruleus. To block unspecific antibody binding sites, the dehydrated sections were pre-incubated with 10% donkey and goat serum for 10 minutes. Sections were then incubated with primary mouse antibodies against FBXO7 (Abnova, 1/25) and rabbit α-Synuclein (Chemicon, 1/100) overnight at 4°C. Negative control was generated by omission of primary antibodies. All primary antibodies and serum were diluted in PBS containing 1% (w/v) bovine serum albumin. After washing with PBST, sections were then incubated for 1 hour with Cy3-conjugated anti-mouse secondary antibody (Jackson ImmunoResearch, 1/200) and Alexa 488-conjugated anti-rabbit secondary antibody (Invitrogen, 1/200). To quench autofluorescence of brain tissue, the sections were treated with 0.1% Sudan Black B (Sigma-Aldrich) in dark. The slides were then covered by cover slip and mounted with DAKO. Fluorescence images were collected using a Leica SP5 confocal microscope (Leica Microsystems), and analyzed with the Leica confocal software. The number of FBXO7-positive LBs in sections of substantia nigra was expressed as the percentage of the α-Synuclein positive inclusions (N=90) counted in the same sections.

ACKNOWLEDGEMENTS

This study was supported by grants from the “Internationaal Parkinson Fonds” (The Netherlands), and the Netherlands Organization for Scientific Research (NWO, VIDI grant) to VB. We thank Diana Nijholt (Erasmus MC, Rotterdam) for help with immunostaining, and Tom de Vries-Lentsch (Erasmus MC, Rotterdam) for artwork.

REFERENCES

1. Lang AE, Lozano AM (1998) Parkinson's disease. First of two parts. N Engl J Med 339: 1044-1053.
2. Fahn S (2003) Description of Parkinson's disease as a clinical syndrome. Ann N Y Acad Sci 991: 1-14.
3. Jankovic J (2008) Parkinson's disease: clinical features and diagnosis. J Neurol Neurosurg Psychiatry 79: 368-376.
4. Dickson DW, Braak H, Duda JE, Duyckaerts C, Gasser T, et al. (2009) Neuropathological assessment of Parkinson's disease: refining the diagnostic criteria. Lancet Neurol 8: 1150-1157.
5. Braak H, Ghebremedhin E, Rub U, Bratzke H, Del Tredici K (2004) Stages in the development of Parkinson's disease-related pathology. Cell and tissue research 318: 121-134.
6. Tofaris GK, Spillantini MG (2005) Alpha-synuclein dysfunction in Lewy body diseases. Movement disorders : official journal of the Movement Disorder Society 20 Suppl 12: S37-44.
7. Bonifati V (2007) Genetics of parkinsonism. Parkinsonism Relat Disord 13 Suppl 3: S233-241.
8. Spillantini MG, Goedert M (2000) The alpha-synucleinopathies: Parkinson's disease, dementia with Lewy bodies, and multiple system atrophy. Ann N Y Acad Sci 920: 16-27.
9. Corti O, Lesage S, Brice A (2011) What genetics tells us about the causes and mechanisms of Parkinson's disease. Physiol Rev 91: 1161-1218.
10. Di Fonzo A, Dekker MC, Montagna P, Baruzzi A, Yonova EH, et al. (2009) FBXO7 mutations cause autosomal recessive, early-onset parkinsonian-pyramidal syndrome. Neurology 72: 240-245.
11. Zhao T, De Graaff E, Breedveld GJ, Loda A, Severijnen LA, et al. (2011) Loss of nuclear activity of the FBXO7 protein in patients with parkinsonian-pyramidal syndrome (PARK15). PLoS One 6: e16983.
12. Spillantini MG, Crowther RA, Jakes R, Hasegawa M, Goedert M (1998) alpha-Synuclein in filamentous inclusions of Lewy bodies from Parkinson's disease and dementia with lewy bodies. Proc Natl Acad Sci U S A 95: 6469-6473.
13. Shojaee S, Sina F, Banihosseini SS, Kazemi MH, Kalhor R, et al. (2008) Genome-wide linkage analysis of a Parkinsonian-pyramidal syndrome pedigree by 500 K SNP arrays. Am J Hum Genet 82: 1375-1384.
14. Sharma S, Bandopadhyay R, Lashley T, Renton AE, Kingsbury AE, et al. (2011) LRRK2 expression in idiopathic and G2019S positive Parkinson's

disease subjects: a morphological and quantitative study. Neuropathol Appl Neurobiol 37: 777-790.

15. Gandhi S, Muqit MM, Stanyer L, Healy DG, Abou-Sleiman PM, et al. (2006) PINK1 protein in normal human brain and Parkinson's disease. Brain 129: 1720-1731.
16. Ho MS, Ou C, Chan YR, Chien CT, Pi H (2008) The utility F-box for protein destruction. Cell Mol Life Sci 65: 1977-2000.

6

General discussion

General discussion

The aim of the work described in this thesis is to study the role of FBXO7 protein in early-onset Parkinsonism. Our work started with the characterization of pathogenic mutations in the *FBXO7* gene in two families with early-onset parkinsonian-pyramidal syndrome (Chapter 2). This work provided the conclusive evidence, after the initial study in an Iranian pedigree [1], that *FBXO7* is the disease-causing gene in this newly-identified form of parkinsonism [2]. The Iranian study provided the original genome-wide linkage mapping to the chromosome 22, and the identification of a single homozygous *FBXO7* mutation, predicted to lead to a missense change in the encoded protein [1]. However, it is well known that the detection of a single mutation in a positional candidate gene (a gene located within the linkage critical region) in a single family is not sufficient to prove causation. The role of *FBXO7* mutations remained therefore to be demonstrated. Our identification of different pathogenic *FBXO7* mutations in two novel, unrelated families, showed unambiguously that recessive *FBXO7* mutations cause this novel neurodegenerative disease [2].

Of note, we also showed that the phenotypic spectrum associated with *FBXO7* mutations is much broader than that present in the Iranian pedigree. Indeed, the patients in that pedigree had prominent, early signs of pyramidal disturbances, and only some of them subsequently developed parkinsonian signs. The parkinsonism was responsive to levodopa therapy in the case who received this treatment [1]. By contrast, the patients described in our study (Chapter 2) are characterized by a combination of early-onset, progressive parkinsonism with associated milder pyramidal signs, matching therefore clinically the “pallido-pyramidal syndrome” of Davison, or the “parkinsonian-pyramidal” syndrome (a more recently proposed term) [2,3]. In these patients, the parkinsonism shows a good response to levodopa, sometimes marked and sustained, but often limited by severe motor and psychiatric side effects. Furthermore, *in vivo* DaTSCAN-SPECT neuroimaging suggested severe loss of dopaminergic nigrostriatal neurons [2]. This dramatic abnormality of the nigrostriatal dopaminergic terminals and the beneficial effects of levodopa indicate that a dopaminergic lesion at the level of the substantia nigra (rather than the globus pallidum) underlies the parkinsonism in these patients. Due to these reasons, we proposed the name PARK15 (Monogenic parkinsonism, type 15), to refer to this newly identified form of human neurodegenerative disease [2], which has been accepted by the HUGO Committee (http://www.genenames.org/guidelines.html).

Mutations in the *FBXO7* gene should therefore be suspected in patients with early-onset parkinsonian-pyramidal syndromes. After the publication of our work, another two families with this disease have been identified, originating from Pakistan and Turkey [4]. Intriguingly, there was again prominent parkinsonism with a marked levodopa responsiveness, which was however limited by psychiatric side effects; the pyramidal disturbances represented a less important phenotypic component. All these features bring the PARK15 disease closer to the other forms of typical early-onset parkinsonism, caused by mutations in *parkin*, *PINK1*, or *DJ-1*. On the other hand, atypical clinical presentations have sometimes been reported in patients with mutations in *parkin* or *DJ-1*, blurring the distinction between clinically "typical" and "atypical" early-onset parkinsonism [5,6].

PARK15 has therefore joined the expanding list of monogenic parkinsonisms [7]. However, in many patients with a similar phenotype, mutations are not found in any of the known genes. Therefore, it is very likely that additional monogenic forms will be identified in the future, adding to the etiologic heterogeneity of the human parkinsonism.

The novel technology of massively parallel DNA sequencing (also termed Next Generation Sequencing) will allow a significant acceleration in the pace of the discovery of disease-causing genes. In particular, whole-exome sequencing (WES), which allows the sequencing of the entire coding part of the human genome (~1% of the whole genome) in a single experiment, is currently adopted as the strategy of choice for the identification of novel disease-causing mutations. This technique is especially powerful when used in combination with classical linkage mapping approaches, because in this way, the target genomic region is significantly reduced, facilitating the identification of the causative mutation among the long list of variants identified by WES. However, WES can also discover a disease-causing mutation in the absence of linkage data, by the analysis of even only a single pair of affected relatives in a single pedigree. One example of the successes of this strategy is the recent identification of a *VPS35* mutation in a Swiss and an Austrian kindred with autosomal dominant PD [8,9]. There is currently great excitement about, and expectations from the implementation of next generation sequencing. However, it is important to keep in mind that WES is still a young and imperfect technology, currently limited by the sub-optimal capture efficiency (particularly in some GC-rich genomic regions); examples of WES failures due to this reason have been already

published, and improvements of the experimental techniques and analytical approaches are warranted [10,11,12].

Since the *FBXO7* mutations cause PARK15 in a recessive fashion, they act by a loss-of-function. Understanding the normal function of the FBXO7 protein might thus provide clues on the mechanisms of this disease, and in particular, on the maintenance of the brain dopaminergic neurons, which are dramatically lost in the patients with PARK15.

However, the protein encoded by *FBXO7* remained very poorly characterized. Two isoforms (also referred to as isoform 1 and isoform 2) were predicted by the transcripts annotated in Genbank. However, experimental confirmation of the existence of these two protein isoforms had remained elusive, and nothing was known about the expression of the FBXO7 protein(s) in the human brain. We therefore initiated a number of studies aimed at the characterization of the FBXO7 protein(s).

The expression of the FBXO7 proteins in cell models

In chapter 3, we showed that two protein isoforms are expressed from the *FBXO7* gene, and that PARK15 patients have in common a severe depletion of the longer isoform, which localizes predominantly in the cell nucleus [13]. We therefore suggested that the activity of FBXO7 in the nucleus might be crucial for the maintenance of brain neurons in humans and the pathogenesis of PARK15 [13]. We also showed that an intact N-terminus is needed for the nuclear FBXO7 localization, as N-terminal modification by PARK15-linked missense mutation, or N-terminus tag leads to cytoplasmic mislocalization [13]. This effect of the N-terminal tagging might also explain some conflicting results reported in previous studies on the sub-cellular cytoplasmic localization of this protein [14,15]. Canonical nuclear localization signals are not present in the N-terminus of FBXO7. However, nuclear localization signals might also consist of one or more short sequences of positively charged lysine or arginine residues, which are indeed present in the N-terminus of FBXO7. The effects of N-terminal tagging would therefore be explained by the masking of these signals. More recently, a functional leucine-rich nuclear export sequence (NES) was identified in the F-box domain, and the subcellular localization of FBXO7 was shown to be regulated by the competitive interaction of FBXO7 between Skp1 and the nuclear export protein exportin 1 (CRM1) [16]. According to this model, the

binding to Skp1 prevents FBXO7 from contacting CRM1, leading to the accumulation of FBXO7 in the nucleus [16].

Clearly much more work remains ahead in order to clarify the exact cellular localization of the two FBXO7 protein isoforms, their functions, and the mechanisms of their dysfunction in PARK15. The development of more sensitive and isoform-specific antibodies will be a crucial step forward in order to reliably detect and distinguish the two endogenous protein isoforms.

A vertebrate model of PARK15 in zebrafish

In parallel with the above-mentioned in vitro experiments, we developed an in vivo model of PARK15 by transient, morpholino-mediated knockdown of the homologue gene of *FBXO7* in zebrafish (Chapter 4). Using whole-mount *in situ* mRNA hybridization we showed abnormal patterning and significant decrease in the number of diencephalic *tyrosine hydroxylase*-expressing neurons, corresponding to the human nigrostriatal dopaminergic neurons. Interestingly, we also showed that the number of the *dopamine transporter*-expressing neurons was much more severely depleted. This discrepancy between the reduction in the th^+ and dat^+ neurons might indicate, in part, a selective loss of dopaminergic (DA) neurons, within the larger compartment of the catecholaminergic neurons. However, this pattern more likely indicates the presence of surviving th^+ DA neurons with down-regulated *dat* expression. The same pattern (reduced DAT in preserved DA neurons) is seen *in vivo* in humans with genetic forms of PD by PET imaging in the earlier stages of DA neuronal degeneration [17]. This represents a compensatory neuronal reaction aimed to maintain sufficient synaptic dopamine levels by down-regulating the DAT-mediated presynaptic reuptake of the neurotransmitter [17]. In addition to the morphologic phenotypes, our zebrafish morphants displayed severe locomotor disturbances (bradykinesia), which were dramatically improved by the dopaminergic agonist apomorphine.

The specificity of the effects in our morpholino (MO)-mediated knockdown model is supported by several arguments. We obtained similar phenotypes using two different morpholino-mediated knockdown strategies. Moreover, the severity of the morphological and behavioral abnormalities correlated with the severity of zebrafish Fbxo7 (zFbxo7) protein deficiency. Last, we excluded off-target p53-effects by co-injecting p53-targeting morpholinos. Unfortunately, we could not show phenotype rescuing by injecting the *FBXO7* mRNA. However, a detailed

analysis of the temporal pattern of expression disclosed a clear discrepancy between the time course of expression of the exogenous hFBXO7 and the endogenous zFbxo7 protein, as the likely explanation of the lack of rescuing effects. The lack of rescue of truly-specific effects is a well-known phenomenon in zebrafish MO-mediated modelling [18,19].

The transient MO-mediated knockdown of other PD-related genes in zebrafish has yielded varying degrees of pathologic and/or behavioural abnormalities, reproducing features of human parkinsonism [20,21,22,23,24,25,26,27,28]. However, the specificity of the effects were not fully controlled in some studies; in several other, only the *th*$^{+}$ expression was used as a marker of the DA neurons; most importantly, almost none of the previous studies yielded both evidence of DA neuronal loss and dopamine-dependent motor phenotypes.

Instead, our novel PARK15 vertebrate model reproduces both the pathologic and behavioral hallmarks of human parkinsonism (dopaminergic neuronal loss and dopamine-dependent bradykinesia), representing therefore a more valid tool for investigating the mechanisms of selective dopaminergic neuronal death, and screening for modifier genes and therapeutic compounds.

These exciting results obtained in our transient knockdown model suggest also that the development of stable knockout models of PARK15 in zebrafish (TILLING strategy) or in other model organisms might provide further important clues. It will be especially interesting to investigate whether the phenotype due to FBXO7 knockdown is rescued by the over-expression of other genes causing early-onset recessive PD (parkin, PINK1, DJ-1). These experiments might help understanding whether the mechanisms of PARK15 and those of other forms are converging on common pathways or not.

Whether the different genetic forms of parkinsonism converge on a single or on multiple pathogenetic pathways is perhaps the most relevant point [29,30,31]. The answer to this question has obvious implications for the design of novel therapeutic approaches. If a single pathogenetic pathway underlies the different forms, a single therapeutic strategy will be successful in all the patients. Conversely, different therapeutic strategies might be necessary if the different genetic forms are due to different pathogenetic mechanisms.

Concerning the autosomal recessive early-onset forms, there is now convincing evidence that parkin and PINK1 proteins are functionally linked, with PINK1 acting upstream of parkin in the same neuroprotective pathway [32,33]. Whether the same pathway is also involved in the patients with *DJ-1* mutations remains controversial [34,35]. It will be very important to understand whether the pathways of the FBXO7 protein are also somehow linked to those of PINK1 and parkin. There are currently no data in support or against this possibility.

The ubiquitin E3 ligase activity of FBXO7 points to the similar biochemical activity of parkin. However, there are many E3 ligases in the human proteome, involved in disparate cellular pathways. It is therefore impossible to predict whether FBXO7 functions in the same pathway of parkin solely on the basis of this biochemical parallelism. The sub-cellular localization of FBXO7, and its depletion in the patients with PARK15 suggest important roles for this protein in the cell nucleus and in the cytoplasm, while PINK1 and parkin converge at the level of the mitochondria.

Expression of FBXO7 proteins in the normal brain and in PD

The few available autopsy studies in patients with monogenic parkinsonisms highlighted some neuropathologic differences in patients with *parkin* mutations compared with classical LB-positive PD [36]. Most patients with *parkin* mutations do not have LBs, and the neuronal loss is limited to the substantia nigra. However, one should be cautious to develop pathogenetic models based only on neuropathologic criteria. It is well known that the brain pathology might be heterogeneous even in different members of the same family with the same disease-causing mutation. For example, in families with *LRRK2* mutations, some patients display LB-positive, and others display LB-negative pathology [36]. Moreover, LB-positive pathology has been reported in patients with *PLA2G6* (PARK14) mutations [36]. A first patient with *PINK1* mutations has been recently studied post-mortem, also showing LB-positive pathology [37]. There are currently no pathologic reports in patients with *DJ-1* or *FBXO7* mutations. Clearly, more studies are needed in order to shed light on the pathologic spectrum associated to these forms and to develop a more coherent framework to inform models and theories of pathogenesis.

In this regards, the pattern of expression of the FBXO7 proteins in the human brain remained poorly characterized. Furthermore, the expression of these proteins in the brain of the patients with late-onset LB-associated PD was not

explored before. Therefore, we studied the expression of the FBXO7 proteins in the brain of normal human subjects and of PD patients (Chapter 5). We found that the FBXO7 immunoreactivity is widespread in neurons across all the brain regions analysed, confirming an important role for these proteins in the human brain. The highest levels of expression were detected in the cerebral cortex, putamen and cerebellum. Furthermore, semiquantitative analysis showed no gross differences between normal controls and PD patients.

Of note, we detected FBXO7 immunoreactivity in the majority of LBs and LNs, where it was co-localized with α-synuclein, the main component and hallmark of these inclusions. The FBXO7 immunoreactivity was mostly concentrated in the halo of Lewy bodies, but occasionally it was present in the entire inclusions. These findings suggest a role for the FBXO7 proteins in the pathogenesis of LB pathology in the common forms of synucleinopathies. These represent potentially very important findings, which, however, need to be confirmed using additional isoform-specific antibodies. It will also be very important to study the distribution of the FBXO7 immunoreactivity in other, related neurodegenerative conditions, and especially the other synucleinopathies (diffuse Lewy body disease, MSA). The FBXO7 protein could play important roles in the pathogenesis of those conditions as well.

Conclusions and future perspectives

PARK15 is a novel, rare form of early-onset recessive parkinsonism, caused by the loss of the neuronal function of the FBXO7 proteins. In order to understand the still unknown function of these proteins, we performed *in vitro* studies using neuronal and non-neuronal cell lines, and PARK15-patient fibroblasts, and we developed the first vertebrate model of this disease in the zebrafish. We finally studied the expression of these proteins in the normal and PD brain, and provided the first evidence of these proteins in the LBs, the characteristic pathologic lesions in the common forms of PD.

Much more work remains ahead to understand the neuronal function of these interesting proteins, and the mechanisms underlying neurodegeneration in the patients with PARK15. It will be of outmost importance to understand whether the pathogenesis of PARK15 is functionally linked to the pathogenesis of other genetic forms of parkinsonism, particularly those caused by mutations in parkin, PINK1, and DJ-1. This can be pursued by functional experiments in cells and in

animal models, including the zebrafish. These animal models might also be helpful in identification and testing of new drugs for PD.

Last, the recent development of the technology for the generation of induced pluripotent stem (iPS) cells from patients fibroblasts, offers an unprecedented opportunity to model disease in the relevant (human, neuronal) cell types. For example, *LRRK2* mutant iPS derived DA neurons were recently shown to exhibit increased susceptibility to oxidative stress, and *PINK1* mutant iPS derived DA neurons displayed impaired recruitment of Parkin to mitochondria [38,39]. These results provided the proof-of-concept for iPS-based cellular modelling of PD. iPS cells obtained from patients with *FBXO7* mutations differentiated into dopaminergic neurons might bring further important insights into the mechanisms of PARK15 and its relationships to other genetic and common (idiopathic) forms of PD.

REFERENCES

1. Shojaee S, Sina F, Banihosseini SS, Kazemi MH, Kalhor R, et al. (2008) Genome-wide linkage analysis of a Parkinsonian-pyramidal syndrome pedigree by 500 K SNP arrays. Am J Hum Genet 82: 1375-1384.
2. Di Fonzo A, Dekker MC, Montagna P, Baruzzi A, Yonova EH, et al. (2009) FBXO7 mutations cause autosomal recessive, early-onset parkinsonian-pyramidal syndrome. Neurology 72: 240-245.
3. Horstink MW, Dekker MC, Montagna P, Bonifati V, van De Warrenburg BP (2010) Pallidopyramidal disease: a misnomer? Mov Disord 25: 1109-1115.
4. Paisan-Ruiz C, Guevara R, Federoff M, Hanagasi H, Sina F, et al. (2010) Early-onset L-dopa-responsive parkinsonism with pyramidal signs due to ATP13A2, PLA2G6, FBXO7 and spatacsin mutations. Mov Disord 25: 1791-1800.
5. Annesi G, Savettieri G, Pugliese P, D'Amelio M, Tarantino P, et al. (2005) DJ-1 mutations and parkinsonism-dementia-amyotrophic lateral sclerosis complex. Ann Neurol 58: 803-807.
6. Wickremaratchi MM, Majounie E, Morris HR, Williams NM, Lewis H, et al. (2009) Parkin-related disease clinically diagnosed as a pallido-pyramidal syndrome. Mov Disord 24: 138-140.
7. Bonifati V (2012) Autosomal recessive parkinsonism. Parkinsonism Relat Disord 18 Suppl 1: S4-6.
8. Vilarino-Guell C, Wider C, Ross OA, Dachsel JC, Kachergus JM, et al. (2011) VPS35 mutations in Parkinson disease. Am J Hum Genet 89: 162-167.
9. Zimprich A, Benet-Pages A, Struhal W, Graf E, Eck SH, et al. (2011) A mutation in VPS35, encoding a subunit of the retromer complex, causes late-onset Parkinson disease. Am J Hum Genet 89: 168-175.
10. Bloch-Zupan A, Jamet X, Etard C, Laugel V, Muller J, et al. (2011) Homozygosity mapping and candidate prioritization identify mutations, missed by whole-exome sequencing, in SMOC2, causing major dental developmental defects. Am J Hum Genet 89: 773-781.
11. Heron SE, Grinton BE, Kivity S, Afawi Z, Zuberi SM, et al. (2012) PRRT2 mutations cause benign familial infantile epilepsy and infantile convulsions with choreoathetosis syndrome. Am J Hum Genet 90: 152-160.
12. Quadri M, Federico A, Zhao T, Breedveld GJ, Battisti C, et al. (2012) Mutations in SLC30A10 cause parkinsonism and dystonia with

hypermanganesemia, polycythemia, and chronic liver disease. Am J Hum Genet 90: 467-477.
13. Zhao T, De Graaff E, Breedveld GJ, Loda A, Severijnen LA, et al. (2011) Loss of nuclear activity of the FBXO7 protein in patients with parkinsonian-pyramidal syndrome (PARK15). PLoS One 6: e16983.
14. Chang YF, Cheng CM, Chang LK, Jong YJ, Yuo CY (2006) The F-box protein Fbxo7 interacts with human inhibitor of apoptosis protein cIAP1 and promotes cIAP1 ubiquitination. Biochem Biophys Res Commun 342: 1022-1026.
15. Kirk R, Laman H, Knowles PP, Murray-Rust J, Lomonosov M, et al. (2008) Structure of a conserved dimerization domain within the F-box protein Fbxo7 and the PI31 proteasome inhibitor. J Biol Chem 283: 22325-22335.
16. Nelson DE, Laman H (2011) A Competitive binding mechanism between Skp1 and exportin 1 (CRM1) controls the localization of a subset of F-box proteins. J Biol Chem 286: 19804-19815.
17. Adams JR, van Netten H, Schulzer M, Mak E, McKenzie J, et al. (2005) PET in LRRK2 mutations: comparison to sporadic Parkinson's disease and evidence for presymptomatic compensation. Brain 128: 2777-2785.
18. Bandmann O, Burton EA (2010) Genetic zebrafish models of neurodegenerative diseases. Neurobiol Dis 40: 58-65.
19. Kabashi E, Brustein E, Champagne N, Drapeau P (2011) Zebrafish models for the functional genomics of neurogenetic disorders. Biochim Biophys Acta 1812: 335-345.
20. Flinn L, Mortiboys H, Volkmann K, Koster RW, Ingham PW, et al. (2009) Complex I deficiency and dopaminergic neuronal cell loss in parkin-deficient zebrafish (Danio rerio). Brain 132: 1613-1623.
21. Fett ME, Pilsl A, Paquet D, van Bebber F, Haass C, et al. (2010) Parkin is protective against proteotoxic stress in a transgenic zebrafish model. PLoS One 5: e11783.
22. Anichtchik O, Diekmann H, Fleming A, Roach A, Goldsmith P, et al. (2008) Loss of PINK1 function affects development and results in neurodegeneration in zebrafish. J Neurosci 28: 8199-8207.
23. Sallinen V, Kolehmainen J, Priyadarshini M, Toleikyte G, Chen YC, et al. (2010) Dopaminergic cell damage and vulnerability to MPTP in Pink1 knockdown zebrafish. Neurobiol Dis 40: 93-101.

24. Xi Y, Ryan J, Noble S, Yu M, Yilbas AE, et al. (2010) Impaired dopaminergic neuron development and locomotor function in zebrafish with loss of pink1 function. Eur J Neurosci 31: 623-633.
25. Bretaud S, Allen C, Ingham PW, Bandmann O (2007) p53-dependent neuronal cell death in a DJ-1-deficient zebrafish model of Parkinson's disease. J Neurochem 100: 1626-1635.
26. Baulac S, Lu H, Strahle J, Yang T, Goldberg MS, et al. (2009) Increased DJ-1 expression under oxidative stress and in Alzheimer's disease brains. Mol Neurodegener 4: 12.
27. Sheng D, Qu D, Kwok KH, Ng SS, Lim AY, et al. (2010) Deletion of the WD40 domain of LRRK2 in Zebrafish causes Parkinsonism-like loss of neurons and locomotive defect. PLoS Genet 6: e1000914.
28. Ren G, Xin S, Li S, Zhong H, Lin S (2011) Disruption of LRRK2 does not cause specific loss of dopaminergic neurons in zebrafish. PLoS One 6: e20630.
29. Ahlskog JE (2009) Parkin and PINK1 parkinsonism may represent nigral mitochondrial cytopathies distinct from Lewy body Parkinson's disease. Parkinsonism Relat Disord 15: 721-727.
30. Cookson MR, Bandmann O (2010) Parkinson's disease: insights from pathways. Hum Mol Genet 19: R21-27.
31. Corti O, Lesage S, Brice A (2011) What genetics tells us about the causes and mechanisms of Parkinson's disease. Physiol Rev 91: 1161-1218.
32. Narendra DP, Youle RJ (2011) Targeting mitochondrial dysfunction: role for PINK1 and Parkin in mitochondrial quality control. Antioxid Redox Signal 14: 1929-1938.
33. Springer W, Kahle PJ (2011) Regulation of PINK1-Parkin-mediated mitophagy. Autophagy 7: 266-278.
34. Thomas KJ, McCoy MK, Blackinton J, Beilina A, van der Brug M, et al. (2011) DJ-1 acts in parallel to the PINK1/parkin pathway to control mitochondrial function and autophagy. Hum Mol Genet 20: 40-50.
35. Kamp F, Exner N, Lutz AK, Wender N, Hegermann J, et al. (2010) Inhibition of mitochondrial fusion by alpha-synuclein is rescued by PINK1, Parkin and DJ-1. Embo J 29: 3571-3589.
36. Poulopoulos M, Levy OA, Alcalay RN (2012) The neuropathology of genetic Parkinson's disease. Mov Disord 27: 831-842.
37. Samaranch L, Lorenzo-Betancor O, Arbelo JM, Ferrer I, Lorenzo E, et al. (2010) PINK1-linked parkinsonism is associated with Lewy body pathology. Brain 133: 1128-1142.

38. Nguyen HN, Byers B, Cord B, Shcheglovitov A, Byrne J, et al. (2011) LRRK2 mutant iPSC-derived DA neurons demonstrate increased susceptibility to oxidative stress. Cell Stem Cell 8: 267-280.
39. Seibler P, Graziotto J, Jeong H, Simunovic F, Klein C, et al. (2011) Mitochondrial Parkin recruitment is impaired in neurons derived from mutant PINK1 induced pluripotent stem cells. J Neurosci 31: 5970-5976.

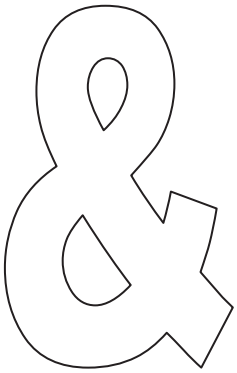

Summary/Samenvatting/总结
Curriculum Vitae
PhD Portfolio
List of Publications
Acknowledgements

Summary

Parkinson's disease (PD) is one of the most common neurodegenerative disorders, which affects ~1-2% of the population above the age of 60 years-old. The clinical features of the disease consist of resting tremor, slowness of movement (bradykinesia), muscular rigidity, and postural instability. This syndrome is caused by the progressive loss of dopaminergic neurons in the substantia nigra of the midbrain, and the formation of alpha-synuclein-containing protein aggregates, termed Lewy bodies, in the surviving neurons. Most PD patients experience the onset of their motor symptoms after the age of 60 years. However, in some patients, the symptoms of the disease develop much earlier. "Early-onset Parkinsonism" is used to indicate the parkinsonian syndromes presenting before the age of 40 years.

Abnormalities in several important cellular pathways and systems are suspected to play important roles in the pathogenesis of PD, including mitochondrial dysfunctions, oxidative stress, proteasomal and autophagic dysfunctions, neuroinflammation, excitotoxicity, and apoptosis. However, the exact molecular mechanisms causing neurodegeneration in PD remain mostly unknown. Over the past few years, genetic studies have provided novel clues for understanding of the molecular pathogenesis of PD. Several Mendelian forms of the disease have been identified, which are transmitted in autosomal dominant or recessive fashion. Mutations in the *FBXO7* gene cause a recently identified form of autosomal recessive parkinsonism with early-onset and additional pyramidal signs. This thesis deals with the role of the protein encoded by this gene (FBXO7) in early-onset parkinsonism.

In **Chapter 2**, we characterized novel pathogenic mutations in the *FBXO7* gene in two unrelated families with early-onset, progressive parkinsonism and pyramidal tract dysfunctions. This work provided the first, conclusive evidence that *FBXO7* is the disease-causing gene in this newly-identified form. The affected subjects displayed parkinsonism with severe defects of the nigrostriatal dopaminergic pathways, and they exhibited good response to levodopa therapy. Thus, the disease caused by *FBXO7* mutations was listed among the monogenic parkinsonisms, and it was designated as PARK15 (for monogenic parkinsonism, type 15).

To investigate the consequences of *FBXO7* mutations, in **Chapter 3** we characterized the expression of the FBXO7 protein in cells derived from PARK15 patients and from normal control subjects. We found that two FBXO7 protein isoforms are expressed in normal human cells, while the common cellular abnormality found in the PARK15 patients from the two families is the depletion of the FBXO7 isoform 1, which normally localizes in the cell nucleus. The activity of FBXO7 in the nucleus appears therefore crucial for the maintenance of brain neurons and the pathogenesis of PARK15.

In parallel with the above-mentioned *in vitro* experiments, in the **Chapter 4** we generated the first *in vivo* model of PARK15 by transient, morpholino-mediated knockdown of the *FBXO7* homologue gene in zebrafish (*zFbxo7*). In these morphants we documented markedly decreased zFbxo7 protein expression, associated with abnormal patterning and significant decrease in the number of dopaminergic neurons. Moreover, the morphants displayed severe locomotor disturbances (bradykinesia), which were dramatically improved by the dopaminergic agonist apomorphine. The severity of these morphological and behavioral abnormalities correlated with the severity of zFbxo7 protein deficiency. Taken together, this novel vertebrate model reproduces pathologic and behavioral hallmarks of human parkinsonism (i.e., dopaminergic neuronal loss and dopamine-dependent bradykinesia), representing therefore a valid tool for investigating the mechanisms of selective dopaminergic neuronal death, and screening for modifier genes and therapeutic compounds.

In **Chapter 5**, we characterized the expression of the FBXO7 protein in the brains of normal human subjects and of PD patients, using a polyclonal antibody against full-length FBXO7. We observed widespread neuronal FBXO7 immunoreactivity throughout all the brain regions. Semiquantitative analysis showed no gross difference in the level of immunoreactivity between normal controls and PD patients. Of note, the FBXO7 immunoreactivity was also detected in some Lewy bodies and Lewy neurites, where FBXO7 co-localized with α-synuclein as confirmed using double immunofluorescence staining. These findings suggest a role for the FBXO7 proteins in the pathogenesis of Lewy-body pathology in the common (non-Mendelian) forms of synucleinopathies (PD and Lewy body dementia).

The last part of the thesis (**Chapter 6**) contains a general discussion of the above-mentioned findings, and some perspectives for future investigations

aimed at the understanding further the role of the FBXO7 proteins in the pathogenesis of the early-onset parkinsonism, and also of the more classical, late-onset forms of neurodegenerative diseases.

Samenvatting

De ziekte van Parkinson (PD) is een van de meest voorkomende neurodegeneratieve aandoeningen met ~1-2% van de bevolking boven de 60 jaar die is aangedaan. De klinische symptomen van de ziekte bestaan uit beven (in rust), traagheid van bewegingen (bradykinesie), spierstijfheid, en posturale instabiliteit. Het syndroom wordt veroorzaakt door het progressieve verlies van dopaminerge neuronen in de substantie nigra van de middenhersenen en de vorming van α-synucleine bevattende eiwit ophopingen, Lewy bodies genaamd, in de resterende zenuwcellen. Bij de meeste patiënten beginnen de symptomen van de motoriek op een leeftijd boven de 60 jaar. Echter bij sommige patiënten ontwikkelen de symptomen van de ziekte veel eerder. “parkinsonisme op jonge leeftijd” is de term die wordt gebruikt om parkinson syndromen aan te duiden die zich reeds op een leeftijd voor de 40 jaar presenteren.

Van verscheidene afwijkingen in belangrijke cellulaire mechanismen en systemen wordt vermoed dat zij een belangrijke rol spelen in het ontstaan van de ziekte van Parkinson, deze omvatten dysfunctie van de mitochondrien, oxidatieve stress, dysfunctie van het proteasoom en autofagie, neuronale ontstekingen, excitotoxiciteit en apoptose. De exacte moleculaire mechanismen die de neurodegeneratie in de ziekte van Parkinson veroorzaken blijven echter grotendeels onbekend. Gedurende de afgelopen jaren hebben genetische studies nieuwe inzichten gegeven in de moleculaire ontwikkeling van de ziekte van Parkinson. Verschillende mendeliaanse vormen de ziekte van Parkinson, die op een autosomaal dominante of recessieve manier worden doorgegeven, zijn geïdentificeerd. Mutaties in het *FBXO7* gen veroorzaken een recent gevonden vorm van autosomaal recessief Parkinsonisme op jonge leeftijd met extra pyramidale tekenen. Dit proefschrift behandeld de rol van het eiwit dat door dit gen (FBXO7) wordt gecodeerd in parkisonisme op jonge leeftijd.

In **hoofdstuk 2**, hebben we nieuwe pathogene mutaties in het *FBXO7* gen in twee niet-verwante families met progressieve parkinsonisme op jonge leeftijd en dysfuncties van het pyramidale traject gekarakteriseerd. Deze studie geeft voor het eerst afdoende bewijs dat *FBXO7* het ziekteveroorzakende gen is in deze nieuw geïdentificeerde vorm van de ziekte. De aangedane patiënten hebben een parkinsonisme met ernstige defecten in nigrostriatale dopaminerge paden en ze reageren goed op behandeling met levodopa. Daarom werd de ziekte veroorzaakt door *FBXO7* mutaties geschaard onder de monogene

parkinsonismen en werd aangeduid als PARK15 (voor monogeen parkinsonisme, type 15).

Om de gevolgen van *FBXO7* mutaties te onderzoeken, hebben we in **hoofdstuk 3**, de expressie van het FBXO7 eiwit in cellen van PARK15 patiënten en normale controles gekarakteriseerd. We hebben aangetoond dat twee FBXO7 isovormen in normale humane cellen tot expressie komen, terwijl de gemeenschappelijke cellulaire afwijking in de PARK15 patiënten uit de twee families de afwezigheid van isovorm 1 is, die normaal in de celkern voorkomt. De activiteit van FBXO7 in de celkern lijkt daarom cruciaal voor het behoud van zenuwcellen in de hersenen en de ziekteontwikkeling in PARK15.

In parallel met de bovengenoemde *in vitro* experimenten, hebben we in **hoofdstuk 4** een eerste *in vivo* model voor PARK15 gemaakt, met behulp van transiente, morpholino gemedieerde knockdown van de zebravis homoloog van *FBXO7, zFbxo7*. In deze "morphants" hebben we een aanzienlijk afgenomen expressie van zFbxo7 laten zien, wat werd geassocieerd met een abnormaal patroon en significante afname van het aantal dopaminerge zenuwcellen. Bovendien hadden de "morphants" een ernstige stoornis in de beweging (bradykinesie), die duidelijk werk verbeterd door de dopaminerge agonist apomorfine. De mate van deze morfologische en gedragsmatige afwijkingen correleren met de mate van het zFbxo7 eiwittekort. Bij elkaar genomen reproduceert dit nieuwe vertebrate model de pathalogische en gedragsmatige kenmerken van humaan parkinsonisme (waaronder verlies van dopaminerge zenuwcellen en dopamine-afhankelijke bradykinesie), daarom is dit een waardevol instrument voor het onderzoeken van de mechanismen van selectieve dopaminerge neuronale celdood, het zoeken naar modificerende genen en therapeutische stoffen.

In **hoofdstuk 5** hebben we de expressie van het FBXO7 eiwit in de hersenen van gezonde personen en van patienten met de ziekte van Parkinson in kaart gebracht, met behulp van een polyclonaal antilichaam tegen het volledige FBXO7 eiwit. We zagen wijdverspreide neuronale FBXO7 immunoreactiviteit in alle hersengebieden. Semiquantitatieve analyse liet geen grote verschillen in immunoreactiviteit zien tussen normale controles and Parkinson patienten. Belangrijk is dat FBXO7 immunoreactiviteit ook werd waargenomen in een aantal Lewy bodies en Lewy neuriten alwaar FBXO7 co-localiseerde met α-synucleine, zoals werd bevestigt met immunofluorescente dubbelkleuring. De

bevindingen suggereren een rol voor het FBXO7 eiwit in de ontwikkeling van Lewy-body pathologie in de algemeen (niet-mendeliaanse) vormen van synucleinopathieen (parkinson en Lewy-body dementie).

Het laatste deel van het proefschrift (**hoofdstuk 6**) bevat een algemene discussie van bovengenoemde bevindingen en enkele suggesties voor toekomstige studies gericht op het verder begrijpen van de rol van FBXO7 eiwit in het ontwikkelen van parkinsonisme op jonge leeftijd en van de meer klassieke, late-onset vormen van neurodegeneratieve ziekten.

总结

帕金森病是最常见的神经退行性疾病之一，大约影响 1-2%的年龄为 60 岁以上的老年人。本病的临床特征包括静止性震颤，运动迟缓，肌强直和姿势步态异常等。帕金森病主要是由中脑黑质多巴胺神经细胞的进行性缺失和神经细胞中 α-突触核蛋白为主的蛋白包涵体（又称为路易小体）的形成而引起的。大部分帕金森病病人在 60 岁以后出现运动系统的症状，然而也有一部分病人在 40 岁以前出现症状，称作早发性帕金森氏症。

细胞旁路和系统的功能异常，例如线粒体功能障碍，氧化应激，细胞凋亡，蛋白酶体及自噬功能障碍等，在帕金森病的发病机制中发挥着重要作用。然而帕金森病中真正引起神经细胞退行性变的分子机制还不清楚。在过去的几年中，致病基因的发现让人们对帕金森病的发病机制有了新的认识。帕金森病可以通过常染色体显性或者隐性的孟德尔遗传方式在家系中进行传播。最近研究发现 *FBXO7* 基因突变能够引起常染色体隐性早发性帕金森氏症，并伴有锥体束病变。本论文论述了 FBXO7 蛋白在早发性帕金森氏症中的作用。

在本论文的第二章中，我们在两个没有关联的早发性帕金森氏症伴有锥体束功能障碍的家系中发现了 *FBXO7* 基因 2 个新的致病性突变。本研究第一次证实了 *FBXO7* 基因是这种新型帕金森病的致病基因。家系中的患者具有帕金森病的典型症状，并伴有严重的黑质纹状体多巴胺旁路的功能缺失。左旋多巴对于该患者的治疗效果显著。鉴于该基因在帕金森病领域的重要性，*FBXO7* 基因突变引起的这种新的疾病类型成为单基因帕金森氏症的新成员，被命名为第 15 类单基因帕金氏症（PARK15）。

在本论文的第三章中，我们分析了正常人和携带 *FBXO7* 基因突变的病人细胞中的 FBXO7 蛋白的表达。我们发现 FBXO7 蛋白的 2 个异构体在正常人的细胞中都有表达，但是 FBXO7 蛋白异构体 1 在病人的细胞中表达缺失。FBXO7 蛋白异构体 1 通常在细胞核中表达，因此，FBXO7 蛋白的细胞核定位及功能对维持脑神经细胞的功能至关重要，同时也与 PARK15 的发病机制密切相关。

除了上述的体外细胞实验，在本论文的第四章中，我们利用斑马鱼构建了第一个 PARK15 的脊椎动物疾病模型。这个模型是利用吗啉反义寡核苷酸技术来定向敲除斑马鱼的 *Fbxo7* 基因（人的 *FBXO7* 同源基因）。在 *Fbxo7* 基因敲除的斑马鱼中，Fbxo7 蛋白表达减少，并引起多巴胺神经细胞表达分布的异常和数量的减少。此外，*Fbxo7* 基因敲除的斑马鱼出现运动迟缓的症状，而该症状能通过应用多巴胺受体激动剂阿朴吗啡而得到明显改善。这些形态及行为的异常都和 Fbxo7 蛋白表达缺失程度密切相关。简而言之，这个新的脊椎动物模型具有多巴

胺神经细胞的缺失和多巴胺依赖的行动迟缓的症状，重现了人类帕金森病的典型的病理和行为特征。因此，这个斑马鱼的疾病模型也成为研究选择性多巴胺神经细胞死亡机制和筛选新型疾病治疗药物的有效工具。

在本论文的第五章中，我们利用 FBXO7 多克隆抗体研究了 FBXO7 蛋白在正常人人脑和帕金森病病人人脑中的表达。我们发现 FBXO7 广泛的表达在大脑中所有的区域中。半定量分析表明，病人和正常人并没有蛋白表达水平上的差异。而值得注意的是，我们在路易小体和路易神经突起中检测到了 FBXO7 蛋白的表达。路易小体和路易神经突起富含 α-突触核蛋白，因此 α-突触核蛋白是识别路易小体和路易神经突起结构的分子标记。双重免疫荧光染色结果进一步证实，FBXO7 和 α-突触核蛋白共定位于路易小体和路易神经突起中。这些结果有助于进一步理解 FBXO7 蛋白在通常（非孟德尔形式）的突触核蛋白病（帕金森病和路易体痴呆病）的路易小体中的病理作用。

在本论文的第六章中，我们综合讨论了上述的研究发现并对今后研究的方向进行了展望。我们今后会进一步研究 FBXO7 蛋白在早发性帕金森氏症以及更典型的晚发性神经退行性疾病中的致病机理。

Curriculum Vitae

Tianna Zhao was born on September 1st 1980, in Zaozhuang, Shandong, China. She obtained the bachelor degree of Clinical Medicine from Shandong University in 2003. In the same year, she started her scientific career in Shandong Academy of Medical Sciences under the supervision of Prof. dr. J. Han and Dr. S. Wang. After obtaining the master degree of Medicine in 2006, she worked as a visiting scholar in Hong Kong Baptist University, Hong Kong, China.

In 2007, she came to the Netherlands, and worked as a PhD student in the department of Clinical Genetics of Erasmus MC Rotterdam, under the supervision of Prof. dr. V. Bonifati and Prof. dr. B.A.Oostra. The results obtained from her PhD research were presented in international conferences, and have been submitted or published in peer-reviewed scientific journals. After her PhD, Tianna would like to continue her academic career with a post-doctoral position.

PhD Portfolio

Summary of PhD training and teaching activities

Name PhD student:	Tianna Zhao	PhD period:	November 2007 - October 2012
Erasmus MC Department:	Clinical Genetics		
Research School:	Medical Genetics Centre (MGC) South-West Netherlands	Promotor(s):	Prof. dr. V. Bonifati Prof. dr. B.A. Oostra
		Supervisor:	Prof. dr. V. Bonifati

1. PhD training

	Year	Workload
General academic skills		
Safely working in the Laboratory	2008	8 hours
Biomedical English Writing and Communication	2010	80 hours
Research skills		
Technology and facilities	2009	24 hours
From development to disease	2009	24 hours
Epigenetic Regulation	2010	16 hours
Photoshop and Illustrator	2010	16 hours
Confocal Microscopy	2012	3 hours
Presentations		
Clinical genetics work discussion	2007-2012	320 hours
Parkinson disease group work discussion	2007-2012	320 hours
Parkinson disease group journal club	2009-2010	64 hours
International conferences		
17th World Congress on Parkinson's Disease and Related Disorders, Amsterdam, The Netherlands	2007	32 hours
2nd World Parkinson Congress, Glasgow, United Kingdom (poster presentation)	2010	32 hours
16th International Congress of Parkinson's Disease and Movement Disorders, Dublin, Ireland (poster presentation)	2012	40 hours
Seminars and workshops		
16th PhD workshop, Brugge (poster presentation)	2009	30 hours
Neurogenetics: from gene to therapy	2009	16 hours
Stepping stones for research funding	2011	6 hours
22th MGC Symposium, Leiden	2012	8 hours

2. Teaching activities

	Year	Workload
Supervising		
Master thesis: “Analysis of FBXO7 proteins in families with PARK15 (Parkinsonian-pyramidal syndrome)” by Agnese Loda	2010	6 months

List of Publications

Zhao T, Severijnen LA, van der Weiden M, Zheng PP, Oostra BA, Willemsen R, Kros JM, Bonifati V. The expression of the FBXO7 proteins in the normal human brain and in Parkinson's disease. ***To be submitted***.

Zhao T, van der Linde HC, Severijnen LA, Oostra BA, Willemsen R, Bonifati V. Dopaminergic neuronal loss and dopamine-dependent locomotor defects in Fbxo7-deficient zebrafish. ***Submitted to PLoS ONE.***

Quadri M, Federico A, **Zhao T**, Breedveld GJ, Battisti C, Delnooz C, Severijnen LA, Di Toro Mammarella L, Mignarri A, Monti L, Sanna A, Lu P, Punzo F, Cossu G, Willemsen R, Rasi F, Oostra BA, van de Warrenburg BP, Bonifati V. Mutations in SLC30A10 cause parkinsonism and dystonia with hypermanganesemia, polycythemia, and chronic liver disease. ***Am J Hum Genet.*** 2012 Mar 9;90(3):467-77.

Zhao T, De Graaff E, Breedveld GJ, Loda A, Severijnen LA, Wouters CH, Verheijen FW, Dekker MC, Montagna P, Willemsen R, Oostra BA, Bonifati V. Loss of nuclear activity of the FBXO7 protein in patients with parkinsonian-pyramidal syndrome (PARK15). ***PLoS ONE.*** 2011 Feb 11;6(2):e16983.

Di Fonzo A, Dekker MC, Montagna P, Baruzzi A, Yonova EH, Correia Guedes L, Szczerbinska A, **Zhao T**, Dubbel-Hulsman LO, Wouters CH, de Graaff E, Oyen WJ, Simons EJ, Breedveld GJ, Oostra BA, Horstink MW, Bonifati V. FBXO7 mutations cause autosomal recessive, early-onset parkinsonian-pyramidal syndrome. ***Neurology.*** 2009 Jan 20;72(3):240-5.

Acknowledgements

Looking back to the life during the last five years, working as a PhD student was a unique experience for me, and it has become sweet memory in my mind. As this PhD journey is approaching its destination, one of the joys of completion is to thank all the colleagues, friends, and my relatives who have helped and supported me along this long but fruitful road.

First of all, I would like to thank my promoters, **Prof. dr. Vincenzo Bonifati** and **Prof. dr. Ben A Oostra,** for the valuable guidance and advice. Thank you for giving me the great opportunity to work in the department of Clinical Genetics, to learn from you, and to have the best environment to develop my scientific career. **Prof. Bonifati,** dear **Vincenzo,** thank you for offering me to work as a PhD student in your laboratory. Your broad academic knowledge and rigorous attitude to science impressed me deeply and showed me the best example of how to be a real and good scientist. You guided me in the field of Parkinson's disease, and taught me how to analyze and interpret data, how to work precisely, and how to write scientific papers. I can not express enough gratitude for your great help for almost everything. **Prof. Oostra,** dear **Ben,** you always gave me valuable suggestions, and you provided encouragement and support to finish my PhD.

I would also like to express my deep and sincere gratitude to my thesis committee member. **Dr. Niels Galjart**, **Prof. Oliver Bandmann**, **Prof. Eleonora Aronica**, and **Prof. Joost Gribnau**. I appreciate all the time and energy you have invested and all your constructive comments to improve and complete this thesis.

My research projects would not have been finished without fruitful collaborations. Dear **Dr. Rob Willemsen**, thank you so much for your kind help and valuable suggestions in our collaboration. Dear **Dr. Esther de Graaff**, the memory of the beginning of my PhD was unforgettable. I often rushed into your office with odd problems and questions, and you always explained and solved them with patience despite of my poor English. Thank you very much for teaching me many techniques, for discussing the results, and for always encouraging me to pursuit my interests. Dear **Lies-Anne Severijnen**, I highly appreciate your technical support in my research and kind help as paranimf. Dear **Herma Zondervan-van der Linde**, your professional experience and kind helps have

driven our projects smoothly! Dear **Edwin Romme**, thank you for your kind help on microinjection. Without your considerate culture, our fish won't be happy. Dear **Prof.** dr. **Max Kros, Dr. Pingpin Zheng, Dr. Adriana T Nijholt** and **Marcel van der Weiden**, thank you for your kind help and support in the brain pathology studies. **Dr. Frans Verheijen, Dr. Cokkie Wouters** and **Laurette Dubbel-Hulsman,** thank you for the generation of lymphoblast and fibroblast cell lines. **Dr. Inge Huitinga** and **Michiel Kooreman** (Netherlands Brain Bank), thank you for providing the samples necessary for our brain studies. **Dr. Marieke Dekker, Prof. Pietro Cortelli** and **the late Prof. Pasquale Montagna**, thank you for your collaboration for the clinical studies of the PARK15 patients.

Dear Parkinson group members, the pipetting work were not lonely and boring because of your nice accompany for five years. Dear **Isa**, it has been such a pleasure to work with you during the last four years. We shared both excitement and frustration from our results, exchanged the ideas and opinions in PD congresses, and enjoyed great fun in office, coffee bar and our apartments! You are really an organized person in both science and life. Six months before my PhD defense, you already started to arrange defense-related work, and I thank you very much for helping me as paranimf. I wish you all the best in your research! **Guido**, you have been my mentor when I performed my first sequence project in our lab. My successful genetic results definitely benefited from your professional skills. Moreover, your "private stellingen" will influence me for my future scientific career. **Erik**, your precise work and excellent cooking are impressive for me. **Simone**, thank you for sharing some Italian traditions and stories, and I wish you good luck with your PhD. **Josja**, we knew each other from the zebrafish project, and many success with your work. **Alessio**, **Janneke**, **Agnese**, **Kate**, **Marina**, **Dorothea** and **Christian**, thanks for providing the different cultures, different traditions, and different ideas. **Anna**, my first friend in Rotterdam, we knew each other very well and became friends quickly. Thank you for coming to my wedding in China as bridesmaid. We also had good time in Krakow, and the peaceful Christmas Eve with your family was fabulous and great memory for me.

I always believe that people need good luck to have the best colleagues, and I am definitely that lucky person. Prof. **Robert Hofstra**, I appreciate your valuable suggestions on work discussions. **Andre, Arnold** and **Aida**, thank you for your valuable and useful suggestions for the research. **Annelies**, thank you for the beautiful evening with your family on Christmas holiday, and your kind invitation

makes me feel like home. **Renate, Mark** and **Elisabeth**, I always bother you with some practical questions, and thank you very much for all your patience, helps and advices on my research. **Femke** and **Josien**, thank you for technical supports in culturing primary neurons, and I wish you all good luck with your new projects. **Edwin** and **Ronald**, when I think of you, I can not help but think of dumplings! Thank you for reminding me to cook some dumplings for you despite of my poor cooking skills. **Edwin**, you always created very cheerful atmosphere in our lab, but your interests on the "special Chinese words" really impressed me. **Ronald**, thank you for reminding me to take more and more chocolate. However, I have one thing against you. Sofie is a very sweet girl, and please do not train her to be your dumpling cooker. **Francesca**, thank you for sharing the experience of your PhD defense. We had a lot of fun when we talk about some similar traditions of our countries. **Bianca**, I like to listen to your great adventures in many countries where you have been. Thank you for organizing the wonderful "girls evening", and I highly appreciate the valuable advice on traveling. **Judith**, **Andreea**, **Celine**, **Christina**, **Sotirios**, **Shimriet**, **Vanessa**, **Luna**, **Cathryn**, **Yunia**, **Maria**, **Danny**, **Rajendra**, **Danielle**, **Elisabeth**, **Anna**, **Erwin**, **Pim**, and **Atze**, thank you for sharing broad knowledge and your excellent research in work discussions, which absolutely expanded my vision in different scientific fields. **Ingeborg**, **Leontine**, **Marianne**, **Rachel**, **Marian**, **Asma**, **Christan**, **Linda**, **Bert**, **Hannie**, and **Jolanda**, without your dedicated work, the experiments will never work easily. **Gert van Cappellen** and **Gert-Jan Kremers**, thank you for teaching me the theories and techniques of confocal microscope. Your professional image skills convinced me that science can be art! **Jeannette, Benno** and **Marjoleine**, thank you for assisting me to settle down in Rotterdam and all the help that you gave me in the last five years. Especially, I would like to thank **Tom de Vries Lentsch** and **Ruud Koppenol** for the artwork. **Elisa, Akiko, Cristina, Catherine, Eskeatnaf, Eveline, Tahsin-Stefan, Chiara, Romana, Karina**, **Tamrat**, **Adriana**, **Claudia**, **Mesut, Widagdo,** and **Rebecca**, thank you for our nice discussion for both work and life.

I have been to many cities in Europe, but Hong Kong is still my favorite city not only because of its fashion, but also because of my good colleagues and friends. **Prof. Wong** and **Dr. Liang**, thank you for offering me an opportunity to work in CIES. Although six month is not long, it is my pleasure to know my good colleagues, **Huachang**, **Weixi**, **Anna**, **Joanne**, **Wang Fang**, **Yanyan**, **Feng**, **Gao Yan**, **Laiqing**. Dear **Maggie**, **Janet, Brian**, **Eric**, and **Martin**, I had so much fun to work with you, and I forgot my homesickness since you guys created a

relaxing atmosphere in the lab. Special thanks go to **Guanhua**. We have so much in common, and I appreciate our precious friendship. The conversation between us as if happened yesterday in my mind, and this memory is just sweet!

Furthermore, I would like to thank my previous supervisors and colleagues during my master. 衷心感谢在硕士期间，我的导师韩金祥和王世立研究员对我的指导。在医科院的学习为我能够顺利完成博士学业打下了坚实的科研基础。感谢卞翠荣教授对我的关心。特别感谢张长铠教授，陈雅丽教授以及晗星对我的教导和关照。向曾经帮助过我的朱有名，常晓天，高雪芹，宋长征，崔亚洲，朱波，窦建华老师表示诚挚的敬意和感谢。

I am indebted to my many Chinese friends for providing a stimulating and joyful environment in which to learn and grow in the Netherlands. 时光荏苒，岁月如梭，在荷兰生活五年的日子有欢笑，也有泪水。由于认识了很多善良可爱，有爱心，有正义感的好朋友，国外的感觉是幸福而甜美的。侯珺，商鹏，感谢你们这五年的陪伴，我们分享过成功的喜悦，同时也彼此倾听对方的牢骚。感谢温蓓，刘凡，姜涛，石颖给我们无趣的荷兰生活带来的无限欢乐。张磊，于晓，王田田，陈韬，Lisha 和宏伟夫妇，蕾蕾和 Maurizio 夫妇，越丹和 Hans 夫妇，童苗，宝月，海波，康宁，亚迪，高振宇，王永毅，黄玲，谢谢你们的陪伴，有了你们，生活才变得多姿多彩。

In the end, I want to express my deepest gratitude to my parents for believing in me, loving me, tirelessly encouraging me, and to my husband for his endless love, understanding, and constant supports. Without their loves and supports, the success of this thesis would not be possible. I dedicate this thesis to them. 亲爱的爸爸妈妈，虽然我们远隔万里，但是我们无时无刻不在思念、牵挂着对方。当我在国内，还是温室里的花朵时候，你们无限呵护我的成长；当我决定出国时，你们恋恋不舍的支持我的选择，希望我经历外界的风雨长成参天大树。你们的宠爱如此细微体贴，让我无法用语言，甚至足够的爱来表达对你们的感谢。你们无私的爱与关怀是我坚强的后盾，是我不畏风雨、不断前进的动力。同时也要感谢我的公公婆婆对我生活上的关心照料以及学业的支持。谢谢我的弟弟群群为我毕业论文设计的精美封面。我们分享快乐的童年，一起长大，我了解你的性格和专业技能，相信并期待你的事业成功在不远的将来。最后，我要特别感谢我的老公吕鹏对我生活上的照顾与课题上的建议。无论是工作上的不顺心还是生活上的不开心，我总是直接向你倾诉抱怨，你在耐心的倾听的同时并积极的开导

我。谢谢你的支持和帮助，我才能顺利的完成学业！因为有爱，你是快乐的，我就是幸福的！谨以此书献给我最爱的亲人们！